OCEAN DATA SYSTEMS, INC.

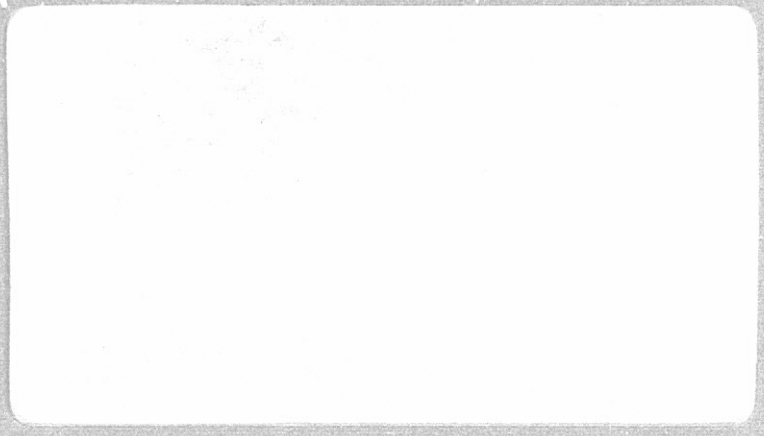

OCEAN DATA SYSTEMS, INC.
2400 GARDEN ROAD, MONTEREY, CALIFORNIA 93940 • 408/649-1133

Submitted to
JET PROPULSION LABORATORY
Pasadena, California

ATMOSPHERIC MODEL DEVELOPMENT IN SUPPORT OF SEASAT

VOLUME IV - FORECAST MODEL SENSITIVITY STUDY

Final Technical Report

Prepared under
JPL Contract Number 954668
(Subcontract of NASA Contract Number NAS7-100)

September 30, 1977

Prepared by
Howard L. Lewit
Philip G. Kesel
OCEAN DATA SYSTEMS, INC.
Monterey, California

EXECUTIVE SUMMARY

This Final Report (in five volumes) was prepared by Ocean Data Systems, Inc. for the Jet Propulsion Laboratory under Contract No. 954668 (as amended) in support of the SEASAT Program.

The objective was to develop atmospheric analysis and prediction models of varying (grid) resolution, and to test the models using real observational data for the purpose of assessing the impact of grid resolution on short-range numerical weather prediction. The work statement was amended to include the performance of sensitivity tests using a coarse-mesh (63 x 63 x 5 level) prediction model in order to identify and order factors which might mask or impair the utility of SEASAT data on short-range weather prediction. Such factors included: initial conditions; topography; surface friction; latent heating; diffusion of momentum and temperature; and computational devices such as tendency truncators, pressure smoothers, and temporal filters.

A. Description

ODSI has completed the sensitivity tests using model version PECHCV (63 x 63 x 5). The model characteristics/parameters which were varied, together with forecast run descriptors, are listed below:

- Temperature diffusion coefficient (K_T)
  - -- $K_T = 10^6$ (standard); Run SF-3
  - -- $K_T = 10^5$; Run SF-4

- Momentum diffusion coefficient (K_M)
  - -- $K_M = 10^6$ (standard); Run SF-3
  - -- $K_M = 10^5$; Run SF-2
  - -- $K_M = f(\sigma)$; Run SF-1

- Surface drag coefficient (C_D)
  - -- $C_D = 0.0015$ (standard); Run SF-3
  - -- $C_D = 0.003$; Run SF-7
  - -- $C_D = 0.00015$; Run SF-9

- Pressure-smoothing coefficient (ε)
  - -- $\varepsilon = 0.01$ (standard); Run SF-3
  - -- $\varepsilon = 0.02$; Run SF-6
  - -- $\varepsilon = 0.0$; Run SF-5
  - -- $\varepsilon = f(t)$; Run SF-12

- Precipitation (large-scale plus convection)
  - -- On (standard); Run SF-3
  - -- Off; Run SF-14

- Temporal filtering
  - -- On (standard); Run SF-3
  - -- Off; Run SF-15

- Multiple modifications
  - -- Standard; Run SF-3
  - -- No diffusion, pressure smoothing, friction, radiation, condensation, evaporation, or sensible heating; Run SF-11
  - -- No radiation, evaporative/sensible exchanges at surface; Run SF-20
  - -- No diffusion (K_T=K_M=0.0); Run SF-10

- Initial wind specification
  - -- Analyzed (standard); Run SF-3
  - -- Derived from balance equation; Run SF-16

- Initial moisture specification
  - -- Parameterized using vorticity patterns (standard); Run SF-3
  - -- RH = 25%; Run SF-17
  - -- RH = 75%; Run SF-18

- Tendency truncation/Terrain tapering
  - -- Tendencies and terrain vanish south of 5°N, and increase smoothly with latitude to full value at 20°N (standard); Run SF-3
  - -- Tendencies and terrain reduced by 50% south of 5°N, with latitudinal increases to full value by 20°N; Run SF-19

- Terrain specification
  - -- Tapered south of 20°N to 5°N equatorward of which it vanishes (standard); Run SF-3
  - -- Smooth earth; Run SF-13

B. Findings

These sensitivity studies have demonstrated that the effects of each process, procedure and parameter contributing to the computer forecast need to be understood, ordered and exploited. Many of the choices are model dependent.

Physical effects are often small when compared to other sources of (possible) variation in a forecast. In fact, some computational/cosmetic devices can mask (or overwhelm) certain physical effects. Consider, for example, pressure-smoothing which has a greater impact on the forecast than surface friction,

mountains or vertical resolution. Momentum diffusion impacts on the forecast as much as (modeled) precipitation. The coefficients for both pressure smoothing and momentum diffusion should be specified only after careful evaluation of numerous forecasts.

Table 1 summarizes some of the variations between two forecasts due to specified modifications in a procedure, coefficient or effect. Precipitation amounts appear to be affected mainly by changes in the horizontal resolution and/or in the initial moisture specification. The average storm intensity is affected by horizontal resolution, too. Vertical resolution increase (from five to ten layers) had minimal impact on storm centers. Pressure smoothing and momentum diffusion have as much effect on lows as precipitation or surface friction. With respect to the kinetic energy change predicted at the lowest model level, note that momentum diffusion has greater impact than tripling the horizontal resolution. Pressure smoothing has the same effect as does surface friction or precipitation. Both radiation and temporal filtering appeared to have only minor (if any) impact on a one-day forecast.

TABLE 1: VARIATIONS IN FORECASTS FROM SPECIFIED MODEL CHANGES.

ITEM	DIFFERENCE BETWEEN TWO FORECASTS		
	PRECIPITATION AMOUNT (%)	AVERAGE STORM INTENSITY (MBS)	KINETIC ENERGY CHANGE AT LOWEST LEVEL (%)
RADIATION (ON-OFF)	∿1	0	0.0
TEMPORAL FILTER (ON-OFF)	1-2	0	0.1
FRICTION (2X CHANGE)	2-3	1.5	14.6
DIFFUSION (10X CHANGE)			
- MOMENTUM	∿5	3.0	66.9
- TEMPERATURE	3-4	1.0	4.7
PRESSURE SMOOTHING (2X CHANGE)	4-5	2.5	14.6
INITIAL WINDS (ANALYZED-DERIVED)	∿5	1.2	12.7
MOUNTAINS (IN-OUT)	∿6	1.1	21.1
PRECIPITATION (ON-OFF)	N/A	3.0	14.0
VERTICAL RESOLUTION (2X CHANGE)	10-15	0.5	3.5
HORIZONTAL RESOLUTION (3X CHANGE)	80-100	6.3	57.7
INITIAL MOISTURES (75%-25%)	50-75	2.6	19.2

TABLE OF CONTENTS

TABLE OF CONTENTS (Continued)

LIST OF FIGURES

LIST OF FIGURES (Continued)

LIST OF FIGURES (Continued)

LIST OF FIGURES (Continued)

LIST OF FIGURES (Continued)

LIST OF TABLES

LIST OF TABLES (Continued)

LIST OF TABLES (Continued)

LIST OF TABLES (Continued)

I. INTRODUCTION

This Final Report (in five volumes) was prepared by Ocean Data Systems, Inc. for the Jet Propulsion Laboratory under Contract No. 954668 (as amended).

The objective was to develop atmospheric analysis and prediction models of varying grid resolution, and to test the models using real data for the purpose of assessing the impact of resolution on short-range (1-2 days) forecasts. This work statement was amended to include the performance of model sensitivity studies, using a coarse-mesh (63 x 63 grid with five vertical layers) prediction model, in order to identify and to order some of the factors which might mask or impair the utility of SEASAT data.

This volume contains the descriptions and results of all sensitivity tests performed. Model parameters, procedures and effects were altered singly or in combination to determine the impact on short-range forecasts. These included such things as: initial conditions (winds; moistures); radiation; orography; surface friction; precipitation; diffusion (momentum; temperature); tendency truncation; pressure smoothing; and temporal filtering.

Numerical models, of course, are used to simulate the physical/dynamical processes, effects and interactions taking place in the real atmosphere. These models tend to differ from one another in terms of grid resolution, the physics, initialization, and numerical methods and procedures. Many of these procedures and parameters are discretionary in nature. Thus, there is a need to determine the impact of each procedure and parameter on the forecast.

II. METHOD

Since the inception of numerical weather prediction, numerous computational devices and procedures have been devised and implemented in order to improve either the efficiency, validity or stability of the solutions. Such devices have been modified or discarded with experience. The methods employed in NWP are such that smoothers, filters, tendency truncators, mountain tapering (and the like) are necessary to enhance the stability and appearance of the numerical forecasts. On the other hand, their repetitive use can (and does) have harmful side effects.

The purpose of this series of sensitivity tests with a coarse-mesh primitive-equation prediction model is to determine and to order the impacts of such procedures and devices, many of which are discretionary. The actual model (PECHCV) is described in detail in Volume III of this Final Report. The initial conditions for all tests are those for 1200Z, 22 April 1976. Each of the tests will be introduced and described in subsequent paragraphs.

A. Temperature Diffusion

The diffusion terms of the thermodynamic energy equation is given by

$$D_T = D \frac{m^2_{i,j}}{d^2} \quad (\pi \nabla^2 T)^{n-1}_{i,j}$$

The diffusion coefficient, D, varies with latitude according to the relation K $(1-\sin^2\phi)$ with 0.9 taken as a maximum for $\sin\phi$. K is taken to be 10^6.

For the purposes of this study, the model is executed with K = 10^5 (SF4). The notation (SF_ _) denotes the label by which this particular alteration will be referenced in the tables which follow.

B. Momentum Diffusion

The momentum diffusion terms of the momentum equations are normally treated in the same manner as the temperature diffusion term above. For this study, runs were made where the coefficient of the momentum diffusion terms are: 10^5 (SF2) and varying values from 1.6×10^6 to 2.2×10^6 depending upon the level (SF1).

C. Drag Coefficient

Frictional dissipation is accounted for in the gross boundary layer (σ = 1.0 - 0.8) by the stress terms Fx and Fy, respectively, of the momentum equations in the x and y directions. The friction in the x direction is given by:

$$F_x^{n-1} = \frac{gC_D}{\Delta\sigma R} V_s^{n-1} \left(\frac{\pi u}{T}\right)^{n-1}$$

and in the y direction by

$$F_y^{n-1} = \frac{gC_D}{\Delta\sigma R} V_s^{n-1} \left(\frac{\pi v}{T}\right)^{n-1}$$

where $V_s = 0.3[u^2 + v^2]^{1/2}$

and C_D = 0.0015 for sea level and 0.0025 for non-sea level terrain in the baseline version. C_D is experimentally modified to .003 (SF7) and .00015 (SF9) for this study in two separate executions of the model.

D. Pressure Smoother

In order to control small-scale noise in the pressure field (PS), a non-linear smoothing operator is applied every time step. This smoothing operator has been described by Oliger and Wellck (1970) and is given by:

$$\Delta Ps = \frac{\varepsilon}{|\delta Ps|_{max}} \left[|Ps^{n}_{i+1,j} - Ps^{n+1}_{*}| \; (Ps^{n}_{i+1,j} - Ps^{n+1}_{*}) \right.$$

$$- |Ps^{n+1}_{*} - Ps^{n}_{i-1,j}| \; (Ps^{n+1}_{*} - Ps^{n}_{i-1,j})$$

$$+ |Ps^{n}_{i,j+1} - Ps^{n+1}_{*}| \; (Ps^{n}_{i,j+1} - Ps^{n+1}_{*})$$

$$\left. - |Ps^{n+1}_{*} - Ps^{n}_{i,j-1}| \; (Ps^{n+1}_{*} - Ps^{n}_{i,j-1}) \right]$$

where $|\sigma Ps_{max}|$ is the maximum absolute difference between Ps at the point (i,j) and Ps at any of the four immediately neighboring points, and ε is the smoothing coefficient which has been determined to be of the order of 0.01 for control of computational noise. The smoothed surface pressure is then given by:

$$Ps^{n+1}_{*} \text{ (smoothed)} = Ps^{n+1}_{*} + \Delta Ps$$

where Ps_{*} denotes Ps at (i,j). For the purposes of this study, smoothing coefficients of 0 (SF5), .02 (SF6) and values as a function of time (SF12) are demonstrated in three runs.

E. Precipitation

Both large-scale and convective-scale precipitation is modeled ordinarily. In the large-scale mechanism, 100% relative humidity is the criterion. Layers beneath the precipitating layer are checked to see if evaporation is called for, before the precipitation reaches the ground. Three types of cumulus clouds are parameterized, two of which may precipitate. For our sensitivity runs, we turned off these mechanisms (SF-14).

F. Time Filter

In order to achieve damping of the shorter wave length components to avoid non-linear instability and, in particular, to damp the computational mode, the simple leap-frog scheme is modified slightly to time filter the solutions of the momentum, thermodynamic and moisture equations. This procedure is known as time filtering and was originally used by Robert (1966).

Assume that the partial differential equation that we wish to approximate is

$$\frac{\partial A}{\partial t} = F(A)$$

Then, using the leap-frog difference scheme, we have

$$A^{n+1} = A^{n-1} + 2\Delta t\, F(A)$$

This step is modified by Robert to become

$$(A')^{n+1} = A^{n-1} + 2\Delta t\ F(A,A')$$

$$A^n = (1-\alpha)(A')^n + \frac{\alpha}{2}\left[A^{n-1} + (A')^{n+1}\right],\ 0<\alpha<1$$

Note that after A' is computed at the n+1 time level, A' at the nth time level is converted to an A value by the mixing of time levels. This A is then used in the calculation at the n-1 time level.

It can be shown that this procedure damps the meteorological solution and heavily damps the computational mode that is present in the solution of the finite difference equations. For this study, the model is executed, in one case, without the assistance of the time filter (SF15).

G. Heating

In the normal execution of the model, the contributions of solar radiation, terrestrial radiation and sensible heating and evaporation in the planetary boundary layer are computed once each hour and pro-rated over the next one-hour forecast period. For the purposes of this study, a selected run of the model is executed where these contributions are not operative (SF20).

H. Initial Winds

The initial winds in this model are normally obtained from an analysis procedure which gives analyzed winds on pressure surfaces from 1000 to 100 mb, and are computed geostrophically on the 50 mb pressure surface. The model uses wind data on eleven pressure surfaces: 950, 850, 700, 500, 400, 300, 250, 200, 150, 100 and 50 mb. The initial winds on pressure surfaces are then vertically interpolated linearly in the logarithm of pressure to each model sigma surface.

For the purposes of this study, the model is run once with the winds initialized by the solution of the divergence (balance) equation on constant pressure surfaces and the interpolation of the rotational component of the wind to sigma surfaces (SF16).

I. Moisture (Initial Relative Humidity)

The model is affected by moisture, which is normally initialized by a parameterization method, in its lowest three levels. This initialization method is based on the intensity of the geostrophic relative vorticity which is used to define the initial moisture distributions on the

1,000, 900, 700, 500 and 300 mb pressure surfaces. These values are then interpolated linearly in the logarithm of pressure to the three sigma surfaces.

In this study, two runs of the model were made in which a different constant value of RH was specified for the lower three levels. The value of 25% (SF17) was used for one run and 75% (SF18) for the other.

J. Boundary Conditions

The model is bounded in the horizontal by rigid, impermeable vertical walls placed on the grid on the next-to-outermost row of grid points. The boundary is both insulated and slippery; that is, no heat or momentum exchange is permitted across the wall, but a parallel flow is permitted along the wall.

There is also a provision in the model to truncate the computed tendencies south of a specified latitude. In the standard model (SF-3), this procedure was operative. From 20°N to the Pole, full values of the computed tendencies are used. Below 5°N, the tendencies are set to zero. In the region between 5°N and 20°N the amount of the computed tendencies used varies according to the relation $[(\sin\phi-\sin5°)/(\sin20°-\sin5°)]^2$. This procedure results in a persistence forecast in the equatorial areas, and acts as a computational buffer.

In this study, a special run (SF19) of the model was performed in which the truncation tendency was a linear value between 1 and .5 from 20°N to 5°N, and a constant .5 south of 5°N. The terrain is normally tapered south of 20°N by the tendency truncation factor, but in SF19 this tapering is omitted.

K. Terrain

The terrain height is normally area-averaged and gradient-limited. That is, the terrain gradient at any grid point is constrained to be less than 2000m per 381km, the basic 63 x 63 grid size. In addition, the terrain is multiplied by the tendency truncator, thereby tapering it towards sea level around the edges of the grid.

For this study, two runs of the model were made with specially initialized terrain. In one run, the terrain was set to zero (flat earth) (SF13) and in the other, the tapering procedure was omitted thereby representing terrain at its full smoothed height south of 20°N (see F19, above).

In the above expressions,

u = x direction wind component

v = y direction wind component

π = terrain pressure

T = temperature

m = map factor

F_x, F_y = stress components

D_T = temperature diffusion term

n = time step

III. SYNOPTIC PATTERN

All of the experiments described in the previous section were performed as twenty-four hour forecasts with initial conditions at 1200Z 22 April 1976 forecast to verify at 1200Z 23 April 1976. The initial analysis at the surface is shown in Figure III-1 and at 500 mb in Figure III-2. The verifying surface and 500 mb analyses are given in Figures III-3 and III-4, respectively.

It should be pointed out, once more, that these analyses are not the actual synoptic situations at the given times but a simulation of the atmosphere based upon the analysis technique and its constraints, the available data and the quality of the "first guess" field. The verification analyses are in turn dependent upon the initial analyses since the forecasts from the initial analyses were constituents of the verification's first guess fields.

The 24-hour history of some of the primary systems of this synoptic pattern are given in Tables III-1 and III-2. The changes in Figures III-5 and III-6 are due to a combination of system development and movement.

Tables have been prepared in this and the next section to numerically define the degree of error or change between two fields. The tables are summarized by ten-degree latitude bands and for the entire northern hemisphere. The statistics that are summarized are:

Root mean square (RmS)

$$RMS = \left[\frac{\Sigma (T_F - T_V)^2}{N} \right] 1/2$$

Standard Deviation (SD)

$$SD = \left[\frac{\Sigma (T_F - T_V)^2}{N} - \left(\frac{\Sigma (T_F - T_V)}{N} \right)^2 \right]^{1/2}$$

$$Mean = \frac{\Sigma (T_F - T_V)}{N}$$

T_F = forecast parameter

T_V = verifying parameter

N = number of grid points

as well as the algebraic maximum (MAX) and minimum (MIN) values.

Table III-3 is the summary of the 24-hour changes for this synoptic period. The greatest change at the surface, associated with the East Asia low, was 40.8 mb. At 500 mb the greatest change was 381 m, associated with the same system.

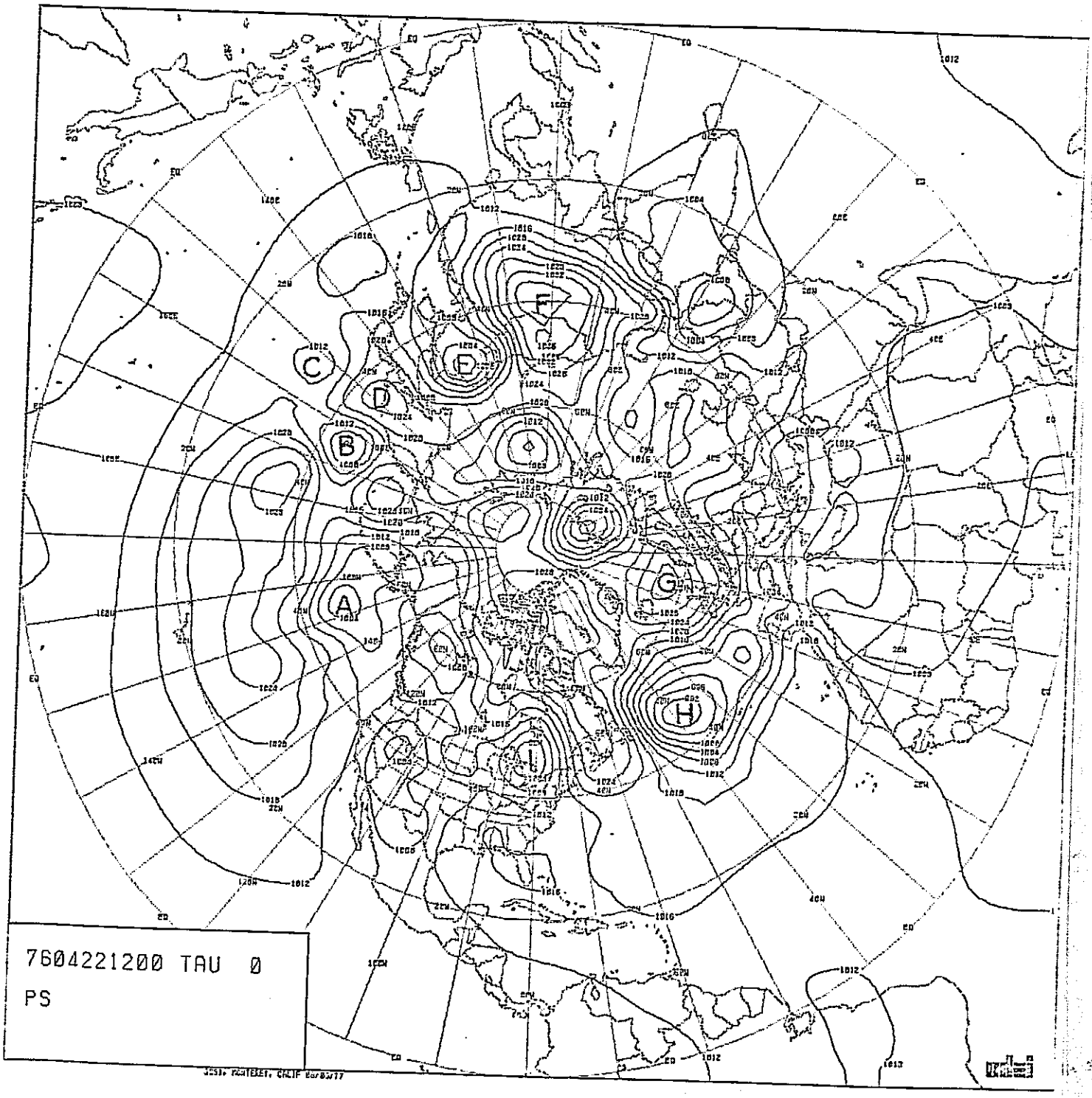

FIGURE III-1: ANALYSIS, SURFACE, 1200z 22 April 1976
(Initial Condition)

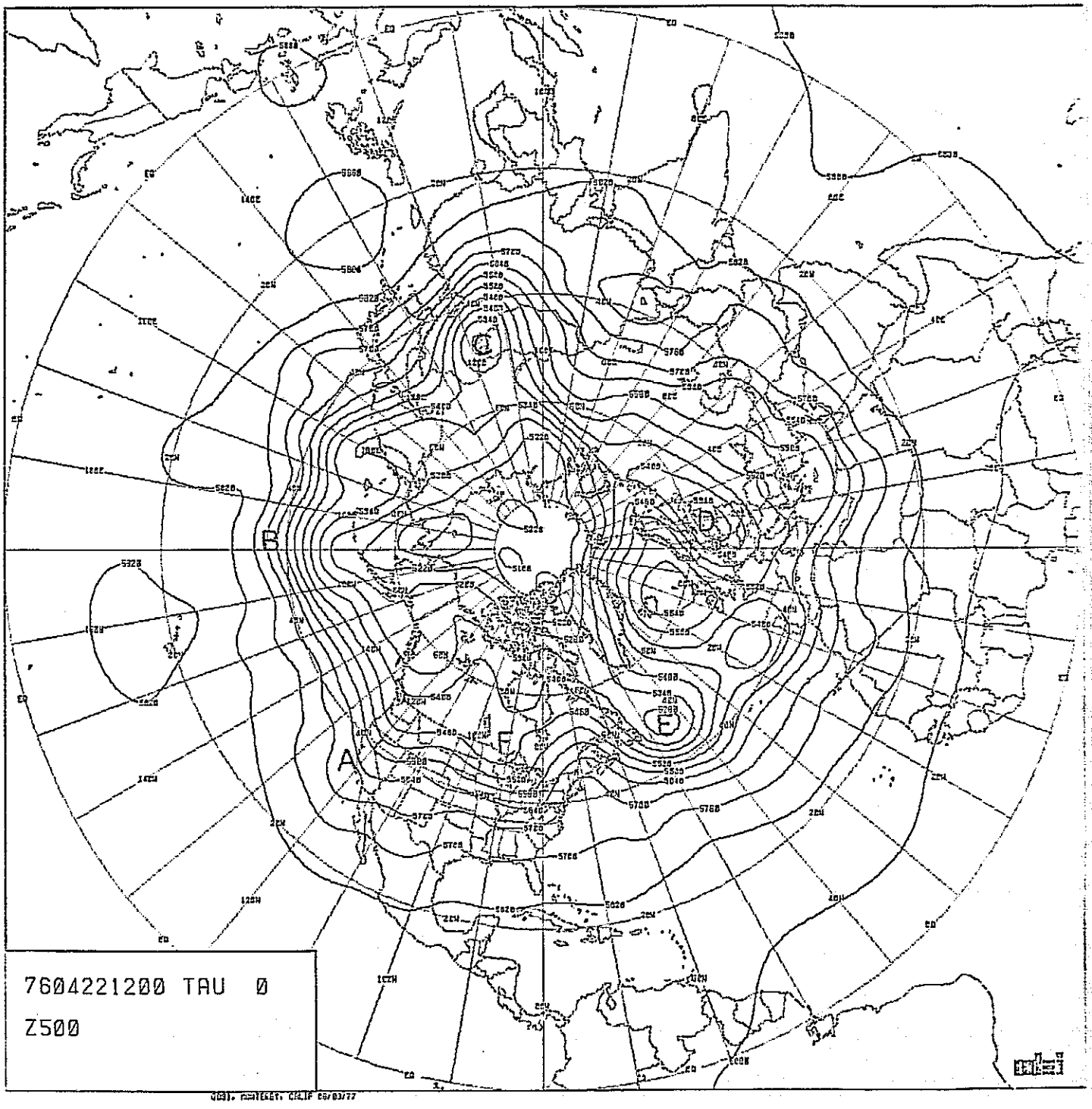

FIGURE III-2: ANALYSIS, 500mb, 1200z 22 April 1976
(Initial Condition)

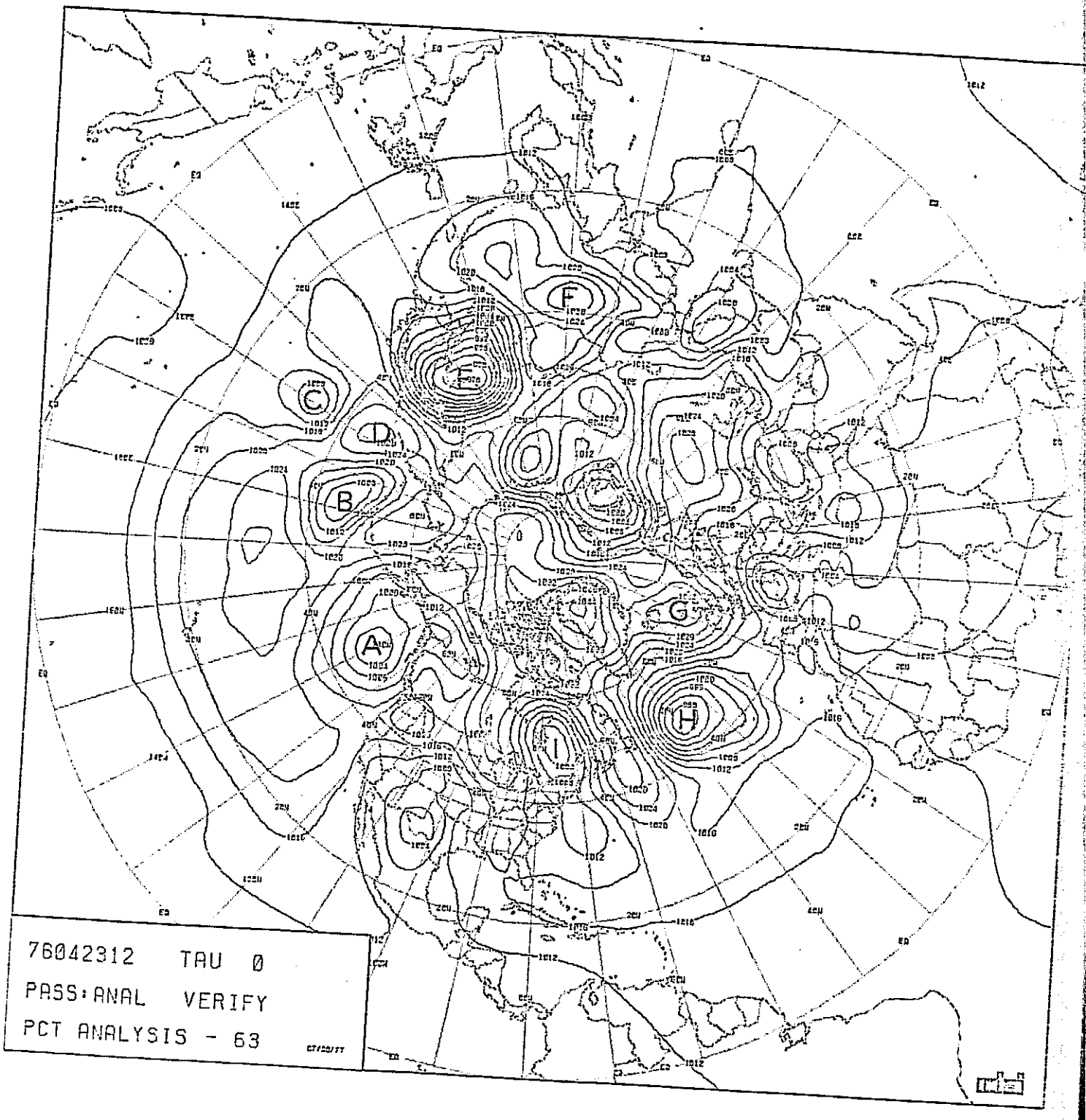

FIGURE III-3: ANALYSIS, SURFACE, 1200z 23 April 1976
(Verification)

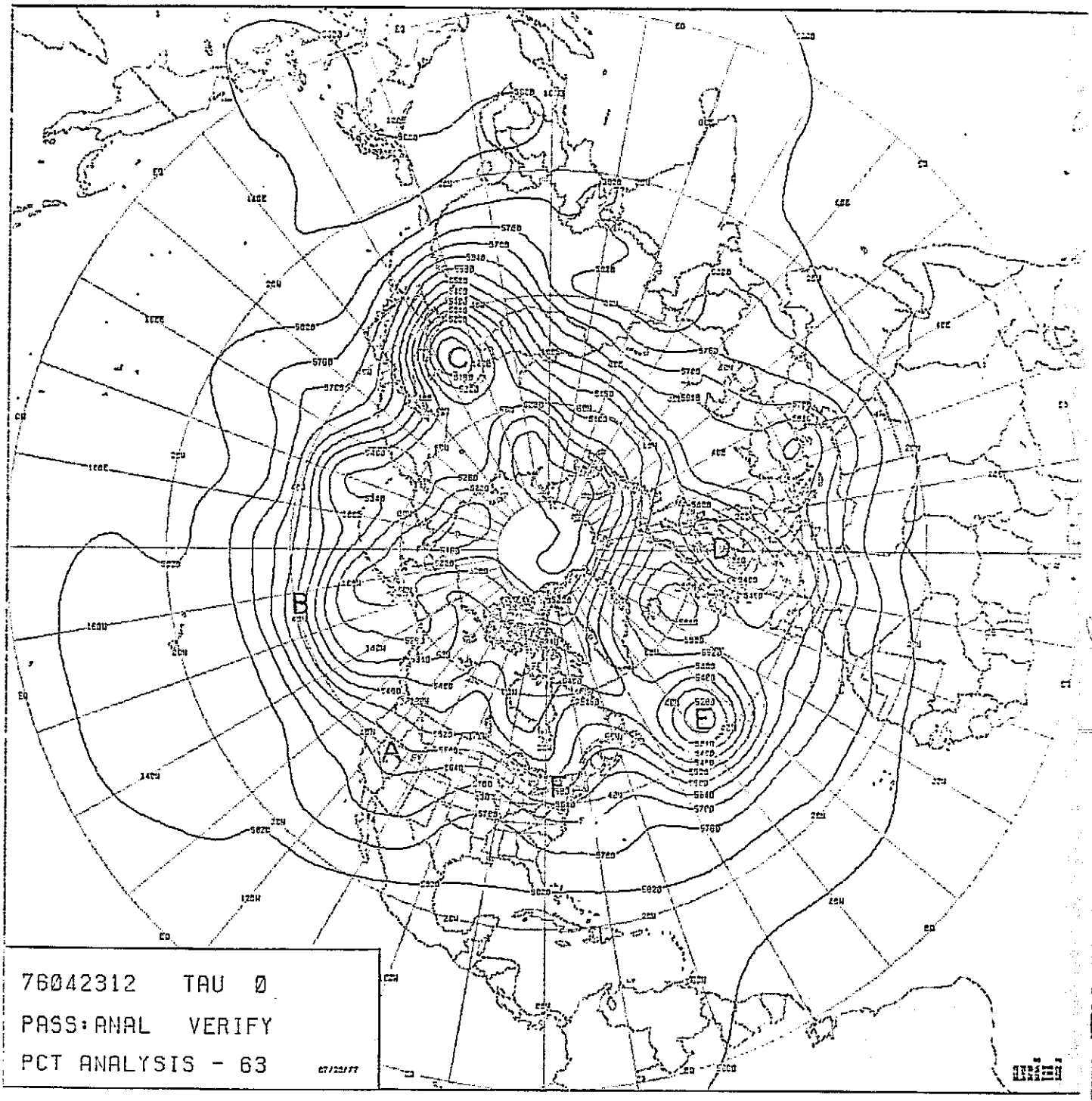

FIGURE III-4: ANALYSIS, 500mb, 1200z 23 April 1976
(Verification)

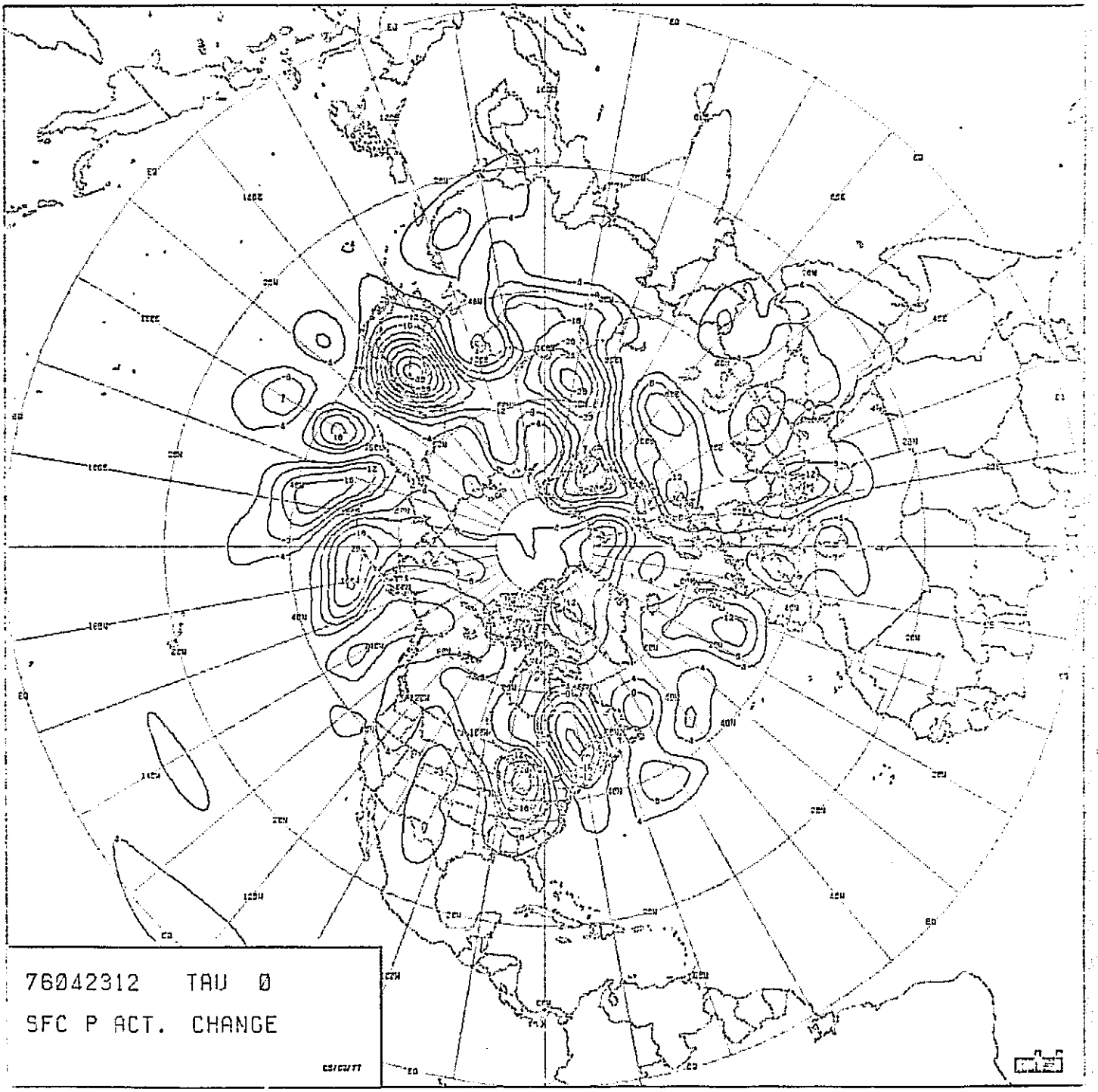

FIGURE III-5: ACTUAL CHANGE, 24-HOUR PERIOD, SURFACE
(4mb Interval)

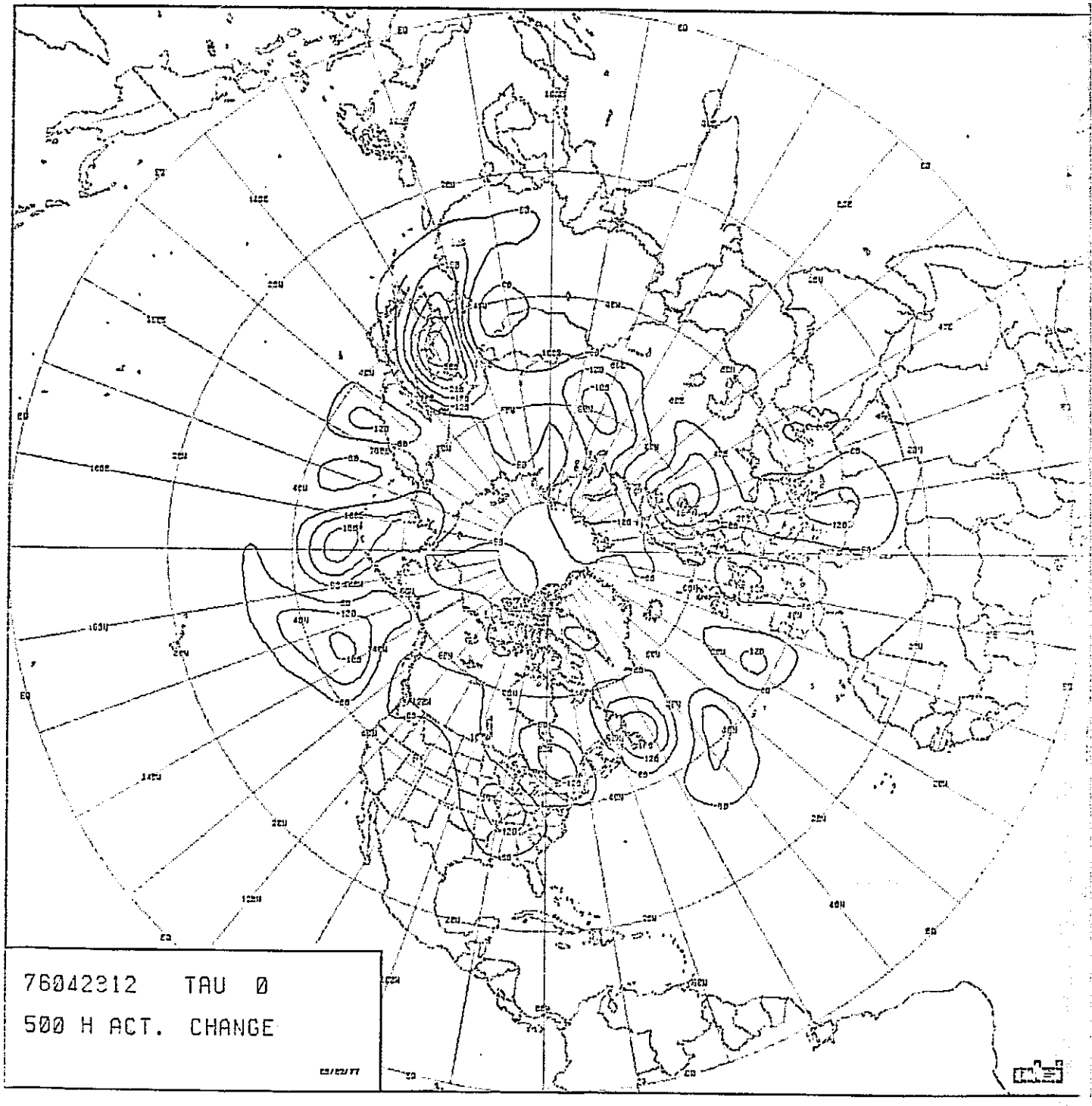

FIGURE III-6: ACTUAL CHANGE, 24-HOUR PERIOD, 500mb
(60M Interval)

TABLE III-1: SURFACE PATTERN HISTORY 1200Z 22 APRIL 1976 to 1200Z 23 APRIL 1976.

LABEL	TYPE	INITIAL PRESSURE (MB)	INITIAL LOCATION	VERIFY PRESSURE (MB)	VERIFY LOCATION
A	Low	1004	48N 154W	1004	48N 140W
B	Low	1004	45N 164E	1004	48N 176W
C	Low	1012	32N 153E	1004	34N 159E
D	High	1024	45N 148E	1028	46N 158E
E	Low	1000	44N 125E	976	49N 129E
F	High	1036	40N 103E	1028	37N 100E
G	High	1032	63N 5W	1032	61N 10W
H	Low	992	46N 38W	988	47N 37W
I	Low	1004	47N 82W	1004	51N 77W (split, low forming off Cape Hatteras)

TABLE III-2: 500 MB PATTERN HISTORY 1200Z 22 APRIL 1976 to 1200Z 23 APRIL 1976.

LABEL	TYPE	INITIAL HT (M)	INITIAL LOCATION	FINAL HT (M) OR COMMENT	FINAL LOCATION
A	Trough	-	along 118W	slightly weaker	along 114W
B	Trough	-	along 170W	low from Aleutians	along 155W
C	Low	5280	48N 117W	5160	48N 126W
D	Low	5340	57N 19E	5340	55N 10E
E	Low	5280	48N 46W	5280	45N 36W
F	Trough	-	Wisconsin to North Carolina	-	L. Erie to SE US Coast

TABLE III-3: 1200Z 22 APRIL 1976 TO 1200Z 23 APRIL 1976 24-HOUR CHANGE STATISTICS.

SURFACE

FROM	TO	RMS	SD	MEAN	MAX	MIN
0	10	.141E+01	.117E+01	.791E+00	.499E+01	-.242E+01
10	20	.168E+01	.168E+01	-.125E-01	.445E+01	-.455E+01
20	30	.260E+01	.258E+01	.345E+00	.963E+01	-.835E+01
30	40	.515E+01	.515E+01	.409E-02	.161E+02	-.195E+02
40	50	.107E+02	.105E+02	-.200E+01	.210E+02	-.408E+02
50	60	.108E+02	.108E+02	-.375E+00	.210E+02	-.288E+02
60	70	.743E+01	.743E+01	.726E-01	.128E+02	-.240E+02
70	80	.883E+01	.859E+01	.205E+01	.144E+02	-.234E+02
80	90	.614E+01	.373E+01	.487E+01	.120E+02	-.623E+01
0	90	.514E+01	.514E+01	.179E+00	.210E+02	-.408E+02

500 MB

FROM	TO	RMS	SD	MEAN	MAX	MIN
0	10	.157E+02	.119E+02	.103E+02	.439E+02	-.292E+02
10	20	.211E+02	.206E+02	.462E+01	.558E+02	-.423E+02
20	30	.298E+02	.297E+02	-.112E+01	.113E+03	-.152E+03
30	40	.661E+02	.655E+02	-.861E+01	.150E+03	-.315E+03
40	50	.101E+03	.101E+03	-.546E+01	.207E+03	-.381E+03
50	60	.912E+02	.910E+02	.559E+01	.218E+03	-.258E+03
60	70	.715E+02	.715E+02	.212E+01	.193E+03	-.188E+03
70	80	.717E+02	.713E+02	-.765E+01	.120E+03	-.145E+03
80	90	.625E+02	.618E+02	-.894E+01	.114E+03	-.109E+03
0	90	.503E+02	.503E+02	.260E+01	.218E+03	-.381E+03

IV. EVALUATION OF FORECASTS

A. General

The run identified as SF3 (see Figures IV-1 and IV-2) is the baseline version of the model for this study. That is, all of the engineering devices and coefficients were set to their generally accepted operational values. The other runs in the study are compared to this version as well as the verification analysis (error charts) and in some cases to each other.

Analyzing the performance of SF3 in detail and with the aid of its error charts, Figures IV-3 and IV-4, it is seen that the following characteristics were demonstrated by the model:

Surface - Low A moved too slowly and deepened in place for an error of 12 mb. Low B showed good movement but was a bit too slow for an error of 8 mb. Most of the development and movement of low C was picked up but it tended to erode the mid-Pacific high too rapidly for an error of 10 mb at about 170E.

The model performed very well in predicting the deepening and movement of low E. Due to the tight gradient of the low and slightly too much eastward extension, a relatively

minor error of about 10 mbs was produced. This compares favorably with the actual change of 40 mb in this area.

The forecast position, intensity and central pressure of low H were excellent and resulted in almost no error.

The forecast status of low I was also excellent and included the low development east of Cape Hatteras.

500 MB - Figure IV-4 shows little error of greater than 30M except for the following:

In the Gulf of Alaska, the model developed the strong westerly flow into a slight ridge rather than a weak trough in advance of the approaching low which resulted in the largest error of 150+M. This error was very close to the actual 24-hour change of 180M.

The intensity and deepening of the western Asian low were excellent. There was, however, a bit too much eastward extension of the low circulation (reflected at the surface) which lead to a 90M error. This was an excellent forecast in an area of a 381M actual change.

The model attempted to develop a weak low north of Thailand for an error of 120M.

The error summary for SF3, Table IV-1, shows the largest error at the surface to be 12.7 mb and 163M at 500 mb.

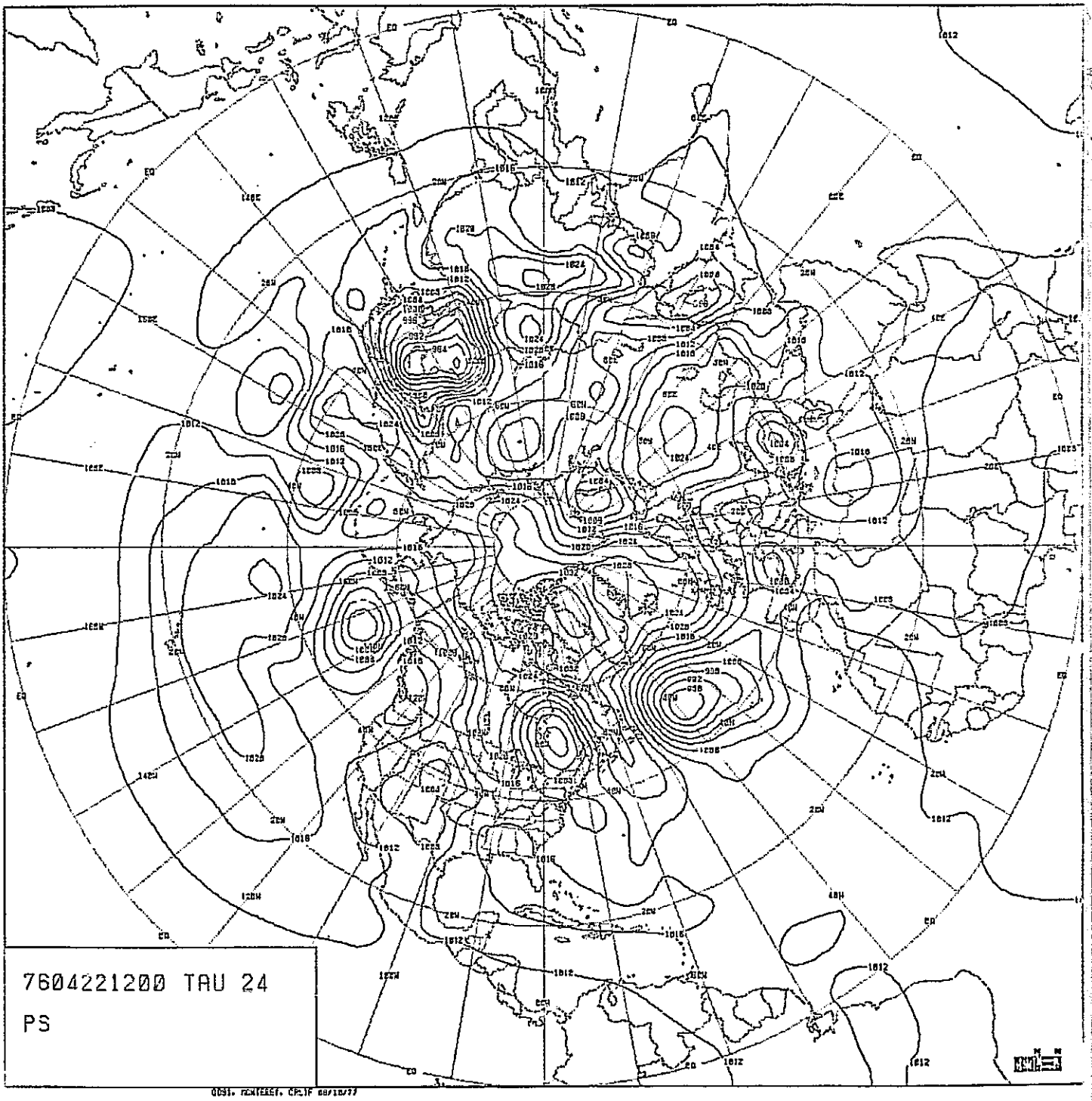

FIGURE IV-1: FORECAST, SURFACE, SF 3 (Baseline)

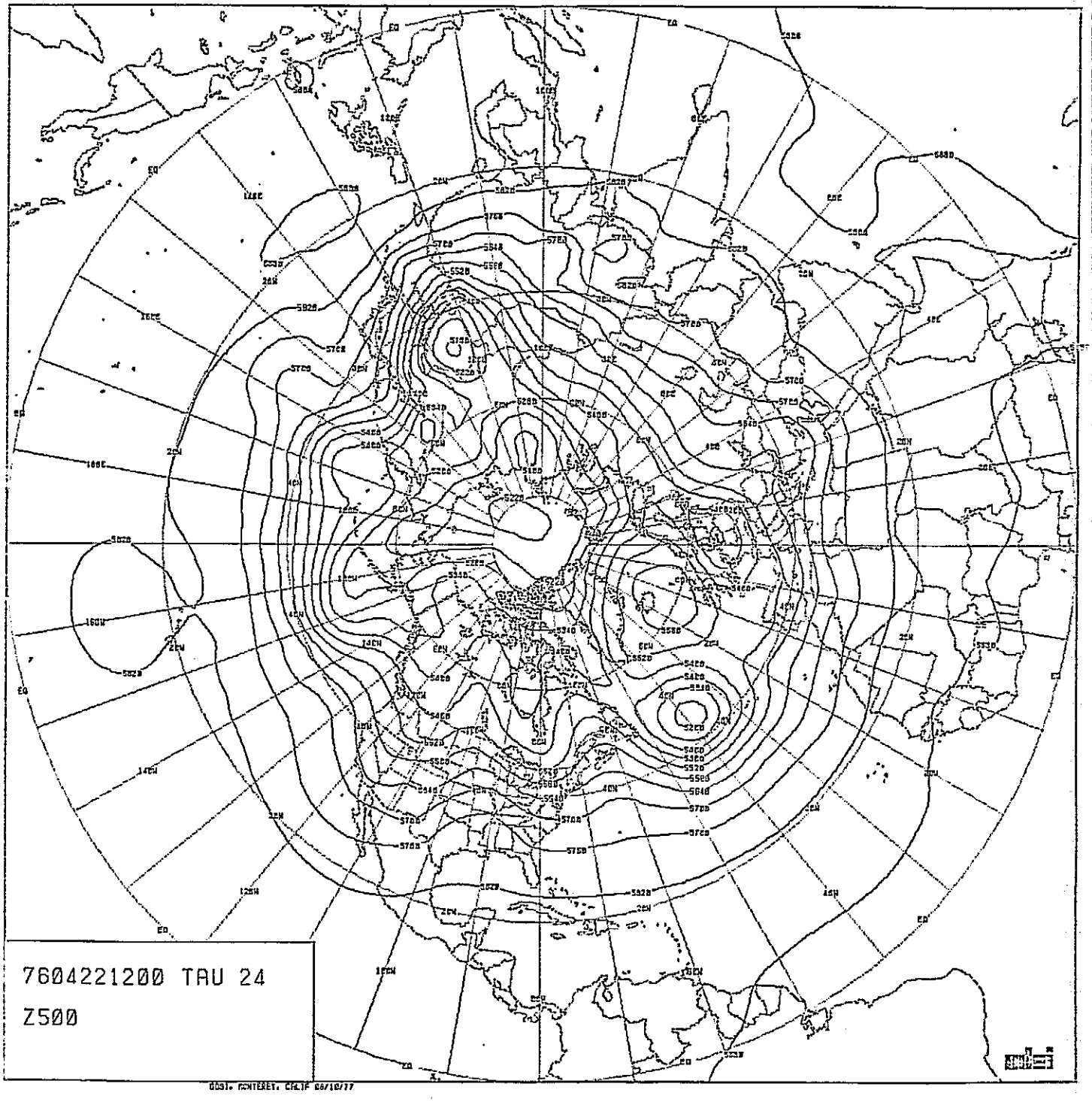

FIGURE IV-2: FORECAST, 500mb, SF3 (Baseline)

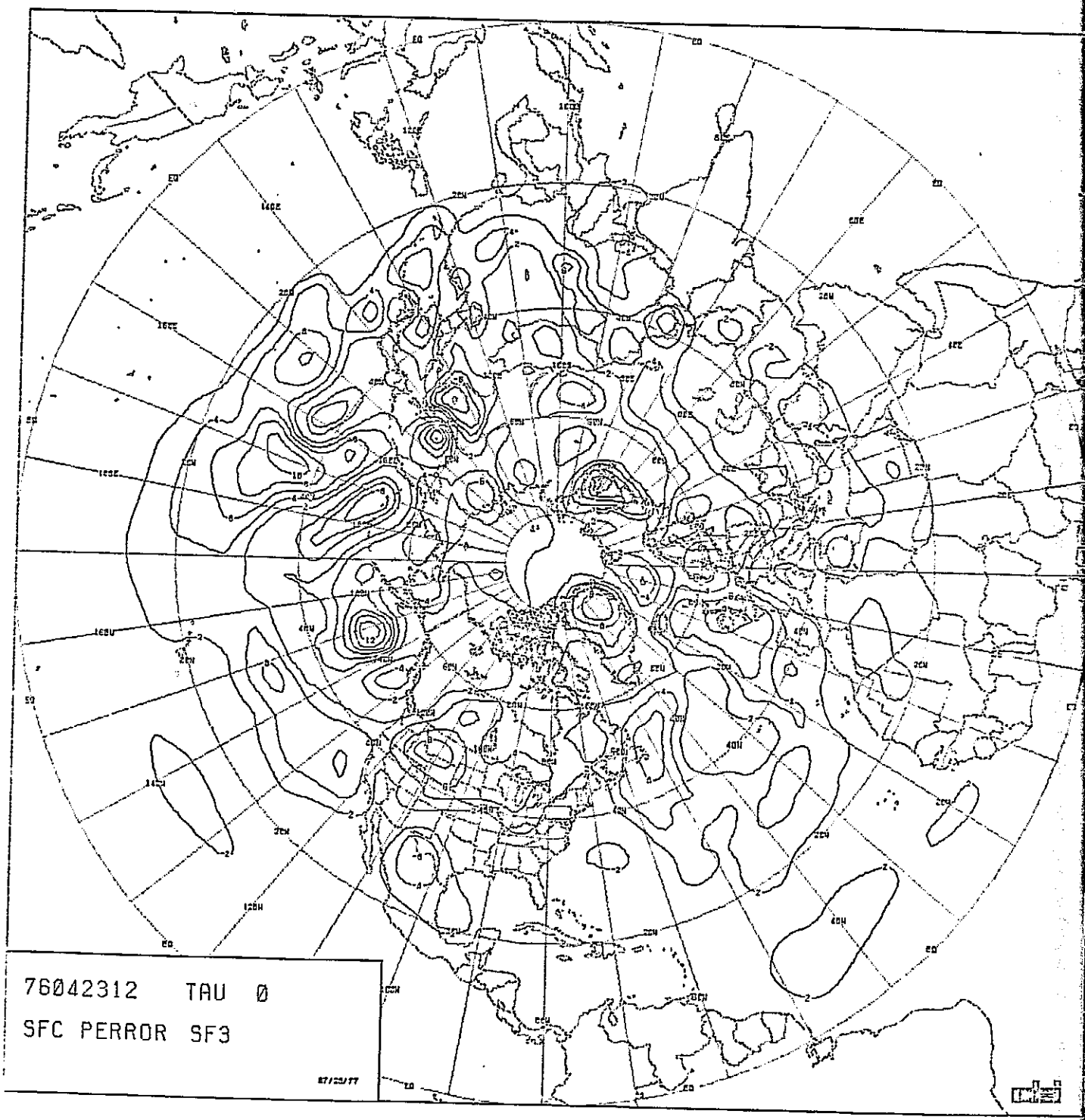

FIGURE IV-3: ERROR PATTERN, SURFACE, SF3

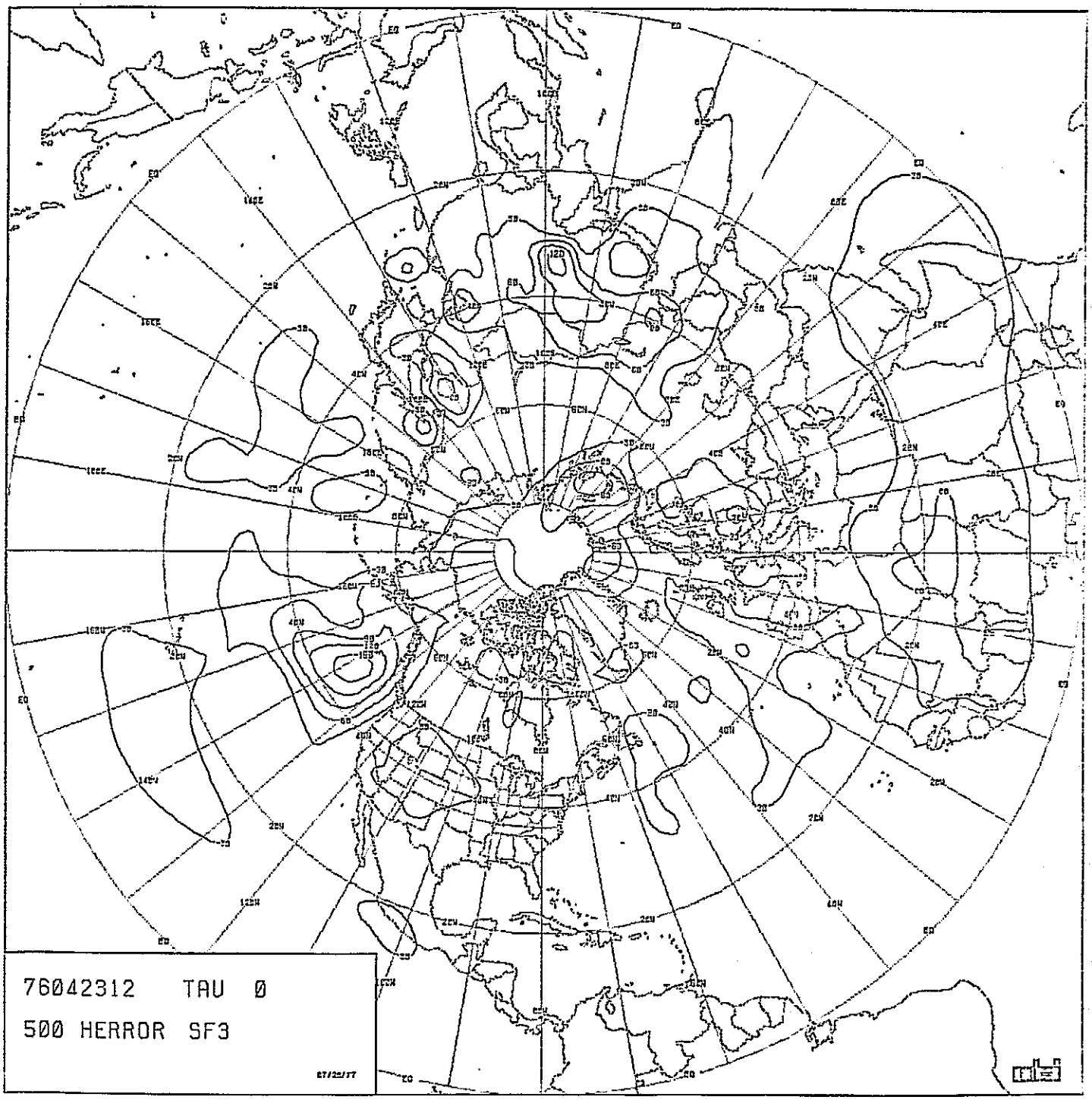

FIGURE IV-4: ERROR PATTERN, 500mb, SF3

TABLE IV-1: ERROR STATISTICAL SUMMARY,
SF3 (BASELINE RUN).

SURFACE

FROM	TO	RMS	SD	MEAN	MAX	MIN
0	10	.710E+00	.672E+00	.230E+00	.242E+01	-.155E+01
10	20	.116E+01	.116E+01	.185E-01	.412E+01	-.282E+01
20	30	.292E+01	.279E+01	.860E+00	.926E+01	-.582E+01
30	40	.339E+01	.304E+01	.150E+01	.112E+02	-.587E+01
40	50	.380E+01	.321E+01	.204E+01	.127E+02	-.774E+01
50	60	.434E+01	.348E+01	.260E+01	.122E+02	-.101E+02
60	70	.332E+01	.275E+01	.185E+01	.775E+01	-.725E+01
70	80	.373E+01	.357E+01	.109E+01	.894E+01	-.900E+01
80	90	.239E+01	.151E+01	.184E+01	.573E+01	-.773E+00
0	90	.250E+01	.236E+01	.819E+00	.127E+02	-.101E+02

500 MB

FROM	TO	RMS	SD	MEAN	MAX	MIN
0	10	.165E+02	.147E+02	.757E+01	.544E+02	-.352E+02
10	20	.266E+02	.247E+02	.991E+01	.623E+02	-.496E+02
20	30	.228E+02	.190E+02	.127E+02	.637E+02	-.423E+02
30	40	.366E+02	.340E+02	.137E+02	.127E+03	-.114E+03
40	50	.478E+02	.476E+02	.428E+01	.112E+03	-.163E+03
50	60	.348E+02	.347E+02	-.283E+01	.777E+02	-.121E+03
60	70	.251E+02	.236E+02	-.876E+01	.538E+02	-.865E+02
70	80	.402E+02	.228E+02	-.331E+02	.911E+01	-.104E+03
80	90	.439E+02	.117E+02	-.423E+02	-.234E+02	-.656E+02
0	90	.285E+02	.277E+02	.665E+01	.127E+03	-.163E+03

B. Variable Momentum Diffusion (SF1)

In this run, the momentum diffusion coefficient was varied as a function of level as follows:

Level	Coefficient
1	1.0×10^6
2	1.9×10^6
3	2.2×10^6
4	2.2×10^6
5	1.0×10^6

Figure IV-5 shows that the SF1 run closely resembles the baseline at the surface with generally minor differences except for the eastern Asia low. There was better control of the eastward extension of this low, and consequently the error chart, Figure IV-6, shows a far less complex error pattern in this area. Figure IV-7, the difference between SF1 and SF3 at the surface, shows as much as a 10-mb difference here. The statistical summary of SF1, Table IV-2, has an overall lower maximum error at the surface than seen in the baseline, Table IV-1.

The differences at 500 mb are less pronounced than at the surface. Figure IV-8 is the SF1 500 mb forecast, Figure IV-9 is the SF1 forecast error, and Figure IV-10 is the

difference between SF1 and SF3 at 500 mb. The latter two figures show an improved treatment of the east Asia low by SF1. Table IV-2 shows very little departure from the baseline in the overall error statistics at 500 mb.

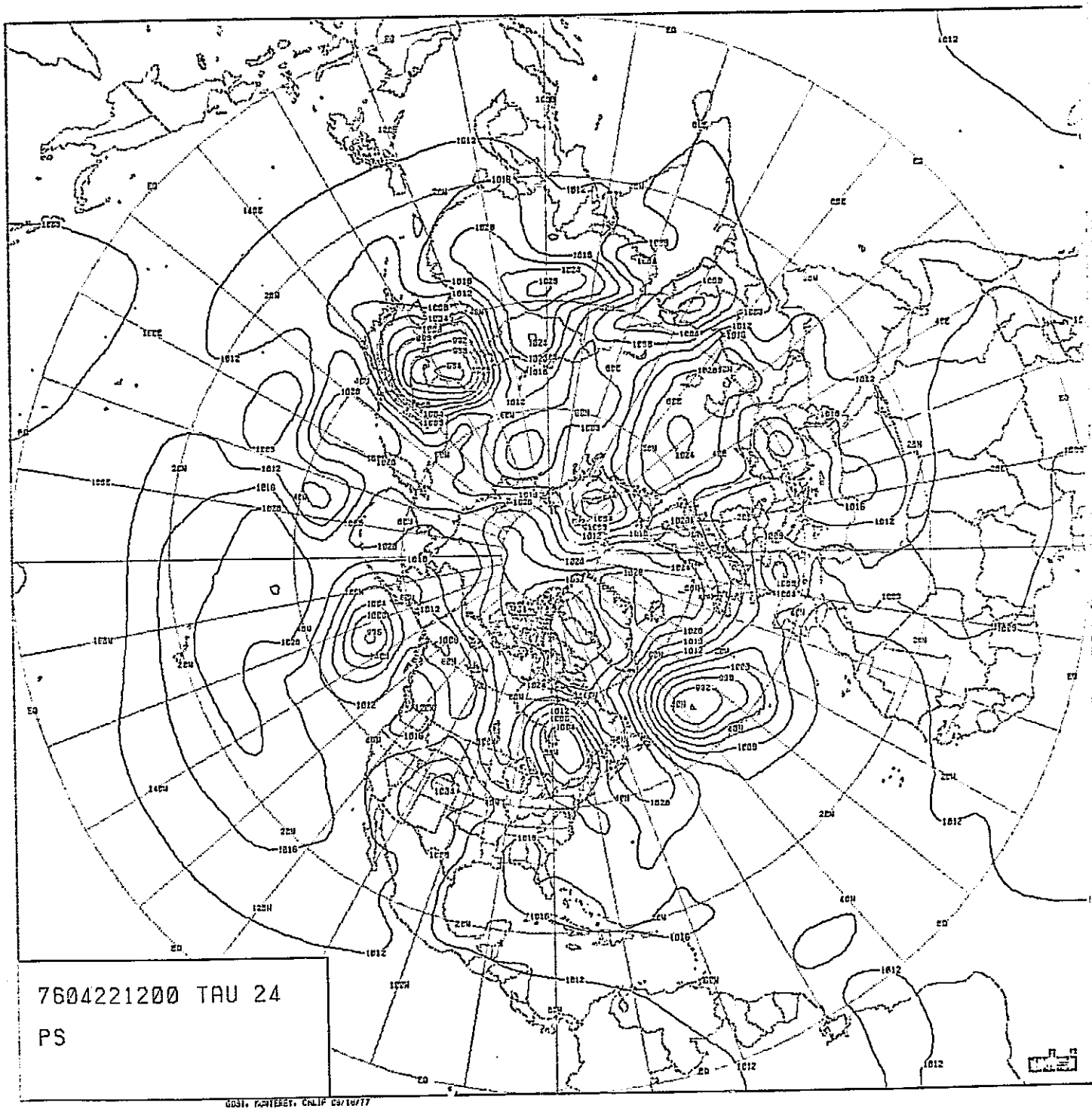

FIGURE IV-5: FORECAST, SURFACE, SF1

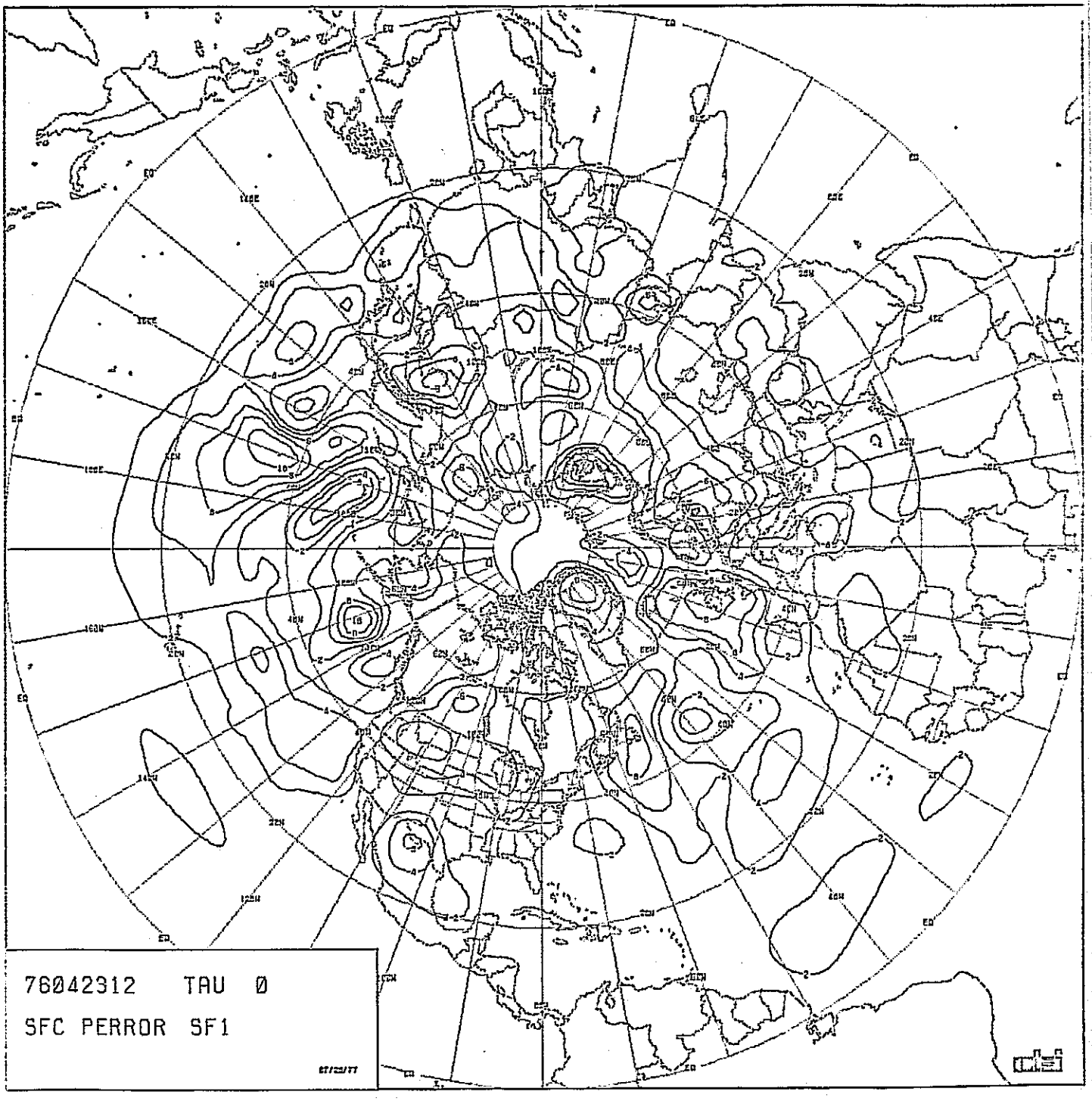

FIGURE IV-6: ERROR PATTERN, SURFACE, SF1

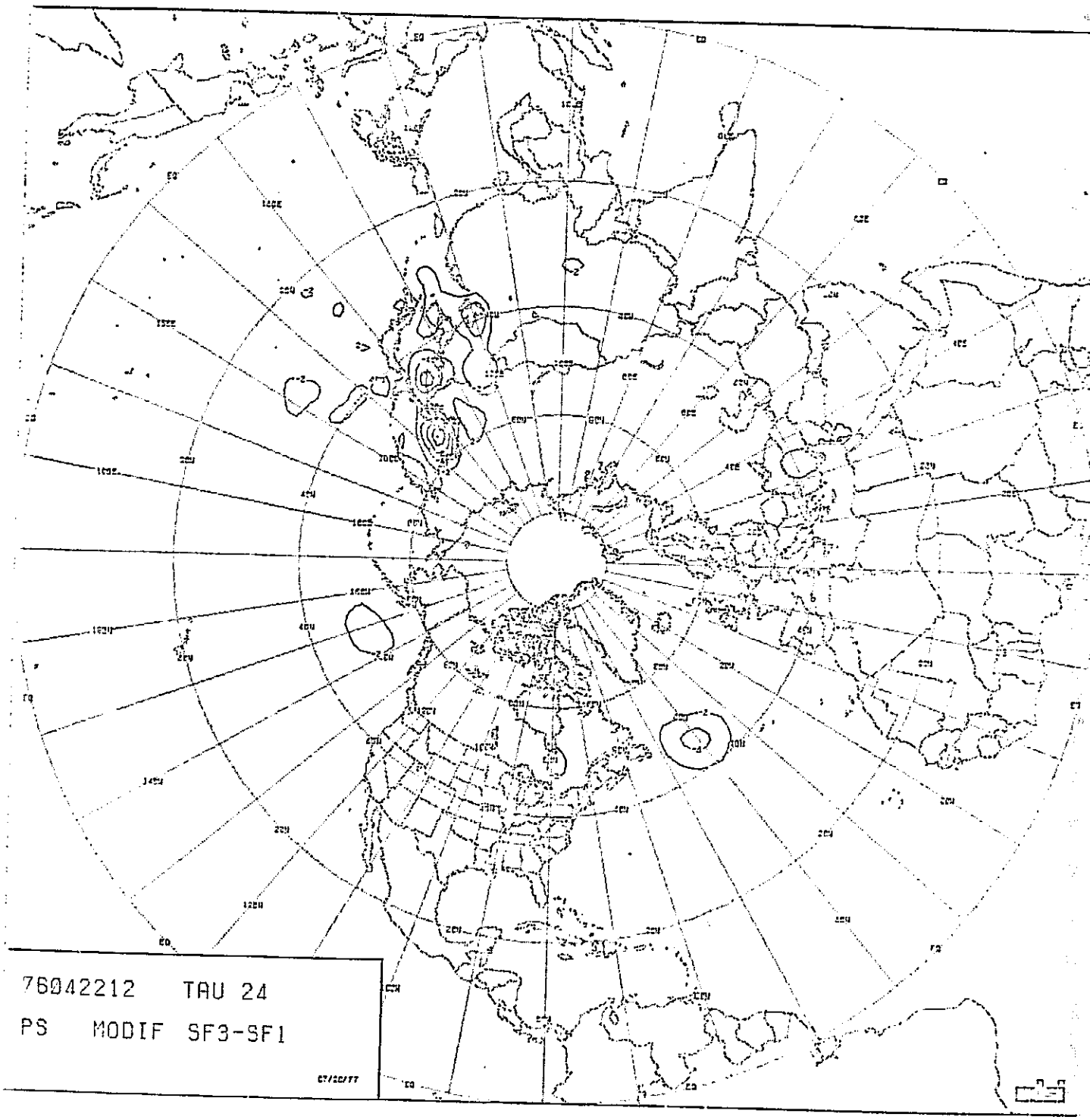

FIGURE IV-7: DIFFERENCE BETWEEN BASELINE AND SF1, SURFACE

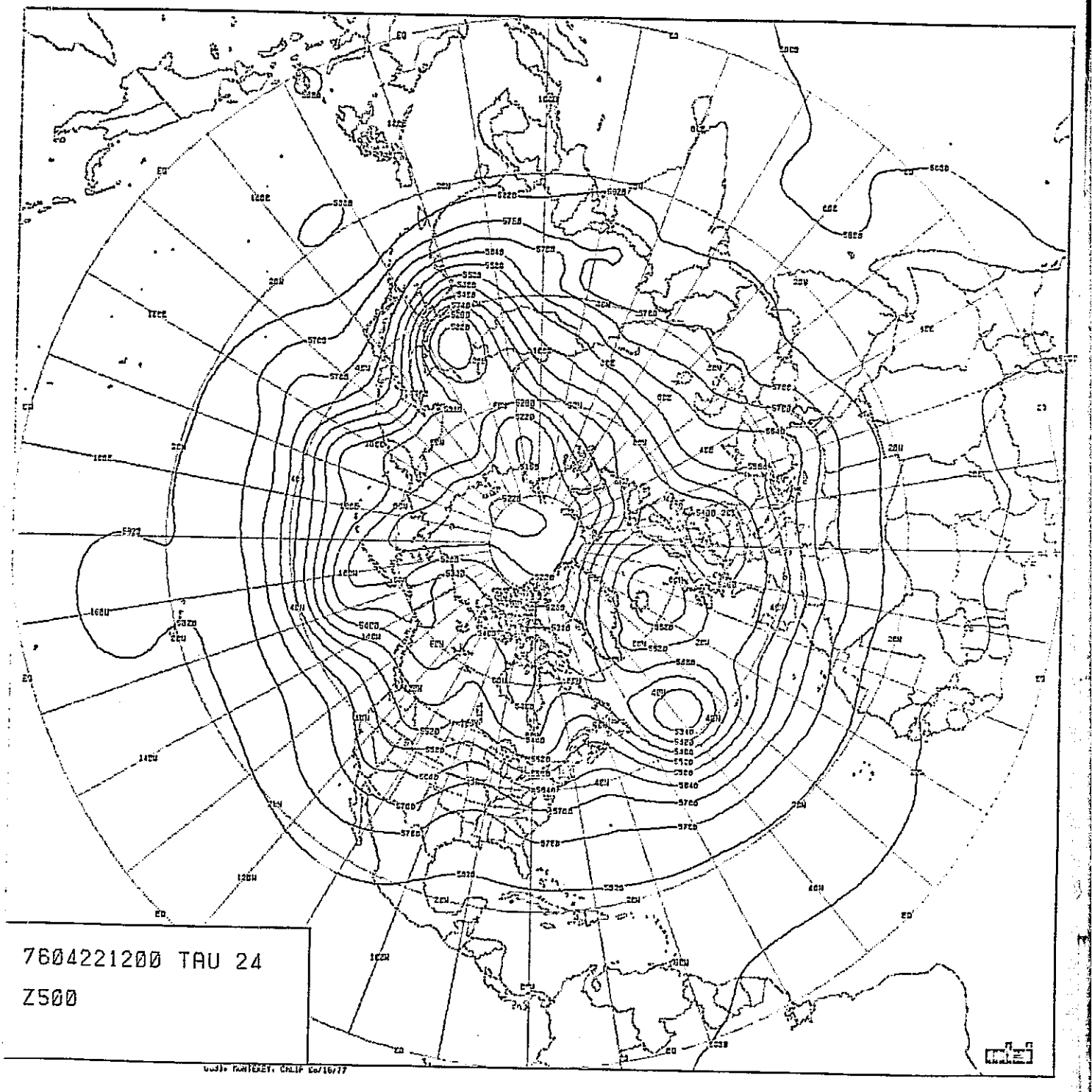

FIGURE IV-8: FORECAST, 500mb, SF1

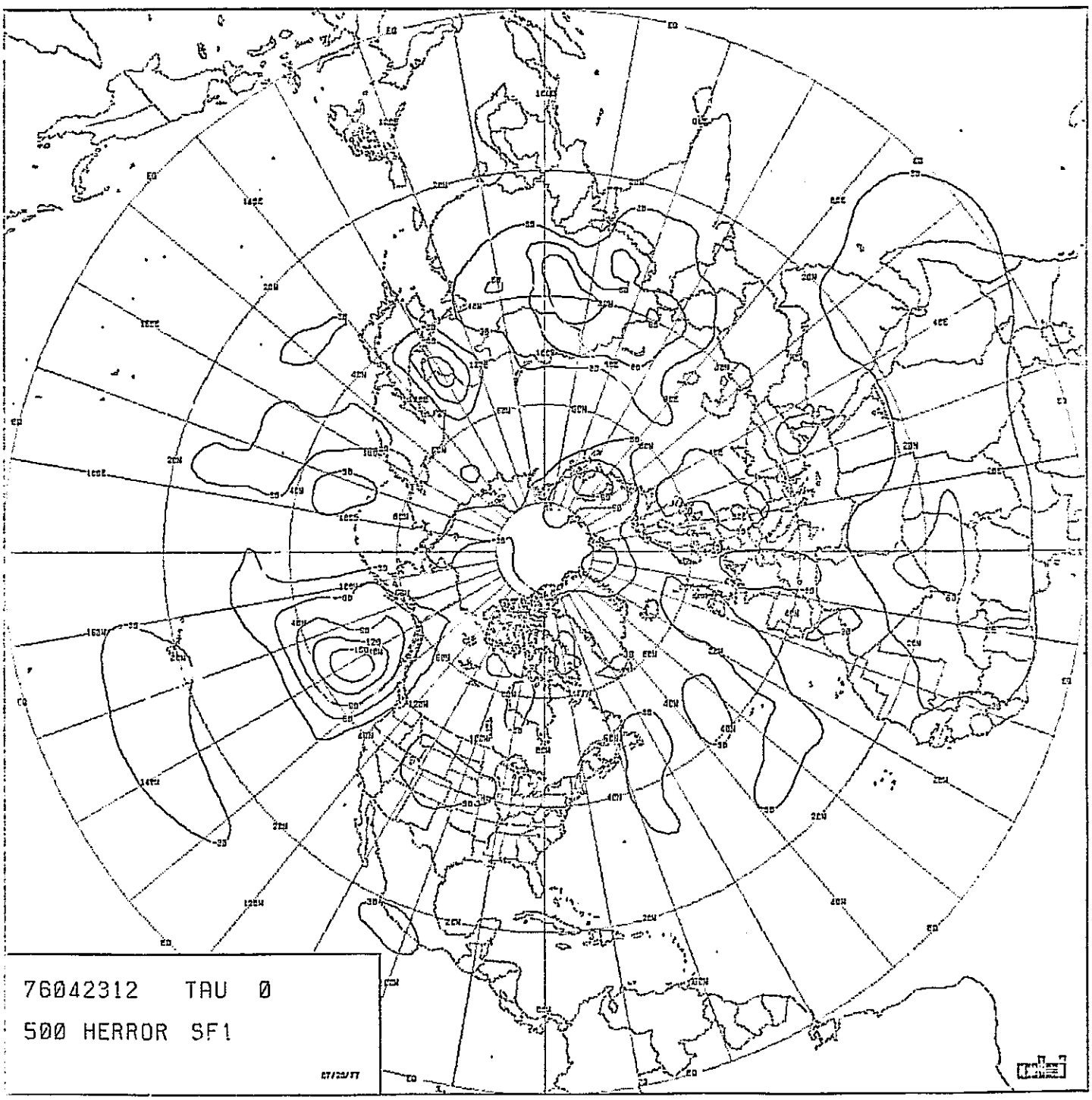

FIGURE IV-9: ERROR PATTERN, 500mb, SF1

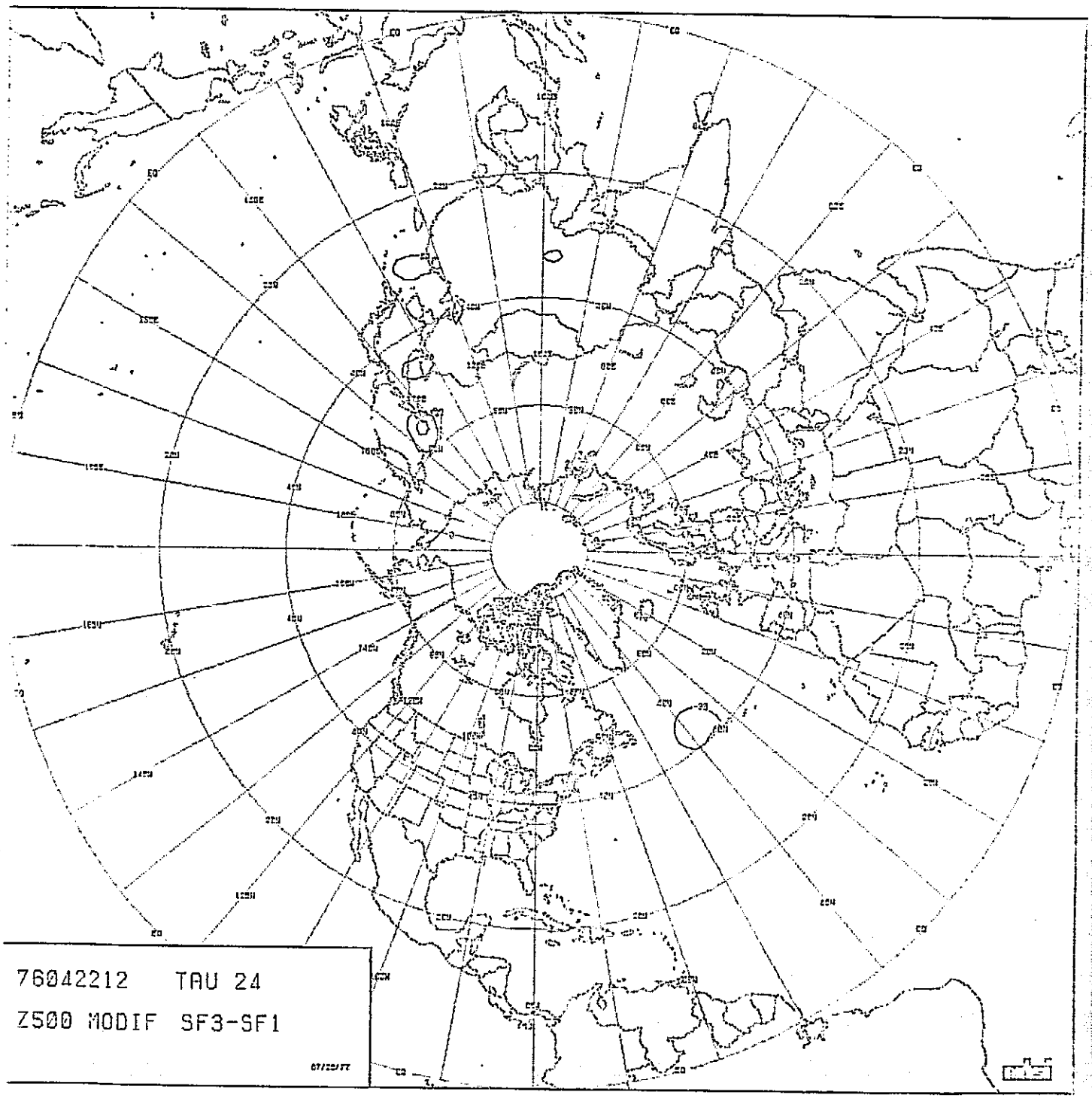

FIGURE IV-10: DIFFERENCE BETWEEN BASELINE AND SF1, 500mb

TABLE IV-2: ERROR STATISTICAL SUMMARY, SF1 (MOMENTUM DIFFUSION COEFFICIENT FUNCTION OF TIME).

SURFACE

FROM	TO	RMS	SD	MEAN	MAX	MIN
0	10	.711E+00	.669E+00	.241E+00	.242E+01	-.156E+01
10	20	.116E+01	.116E+01	.805E-01	.422E+01	-.278E+01
20	30	.293E+01	.270E+01	.847E+00	.969E+01	-.615E+01
30	40	.327E+01	.298E+01	.134E+01	.117E+02	-.584E+01
40	50	.363E+01	.335E+01	.142E+01	.953E+01	-.847E+01
50	60	.395E+01	.321E+01	.229E+01	.963E+01	-.774E+01
60	70	.324E+01	.270E+01	.179E+01	.761E+01	-.748E+01
70	80	.372E+01	.358E+01	.103E+01	.859E+01	-.933E+01
80	90	.233E+01	.159E+01	.171E+01	.534E+01	-.142E+01
0	90	.240E+01	.228E+01	.740E+00	.117E+02	-.933E+01

500 MB

FROM	TO	RMS	SD	MEAN	MAX	MIN
0	10	.166E+02	.147E+02	.766E+01	.539E+02	-.352E+02
10	20	.269E+02	.247E+02	.106E+02	.630E+02	-.497E+02
20	30	.217E+02	.175E+02	.128E+02	.638E+02	-.339E+02
30	40	.355E+02	.332E+02	.125E+02	.114E+03	-.113E+03
40	50	.504E+02	.504E+02	-.238E+00	.113E+03	-.165E+03
50	60	.357E+02	.355E+02	-.367E+01	.626E+02	-.123E+03
60	70	.245E+02	.230E+02	-.848E+01	.492E+02	-.848E+02
70	80	.407E+02	.233E+02	-.334E+02	.725E+01	-.106E+03
80	90	.448E+02	.112E+02	-.434E+02	-.266E+02	-.684E+02
0	90	.288E+02	.281E+02	.627E+01	.114E+03	-.165E+03

C. Momentum Diffusion Coefficient = 10^5 (SF2)

By reducing the momentum diffusion coefficient by one order of magnitude, the importance of this device is seen in the SF2 surface and 500 mb forecasts, Figures IV-11 and IV-12, respectively. Most of the synoptic systems are in about the same locations and have about the same intensities as the baseline case, but considerable instability "noise" has developed. It is likely that this version would become computationally unstable before 72 hours of forecast time.

Systems that appeared to be developing only a little too rapidly on the baseline run are developing much more rapidly on SF2. For example, on the baseline run surface chart, there is a hint of a false extension of the east Asia low to the northeast that lead to an error of about 10 mb. SF2 develops this into a deep, intensive low west of Kamchatka and the main body of the low is split into two distinct centers with southern extensions. At 500 mb, in addition to corresponding incorrect development, the neophyte low north of Cambodia on the baseline has become an intense little low on the SF2.

The corresponding error charts, Figures IV-13 and IV-14, show patterns quite similar to the baseline, except for greatly increased errors in the regions discussed above. In fact,

Figures IV-15 and IV-16 show that the error differences are almost entirely confined to these areas. The statistical summary of SF2, Table IV-3, shows, among other facts, that the size of the maximum errors are about double those of the baseline.

The problem pointed out here as well as the slightly reduced errors in the same areas seen on the SF1 run might suggest more favorable forecasts with a slight increase in the momentum diffusion coefficient to possibly 1.5×10^6 or 2.0×10^6 vice 1.0×10^6.

One should take note of the radical changes in the forecast which can be produced by altering the momentum diffusion coefficient.

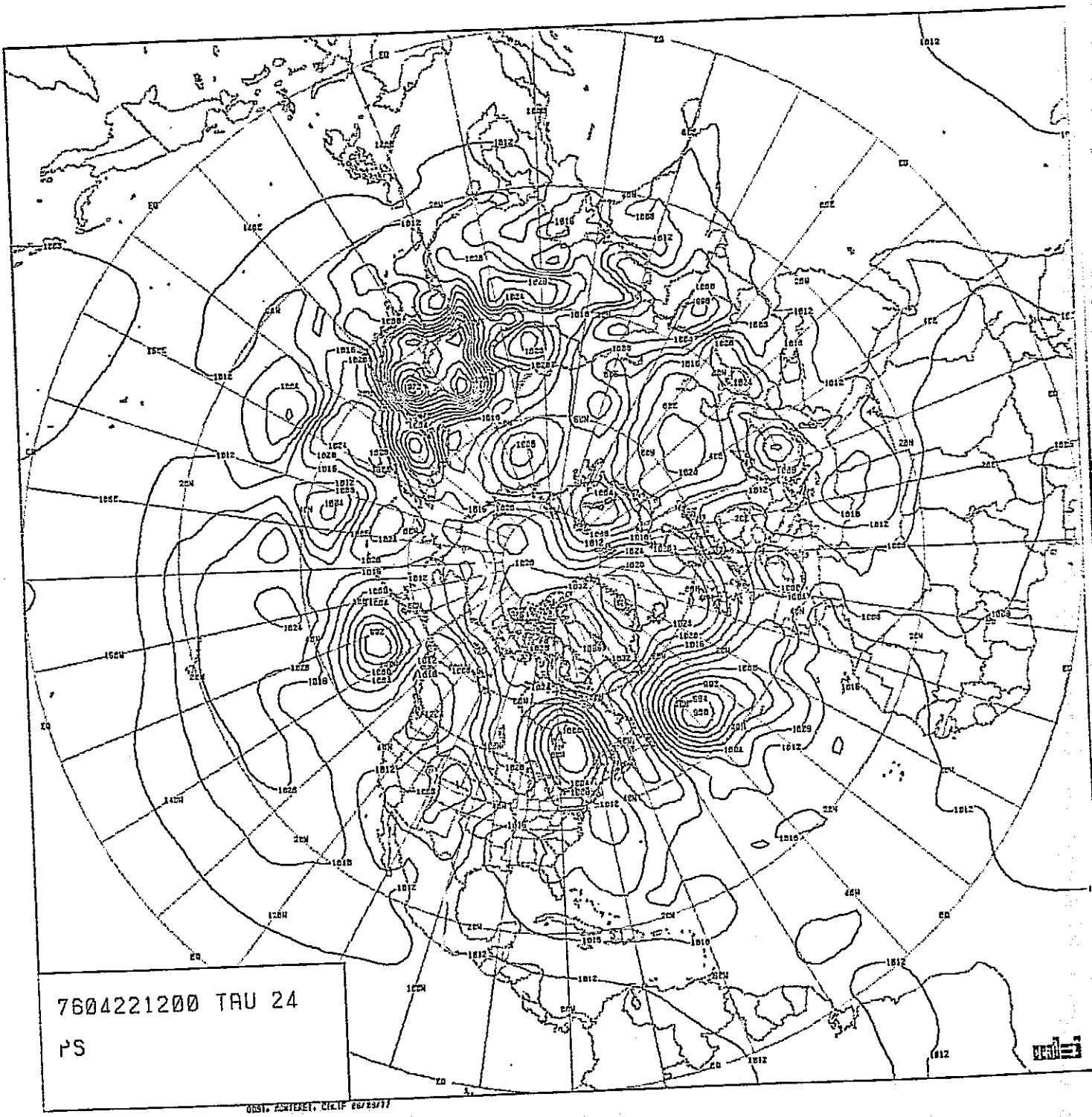

FIGURE IV-11: FORECAST, SURFACE, SF2

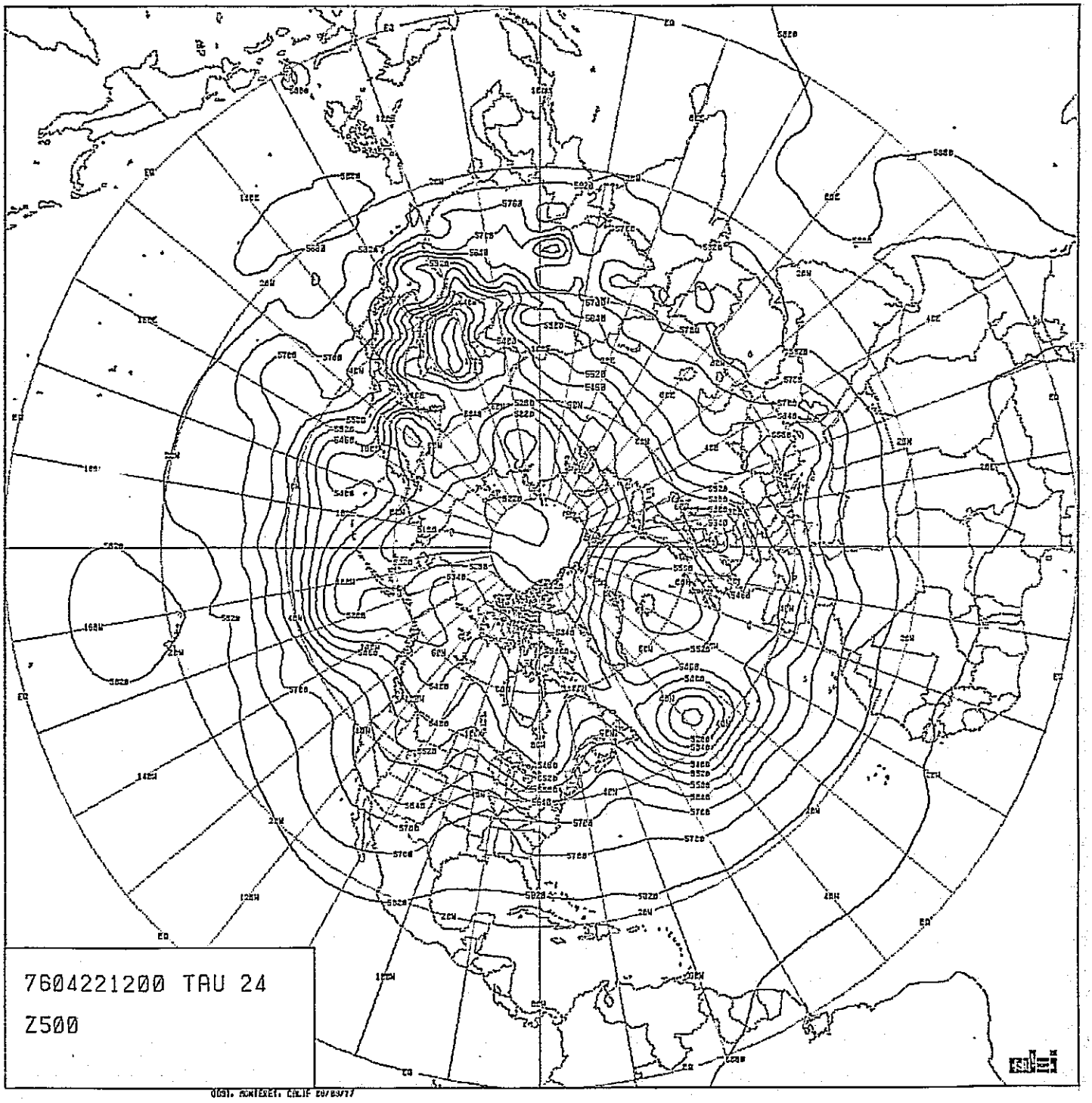

FIGURE IV-12: FORECAST, 500mb, SF2

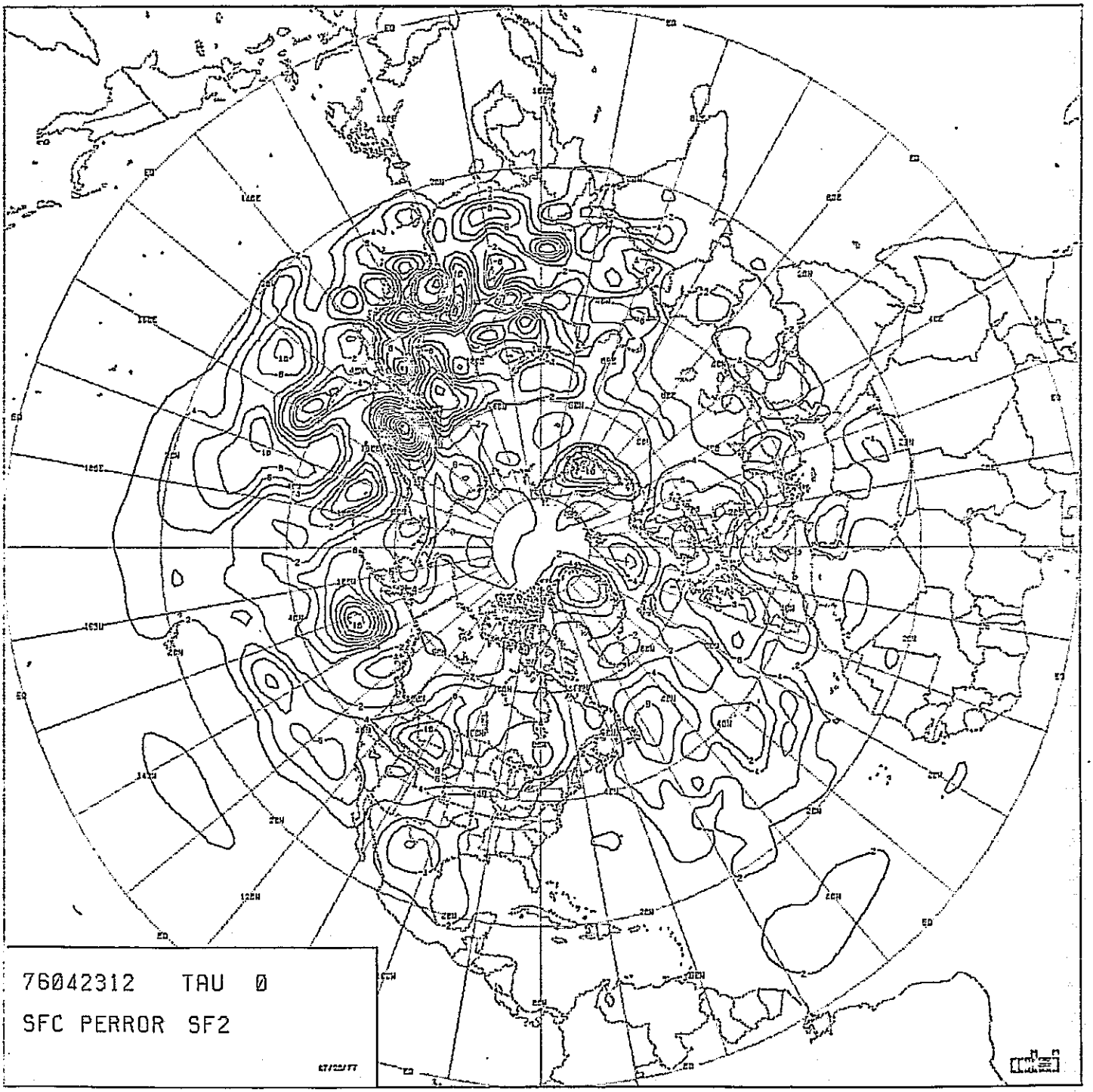

FIGURE IV-13: ERROR PATTERN, SURFACE, SF2

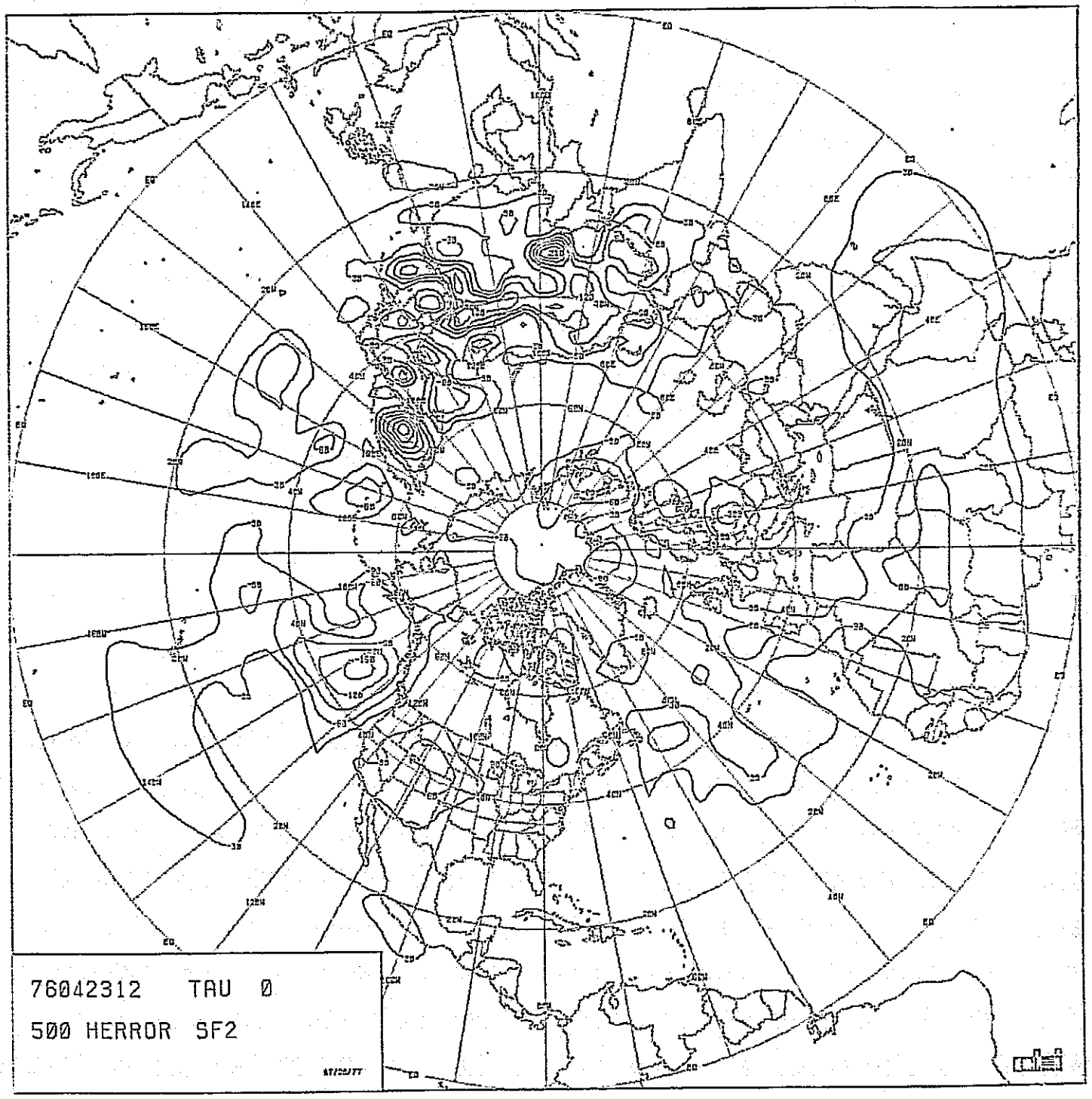

FIGURE IV-14: ERROR PATTERN, 500mb, SF2

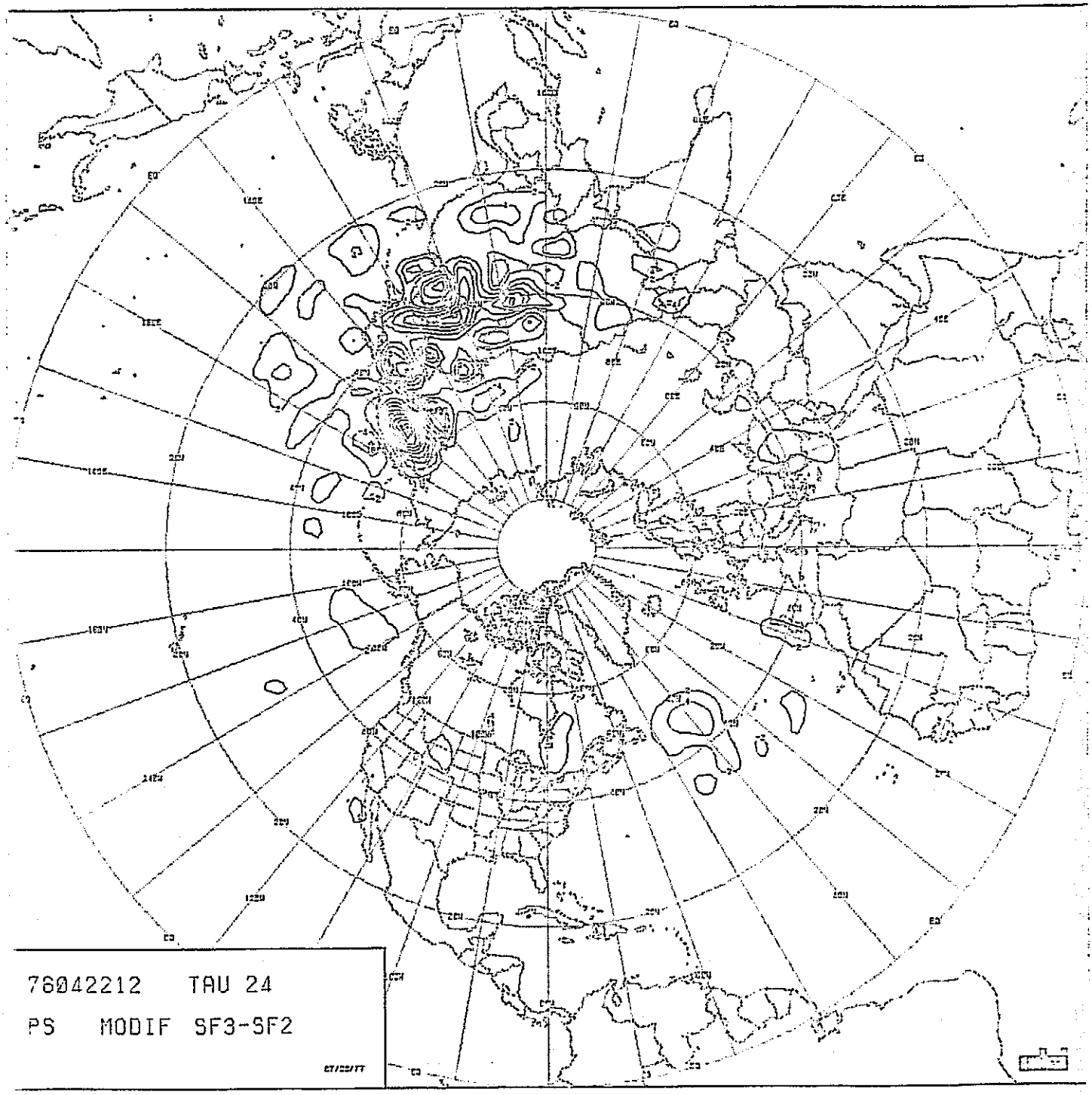

FIGURE IV-15: DIFFERENCE BETWEEN BASELINE AND SF2, SURFACE

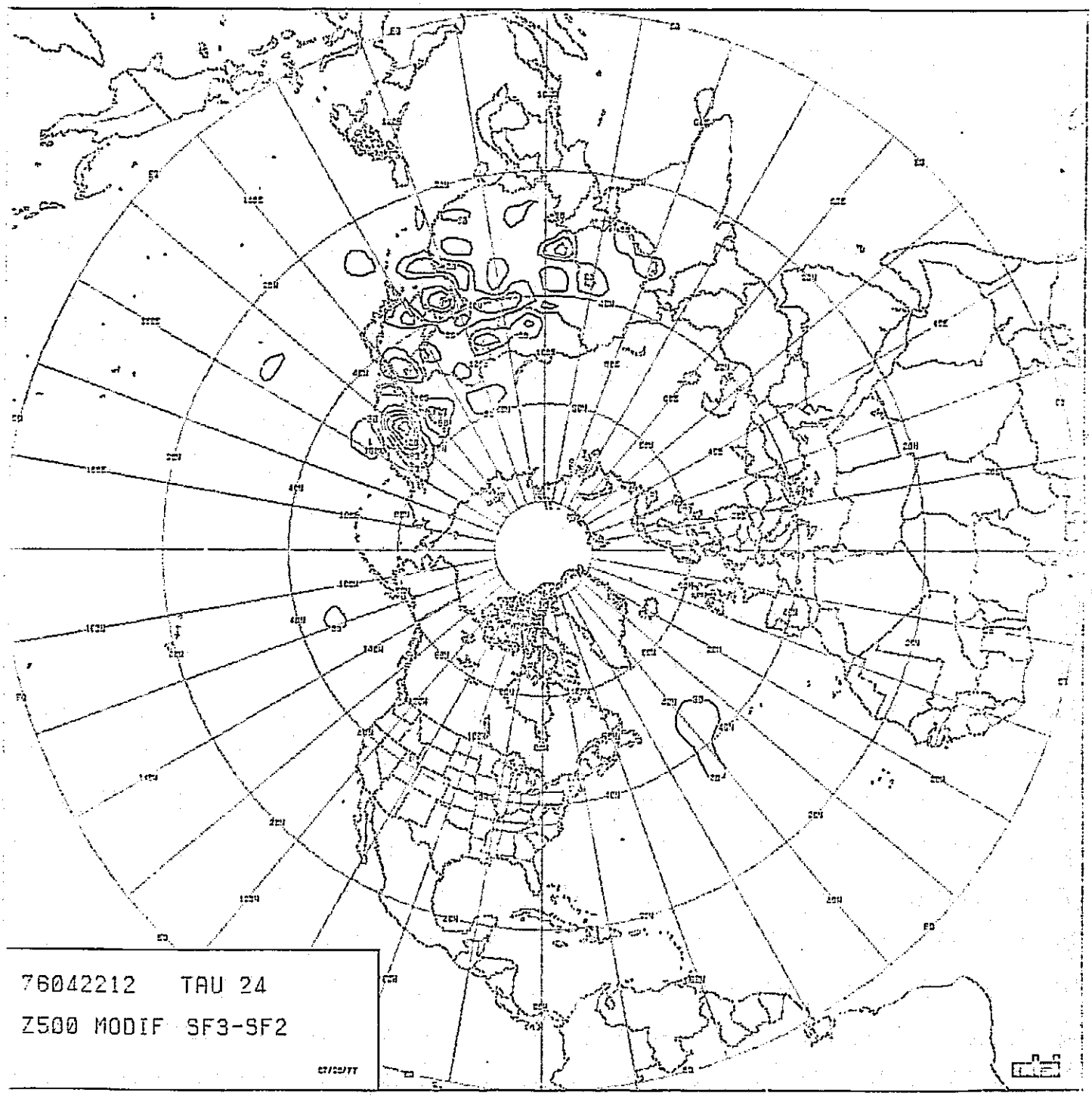

FIGURE IV-16: DIFFERENCE BETWEEN BASELINE AND SF2, 500mb

TABLE IV-3: ERROR STATISTICAL SUMMARY, SF2 (MOMENTUM DIFFUSION COEFFICIENT = 10^5).

SURFACE

FROM	TO	RMS	SD	MEAN	MAX	MIN
0	10	.708E+00	.676E+00	.212E+00	.244E+01	-.154E+01
10	20	.122E+01	.122E+01	-.402E-01	.394E+01	-.291E+01
20	30	.326E+01	.309E+01	.106E+01	.104E+02	-.587E+01
30	40	.426E+01	.383E+01	.186E+01	.158E+02	-.958E+01
40	50	.498E+01	.410E+01	.283E+01	.162E+02	-.993E+01
50	60	.566E+01	.490E+01	.284E+01	.265E+02	-.125E+02
60	70	.357E+01	.301E+01	.193E+01	.849E+01	-.747E+01
70	80	.384E+01	.368E+01	.110E+01	.919E+01	-.689E+01
80	90	.254E+01	.149E+01	.206E+01	.613E+01	-.229E+00
0	90	.302E+01	.287E+01	.959E+00	.265E+02	-.125E+02

500 MB

FROM	TO	RMS	SD	MEAN	MAX	MIN
0	10	.164E+02	.146E+02	.741E+01	.557E+02	-.352E+02
10	20	.268E+02	.252E+02	.912E+01	.631E+02	-.490E+02
20	30	.276E+02	.234E+02	.147E+02	.875E+02	-.553E+02
30	40	.444E+02	.414E+02	.162E+02	.214E+03	-.110E+03
40	50	.522E+02	.515E+02	.881E+01	.136E+03	-.157E+03
50	60	.410E+02	.409E+02	-.260E+01	.207E+03	-.117E+03
60	70	.271E+02	.257E+02	-.888E+01	.592E+02	-.898E+02
70	80	.406E+02	.232E+02	-.334E+02	.102E+02	-.105E+03
80	90	.425E+02	.131E+02	-.404E+02	-.191E+02	-.666E+02
0	90	.315E+02	.306E+02	.743E+01	.214E+03	-.157E+03

D. Temperature Diffusion Coefficient = 10^5 (SF4)

An examination of the SF4 surface and 500 mb levels, Figures IV-17 and IV-18, shows only a hint of the noise seen in SF2. The error charts, Figures IV-19 and IV-20, are only modestly different from those for the baseline which is clearly indicated by the lack of major difference centers on Figures IV-21 and IV-22. Table IV-4 shows that the statistical summary for SF4 is not significantly different from that of the baseline.

In general, a reduction of the temperature diffusion coefficient by one order of magnitude did not have an important effect upon this 24-hour forecast. That is not to say that a longer run, a different synoptic situation or a further reduction of the coefficient would not show a deleterious effect upon the forecast.

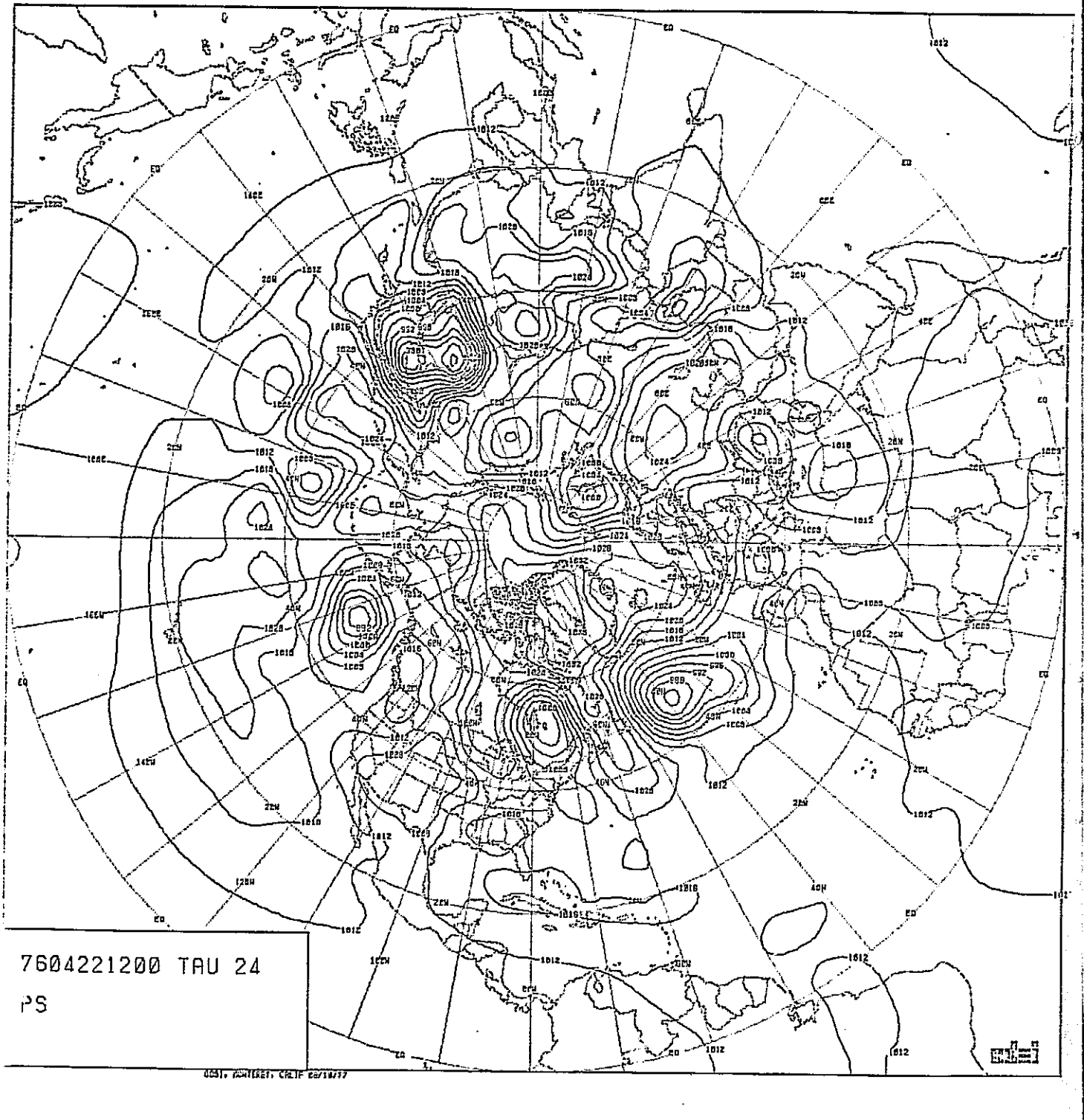

FIGURE IV-17: FORECAST, SURFACE, SF4

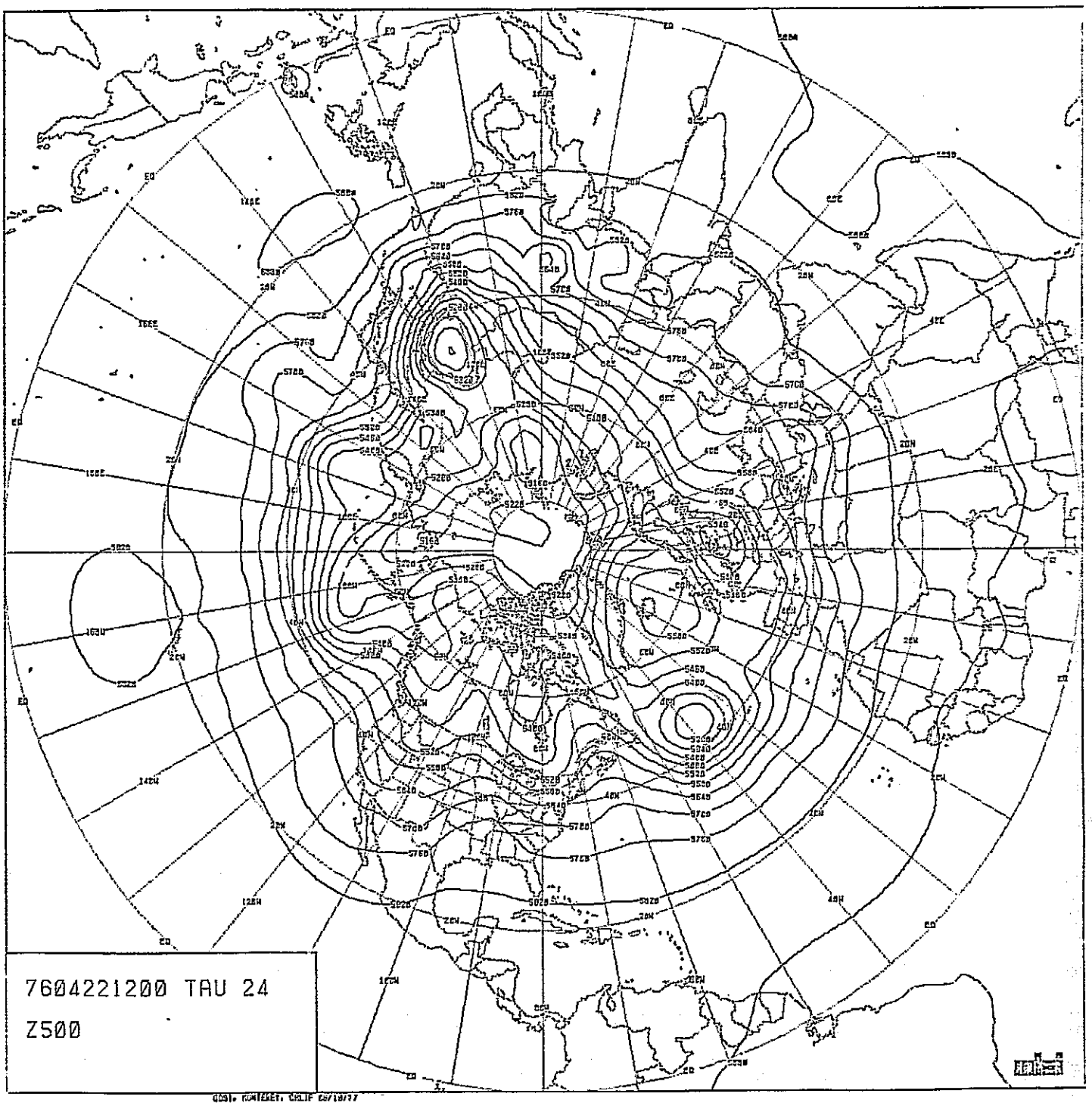

FIGURE IV-18: FORECAST, 500mb, SF4

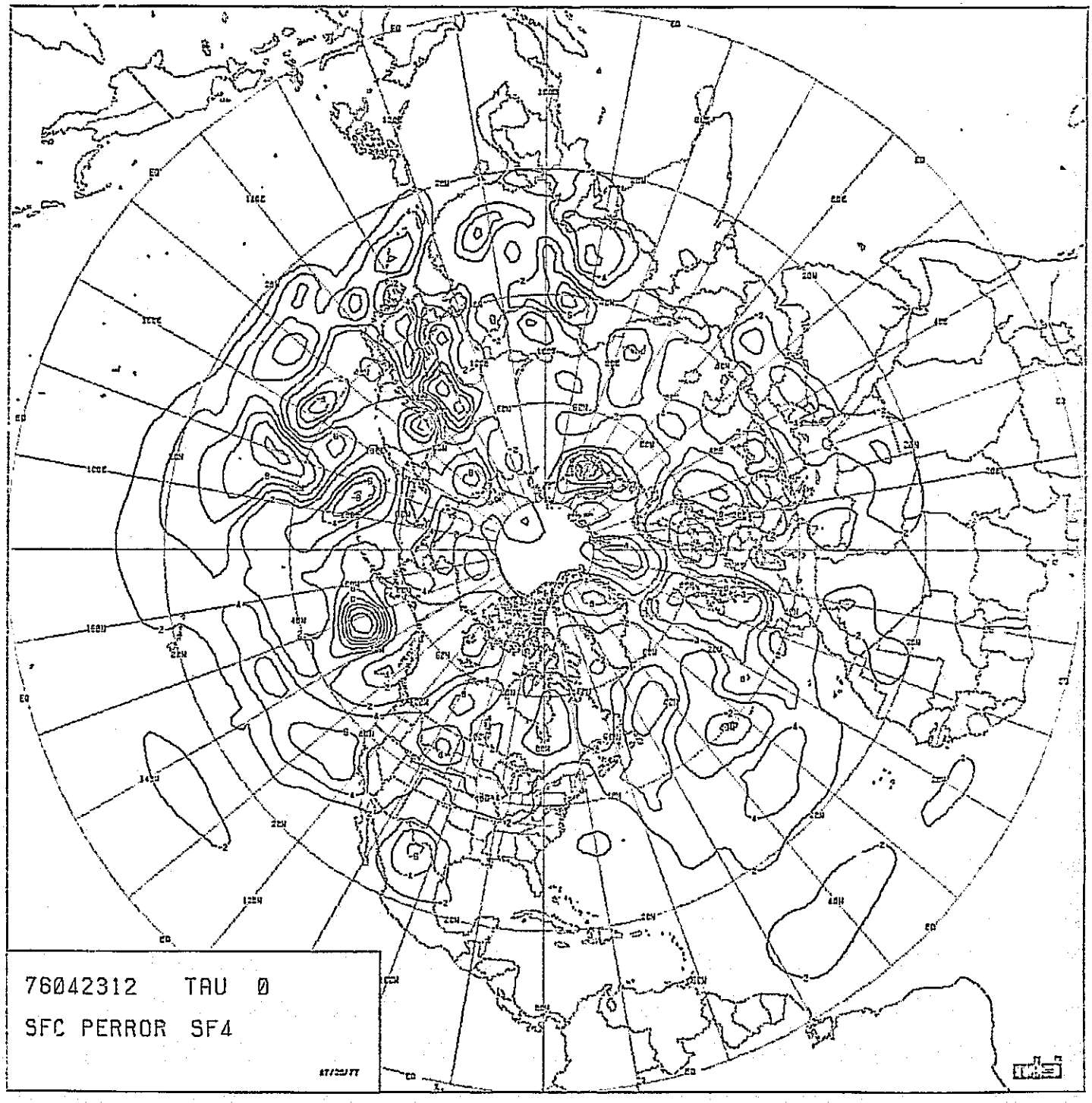

FIGURE IV-19: ERROR PATTERN, SURFACE, SF4

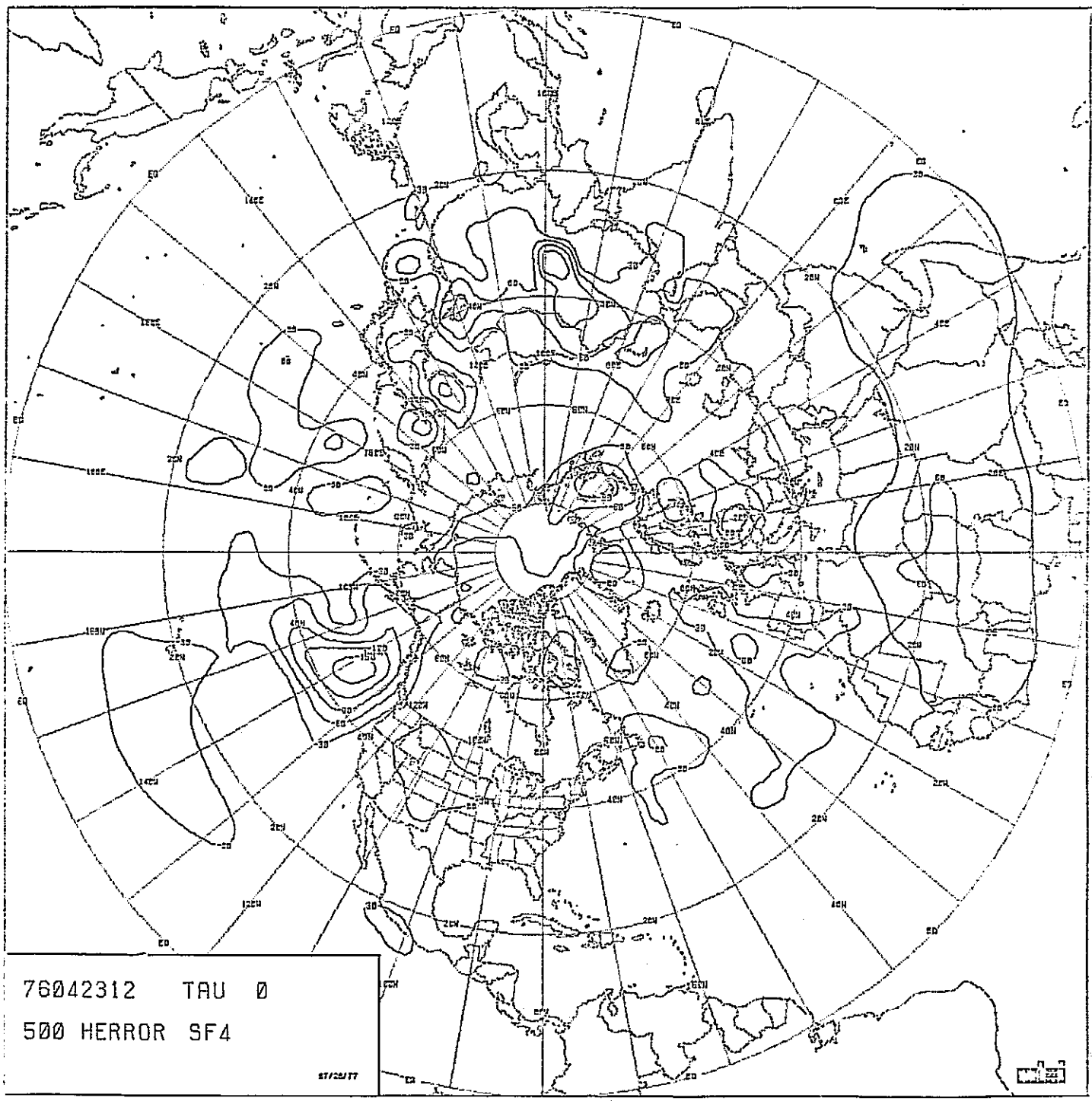

FIGURE IV-20: ERROR PATTERN, 500mb, SF4

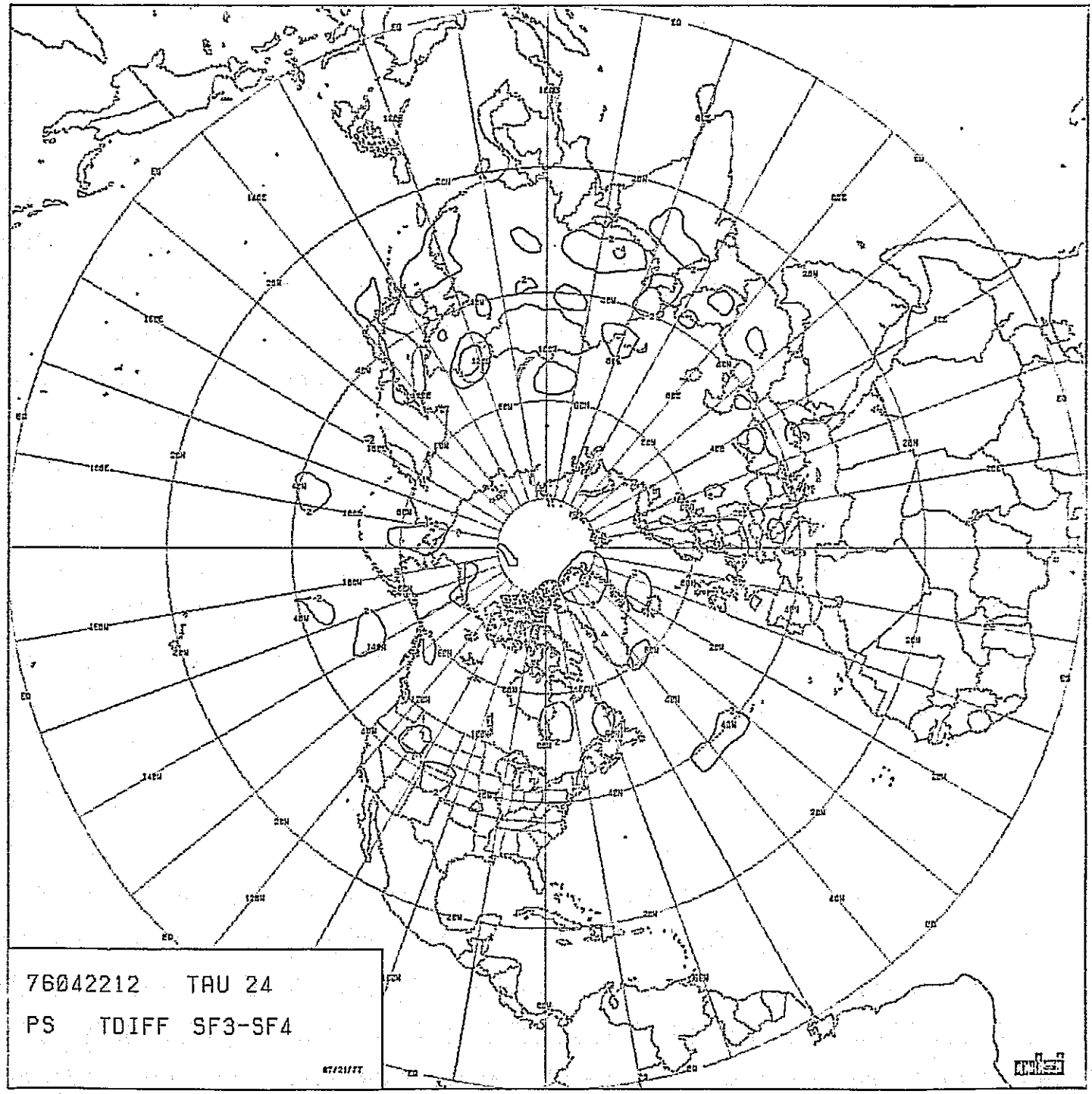

FIGURE IV-21: DIFFERENCE BETWEEN BASELINE AND SF4, SURFACE

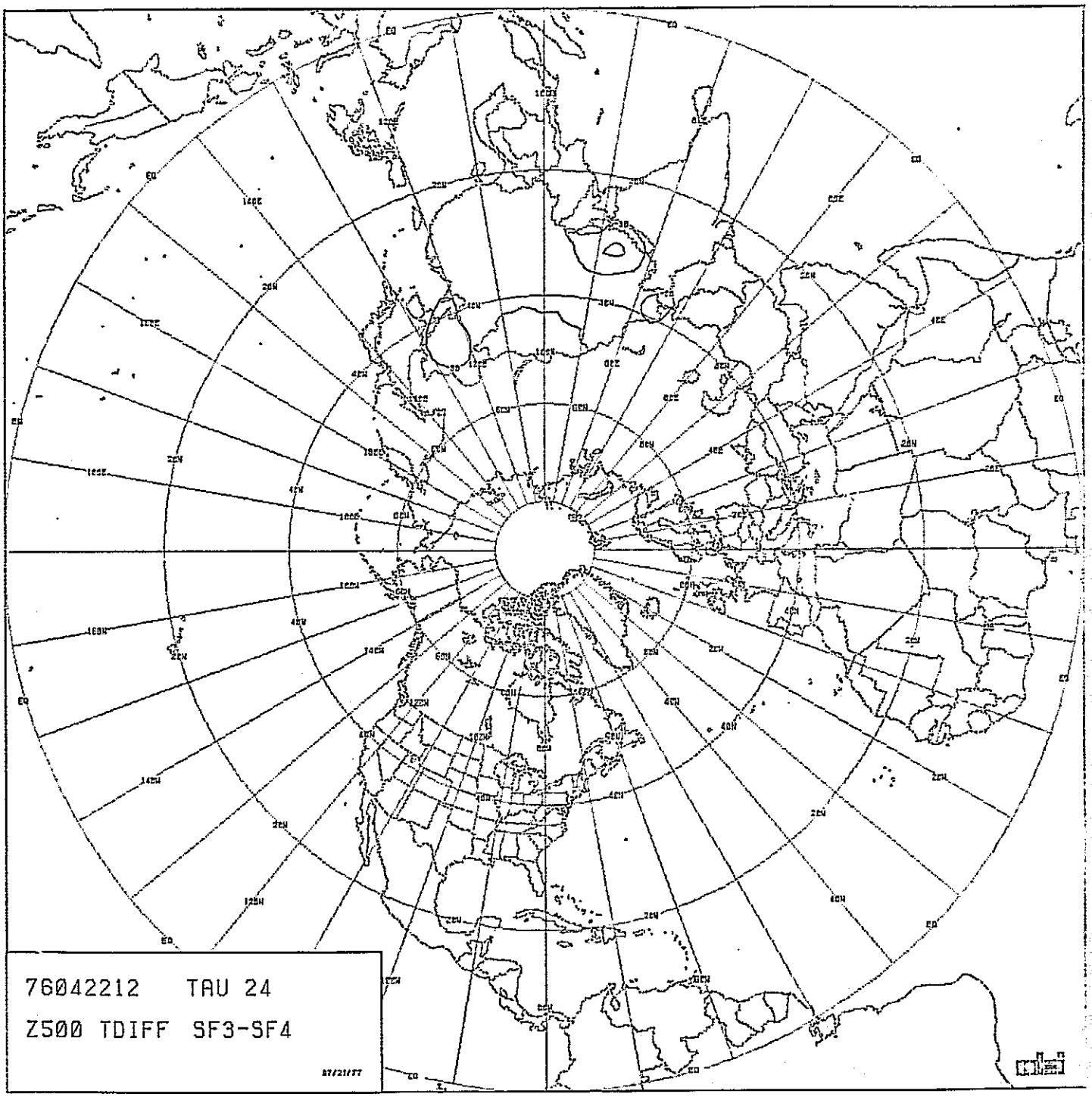

FIGURE IV-22: DIFFERENCE BETWEEN BASELINE AND SF4, 500mb

TABLE IV-4: ERROR STATISTICAL SUMMARY, SF4 (TEMPERATURE DIFFUSION COEFFICIENT = 10^5).

SURFACE

FROM	TO	RMS	SD	MEAN	MAX	MIN
0	10	.713E+00	.675E+00	.230E+00	.244E+01	-.156E+01
10	20	.115E+01	.115E+01	.804E-01	.407E+01	-.284E+01
20	30	.308E+01	.289E+01	.108E+01	.980E+01	-.615E+01
30	40	.365E+01	.336E+01	.143E+01	.124E+02	-.716E+01
40	50	.383E+01	.319E+01	.212E+01	.142E+02	-.908E+01
50	60	.439E+01	.347E+01	.266E+01	.146E+02	-.890E+01
60	70	.338E+01	.274E+01	.197E+01	.880E+01	-.733E+01
70	80	.337E+01	.324E+01	.930E+00	.643E+01	-.818E+01
80	90	.177E+01	.139E+01	.110E+01	.394E+01	-.193E+01
0	90	.257E+01	.242E+01	.867E+00	.146E+02	-.890E+01

500 MB

FROM	TO	RMS	SD	MEAN	MAX	MIN
0	10	.165E+02	.147E+02	.750E+01	.543E+02	-.351E+02
10	20	.266E+02	.250E+02	.923E+01	.618E+02	-.494E+02
20	30	.223E+02	.193E+02	.113E+02	.619E+02	-.437E+02
30	40	.356E+02	.336E+02	.118E+02	.142E+03	-.119E+03
40	50	.476E+02	.471E+02	.689E+01	.112E+03	-.166E+03
50	60	.342E+02	.342E+02	-.176E+00	.795E+02	-.123E+03
60	70	.253E+02	.241E+02	-.767E+01	.604E+02	-.910E+02
70	80	.406E+02	.243E+02	-.318E+02	.165E+02	-.106E+03
80	90	.377E+02	.146E+02	-.348E+02	-.107E+02	-.611E+02
0	90	.282E+02	.274E+02	.657E+01	.142E+03	-.166E+03

E. Smoothing Coefficient = 0 (SF5)

The smoothing operation is performed on the surface pressure, therefore, the effect of eliminating it produced less than 30M of change at 500 mb in SF5.

The surface analysis, Figure IV-23, is almost identical to the baseline, and as seen in Figure IV-24, there is little more than 4 mb difference between the baseline and SF5.

The error summary (Table IV-5) is quite similar to that of the baseline.

The results of omitting the smoothing function are cumulative and the errors that would be introduced accelerate and spread upward through the levels with time so that by 72 hours there would be severe instability throughout the forecast domain.

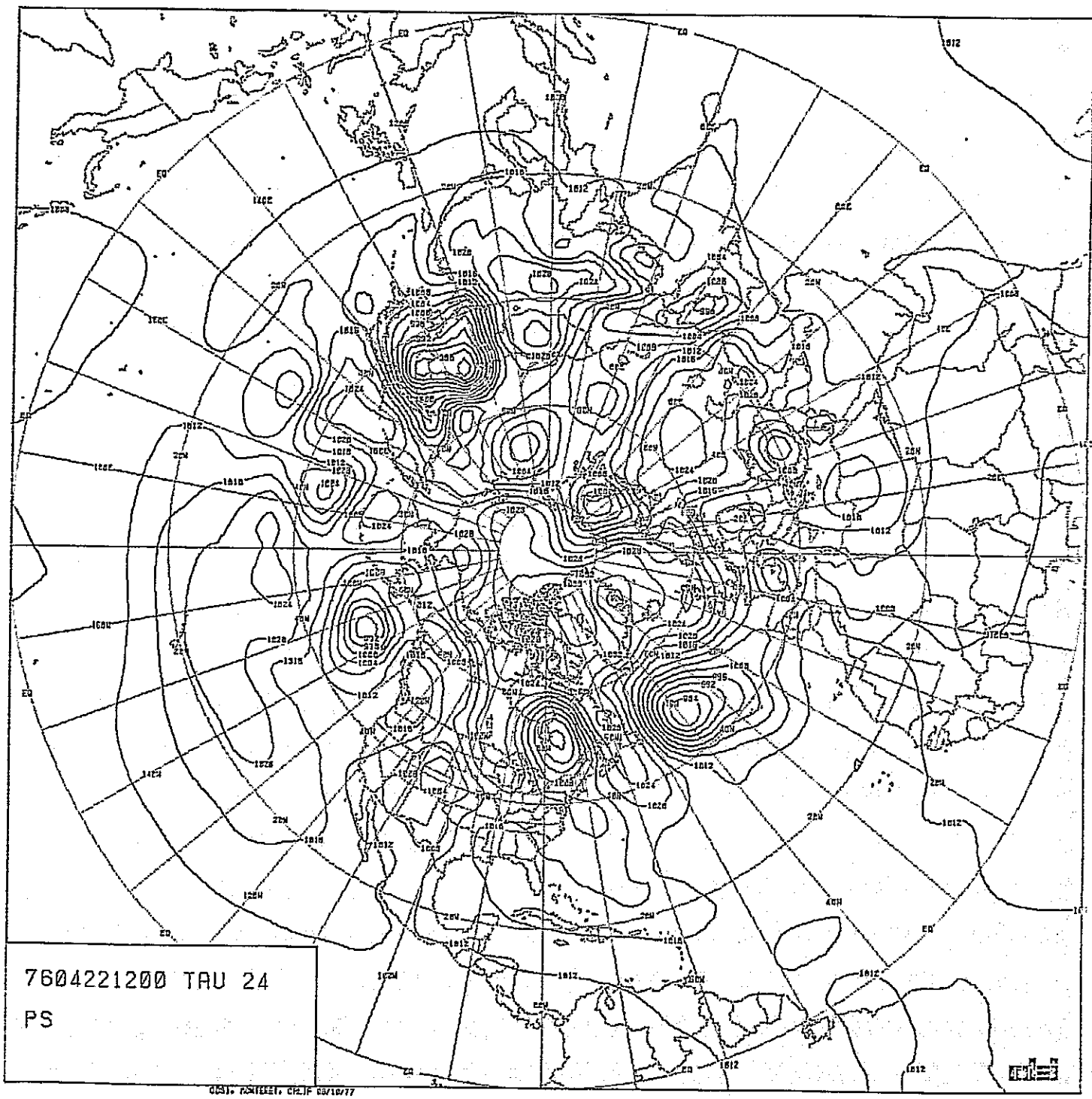

FIGURE IV-23: FORECAST, SURFACE, SF5

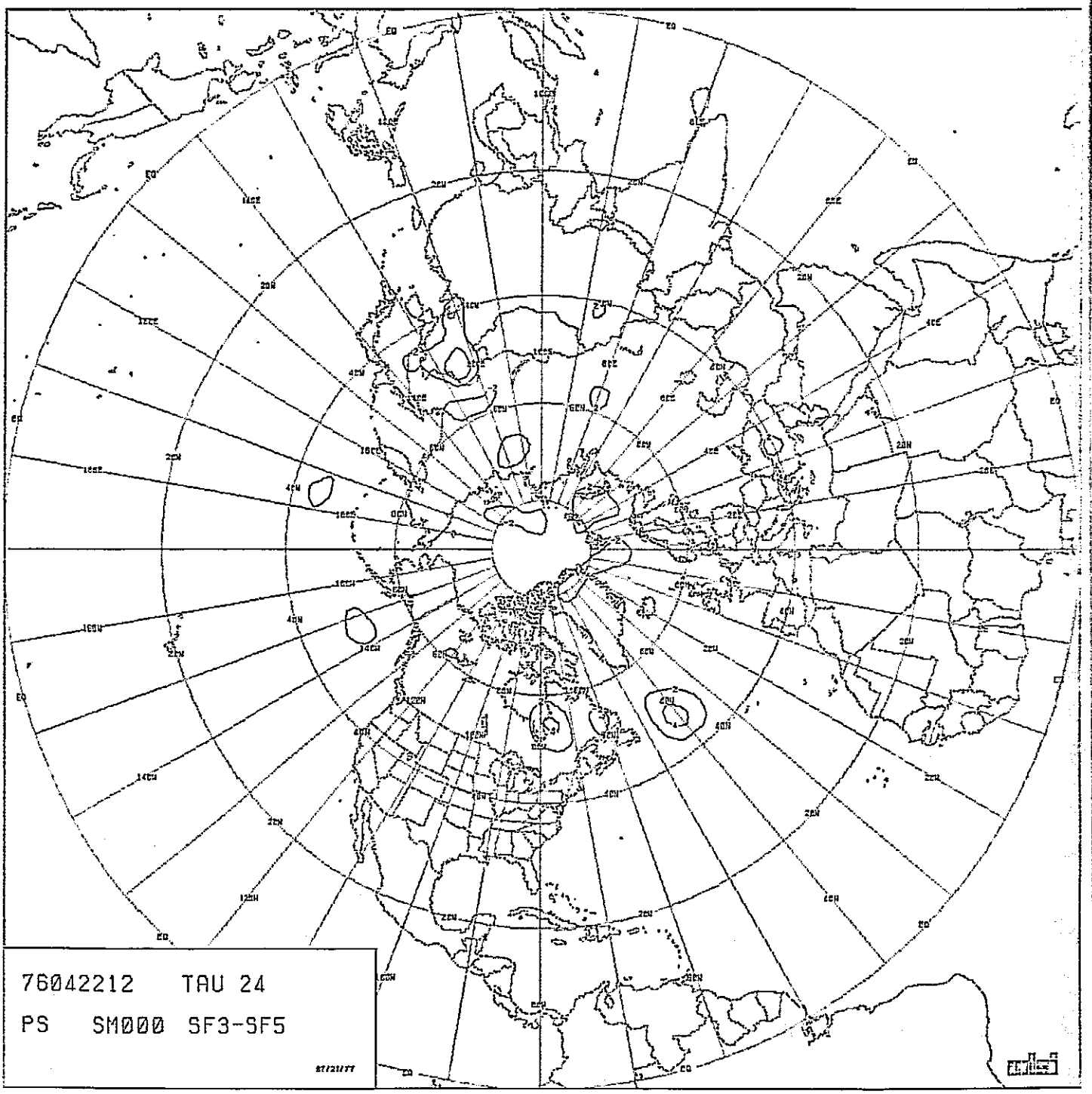

FIGURE IV-24: DIFFERENCE BETWEEN BASELINE AND SF5, SURFACE

TABLE IV-5: ERROR STATISTICAL SUMMARY, SF5
(SMOOTHING COEFFICIENT = 0).

SURFACE

FROM	TO	RMS	SD	MEAN	MAX	MIN
0	10	.714E+00	.680E+00	.215E+00	.247E+01	-.157E+01
10	20	.119E+01	.119E+01	-.143E-01	.406E+01	-.289E+01
20	30	.293E+01	.284E+01	.706E+00	.943E+01	-.590E+01
30	40	.344E+01	.318E+01	.131E+01	.111E+02	-.727E+01
40	50	.398E+01	.331E+01	.220E+01	.149E+02	-.822E+01
50	60	.455E+01	.377E+01	.255E+01	.144E+02	-.110E+02
60	70	.321E+01	.282E+01	.152E+01	.815E+01	-.778E+01
70	80	.374E+01	.364E+01	.829E+00	.886E+01	-.853E+01
80	90	.153E+01	.127E+01	.851E+00	.380E+01	-.117E+01
0	90	.255E+01	.244E+01	.746E+00	.149E+02	-.110E+02

500 MB

FROM	TO	RMS	SD	MEAN	MAX	MIN
0	10	.163E+02	.147E+02	.721E+01	.541E+02	-.354E+02
10	20	.267E+02	.248E+02	.997E+01	.628E+02	-.496E+02
20	30	.231E+02	.190E+02	.130E+02	.632E+02	-.416E+02
30	40	.380E+02	.351E+02	.148E+02	.133E+03	-.114E+03
40	50	.485E+02	.482E+02	.519E+01	.115E+03	-.162E+03
50	60	.358E+02	.357E+02	-.231E+01	.841E+02	-.123E+03
60	70	.253E+02	.236E+02	-.891E+01	.529E+02	-.868E+02
70	80	.417E+02	.237E+02	-.343E+02	.787E+01	-.107E+03
80	90	.455E+02	.122E+02	-.439E+02	-.259E+02	-.680E+02
0	90	.290E+02	.282E+02	.680E+01	.133E+03	-.162E+03

F. Smoothing Coefficient = .02 (SF6)

As in SF5, the effect of altering the smoothing coefficient is generally undetected at 500 mbs. At the surface, Figure IV-25, there is little obvious difference between SF5 and SF6 except that in the latter case the lows are generally not as deep and the gradients around the dominant lows are weaker. The intensity of the differences of SF6 from the baseline, in Figure IV-26, are generally of the same magnitude as seen in Figure IV-24, but of the opposite sign. The total difference between SF5 and SF6 therefore is as much as 10 mb, shown in Figure IV-27.

Table IV-6, the statistical summary for SF6, has little overall difference from the baseline summary but a slight shift of absolute maximum values to the negative.

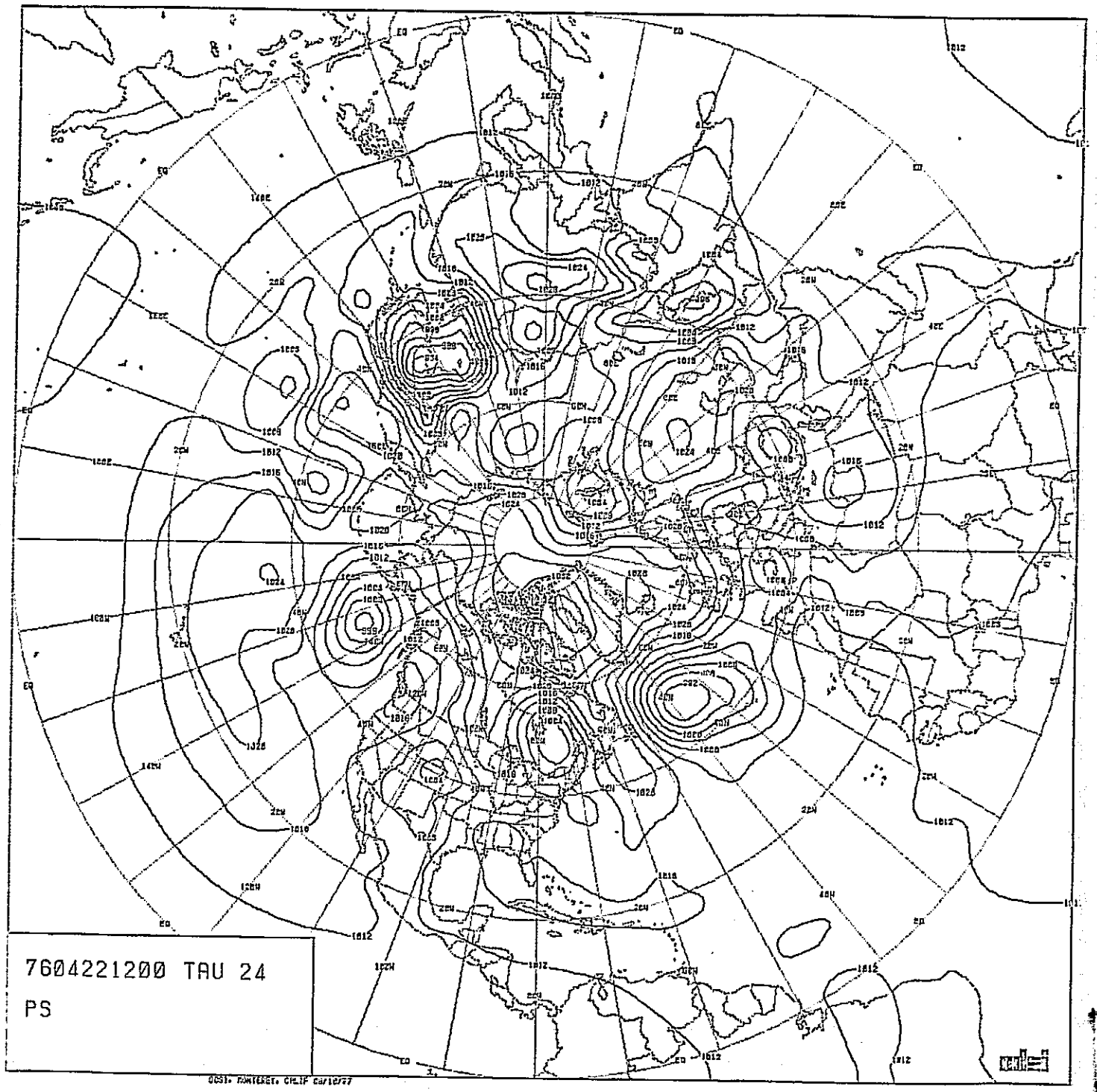

FIGURE IV-25: FORECAST, SURFACE, SF6

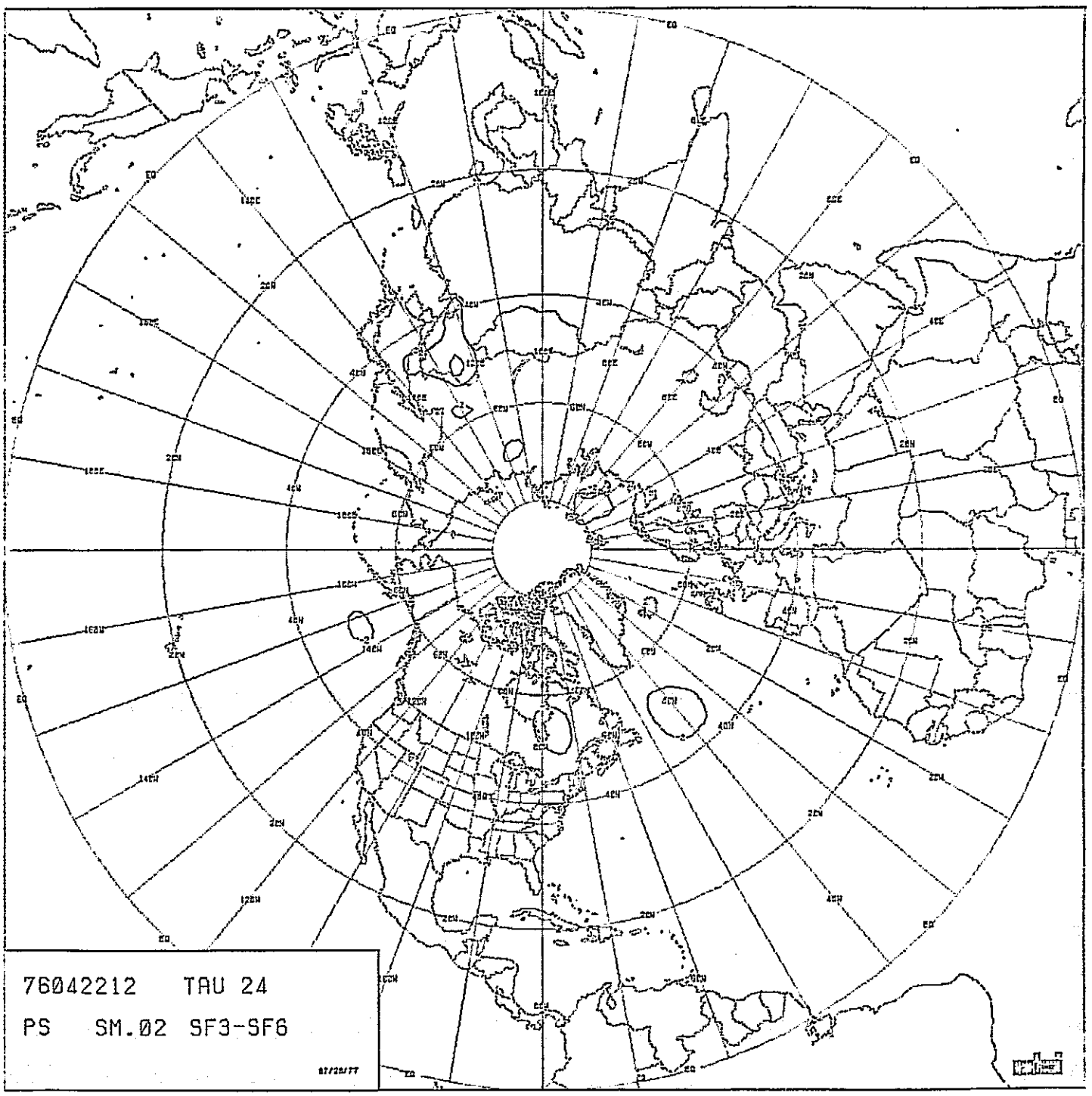

FIGURE IV-26: DIFFERENCE BETWEEN BASELINE AND SF6, SURFACE

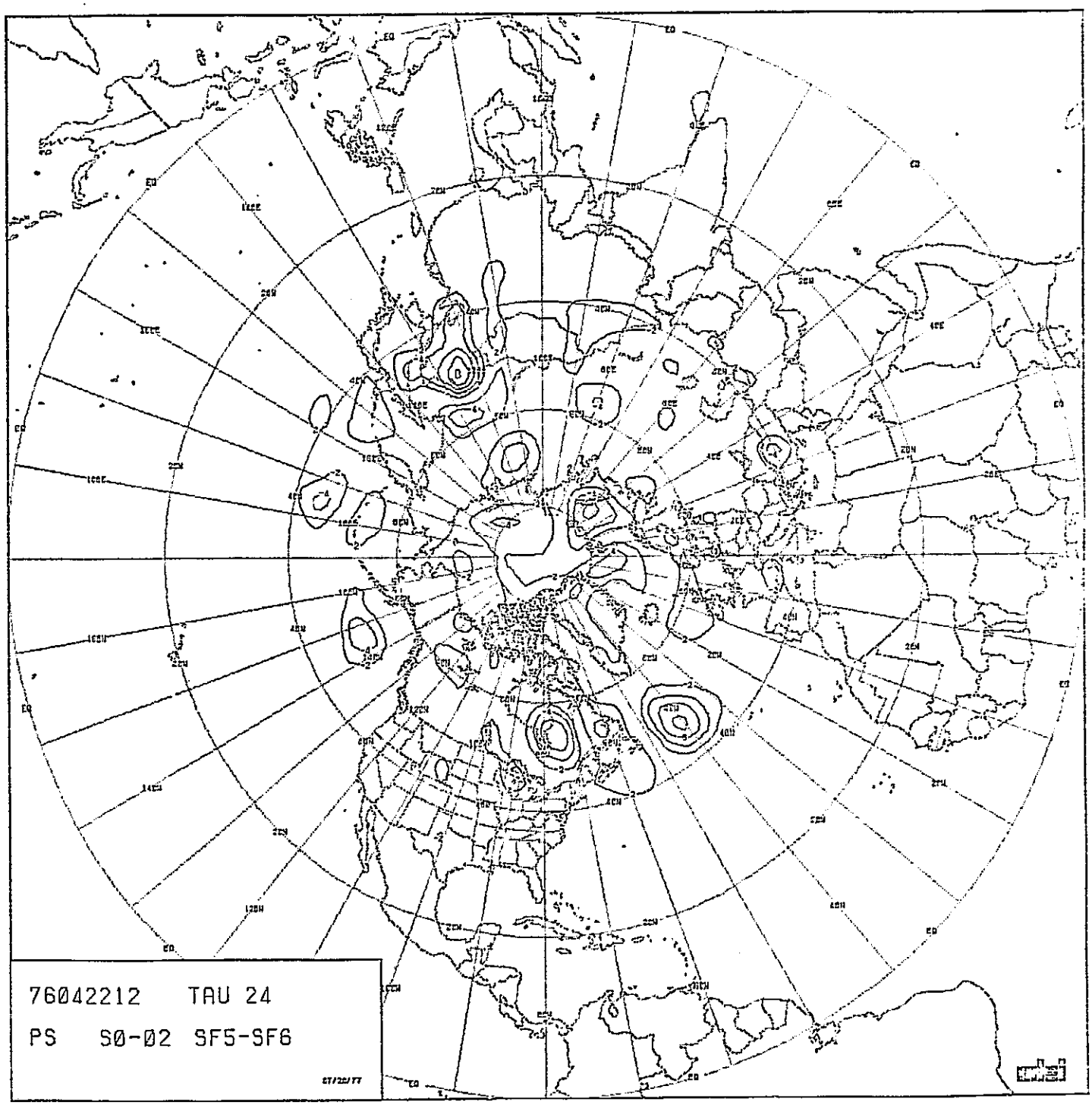

FIGURE IV-27: DIFFERENCE BETWEEN SF5 AND SF6, SURFACE

TABLE IV-6: ERROR STATISTICAL SUMMARY, SF6
(SMOOTHING COEFFICIENT = .02).

SURFACE

FROM	TO	RMS	SD	MEAN	MAX	MIN
0	10	.719E+00	.696E+00	.181E+00	.236E+01	-.160E+01
10	20	.115E+01	.115E+01	-.845E-02	.411E+01	-.284E+01
20	30	.293E+01	.278E+01	.929E+00	.914E+01	-.648E+01
30	40	.335E+01	.296E+01	.158E+01	.110E+02	-.550E+01
40	50	.388E+01	.344E+01	.179E+01	.106E+02	-.103E+02
50	60	.442E+01	.359E+01	.258E+01	.116E+02	-.102E+02
60	70	.356E+01	.289E+01	.207E+01	.811E+01	-.723E+01
70	80	.418E+01	.398E+01	.127E+01	.108E+02	-.992E+01
80	90	.335E+01	.212E+01	.260E+01	.738E+01	-.110E+01
0	90	.255E+01	.242E+01	.816E+00	.116E+02	-.103E+02

500 MB

FROM	TO	RMS	SD	MEAN	MAX	MIN
0	10	.166E+02	.147E+02	.757E+01	.545E+02	-.353E+02
10	20	.266E+02	.247E+02	.973E+01	.624E+02	-.498E+02
20	30	.225E+02	.190E+02	.121E+02	.641E+02	-.428E+02
30	40	.354E+02	.331E+02	.125E+02	.122E+03	-.115E+03
40	50	.473E+02	.471E+02	.341E+01	.110E+03	-.164E+03
50	60	.340E+02	.338E+02	-.327E+01	.713E+02	-.119E+03
60	70	.252E+02	.236E+02	-.869E+01	.546E+02	-.858E+02
70	80	.392E+02	.223E+02	-.322E+02	.960E+01	-.101E+03
80	90	.426E+02	.115E+02	-.410E+02	-.216E+02	-.635E+02
0	90	.281E+02	.274E+02	.632E+01	.122E+03	-.164E+03

G. Smoothing Coefficients as a Function of Time (SF12)

In SF12, the smoothing coefficient was increased each time step linearly from 0 initially to .01 at 24 hours. The output products of this run showed no perceptible difference from the baseline run, and the statistical summary (Table IV-7) showed only slight variations from the statistics produced by the baseline.

TABLE IV-7: ERROR STATISTICAL SUMMARY, SF12 (SMOOTHING COEFFICIENT = FUNCTION OF TIME).

SURFACE

FROM	TO	RMS	SD	MEAN	MAX	MIN
0	10	.712E+00	.672E+00	.236E+00	.245E+01	-.154E+01
10	20	.118E+01	.118E+01	.253E-01	.415E+01	-.283E+01
20	30	.292E+01	.281E+01	.817E+00	.939E+01	-.579E+01
30	40	.342E+01	.310E+01	.146E+01	.112E+02	-.638E+01
40	50	.387E+01	.321E+01	.217E+01	.136E+02	-.781E+01
50	60	.441E+01	.354E+01	.264E+01	.130E+02	-.102E+02
60	70	.325E+01	.274E+01	.174E+01	.767E+01	-.740E+01
70	80	.364E+01	.351E+01	.998E+00	.845E+01	-.856E+01
80	90	.194E+01	.134E+01	.140E+01	.493E+01	-.594E+00
0	90	.252E+01	.238E+01	.815E+00	.136E+02	-.102E+02

500 MB

FROM	TO	RMS	SD	MEAN	MAX	MIN
0	10	.165E+02	.147E+02	.743E+01	.543E+02	-.353E+02
10	20	.266E+02	.247E+02	.994E+01	.623E+02	-.495E+02
20	30	.229E+02	.190E+02	.129E+02	.636E+02	-.419E+02
30	40	.373E+02	.345E+02	.143E+02	.130E+03	-.114E+03
40	50	.482E+02	.479E+02	.483E+01	.114E+03	-.163E+03
50	60	.353E+02	.352E+02	-.257E+01	.779E+02	-.122E+03
60	70	.252E+02	.236E+02	-.891E+01	.532E+02	-.871E+02
70	80	.411E+02	.234E+02	-.338E+02	.876E+01	-.106E+03
80	90	.448E+02	.120E+02	-.431E+02	-.246E+02	-.675E+02
0	90	.288E+02	.280E+02	.675E+01	.130E+03	-.163E+03

H. Time Filter Removed (SF15)

The removal of the time filter produces slight phase errors that increase non-linearly with time. In the first 24 hours, however, there was little to observe in the way of inconsistencies with the baseline. The statistical summary of errors for SF15, Table IV-8, confirms that at this point, SF15 is very much like the baseline.

TABLE IV-8: ERROR STATISTICAL SUMMARY, SF15 (NO TIME FILTER).

SURFACE

FROM	TO	RMS	SD	MEAN	MAX	MIN
0	10	.710E+00	.672E+00	.231E+00	.243E+01	-.154E+01
10	20	.117E+01	.117E+01	.416E-01	.416E+01	-.278E+01
20	30	.292E+01	.278E+01	.890E+00	.932E+01	-.588E+01
30	40	.341E+01	.304E+01	.154E+01	.112E+02	-.587E+01
40	50	.383E+01	.322E+01	.207E+01	.127E+02	-.777E+01
50	60	.438E+01	.351E+01	.263E+01	.123E+02	-.101E+02
60	70	.333E+01	.276E+01	.186E+01	.788E+01	-.716E+01
70	80	.371E+01	.355E+01	.109E+01	.680E+01	-.896E+01
80	90	.239E+01	.154E+01	.183E+01	.583E+01	-.799E+00
0	90	.251E+01	.237E+01	.839E+00	.127E+02	-.101E+02

500 MB

FROM	TO	RMS	SD	MEAN	MAX	MIN
0	10	.165E+02	.147E+02	.754E+01	.544E+02	-.353E+02
10	20	.266E+02	.247E+02	.978E+01	.622E+02	-.497E+02
20	30	.227E+02	.190E+02	.124E+02	.627E+02	-.421E+02
30	40	.366E+02	.340E+02	.135E+02	.124E+03	-.115E+03
40	50	.478E+02	.477E+02	.395E+01	.114E+03	-.164E+03
50	60	.349E+02	.347E+02	-.318E+01	.787E+02	-.120E+03
60	70	.254E+02	.237E+02	-.907E+01	.544E+02	-.881E+02
70	80	.406E+02	.228E+02	-.335E+02	.939E+01	-.104E+03
80	90	.444E+02	.123E+02	-.427E+02	-.243E+02	-.676E+02
0	90	.285E+02	.278E+02	.648E+01	.124E+03	-.164E+03

I. Drag Coefficient = .003 (SF7)

The frictional drag device acts primarily on the lowest level and eventually affects the upper levels. By doubling the drag coefficient to .003, little effect is seen at the surface or 500 mb in 24 hours. The departure from the baseline at the surface, Figure IV-28, shows a maximum of about -4 mb north of Korea. Figure IV-29, the 500 mb level, shows a departure of only 30M. The statistical error summary for SF7, Table IV-9, closely resembles that of the baseline with a slight shift of the maximum value to the negative.

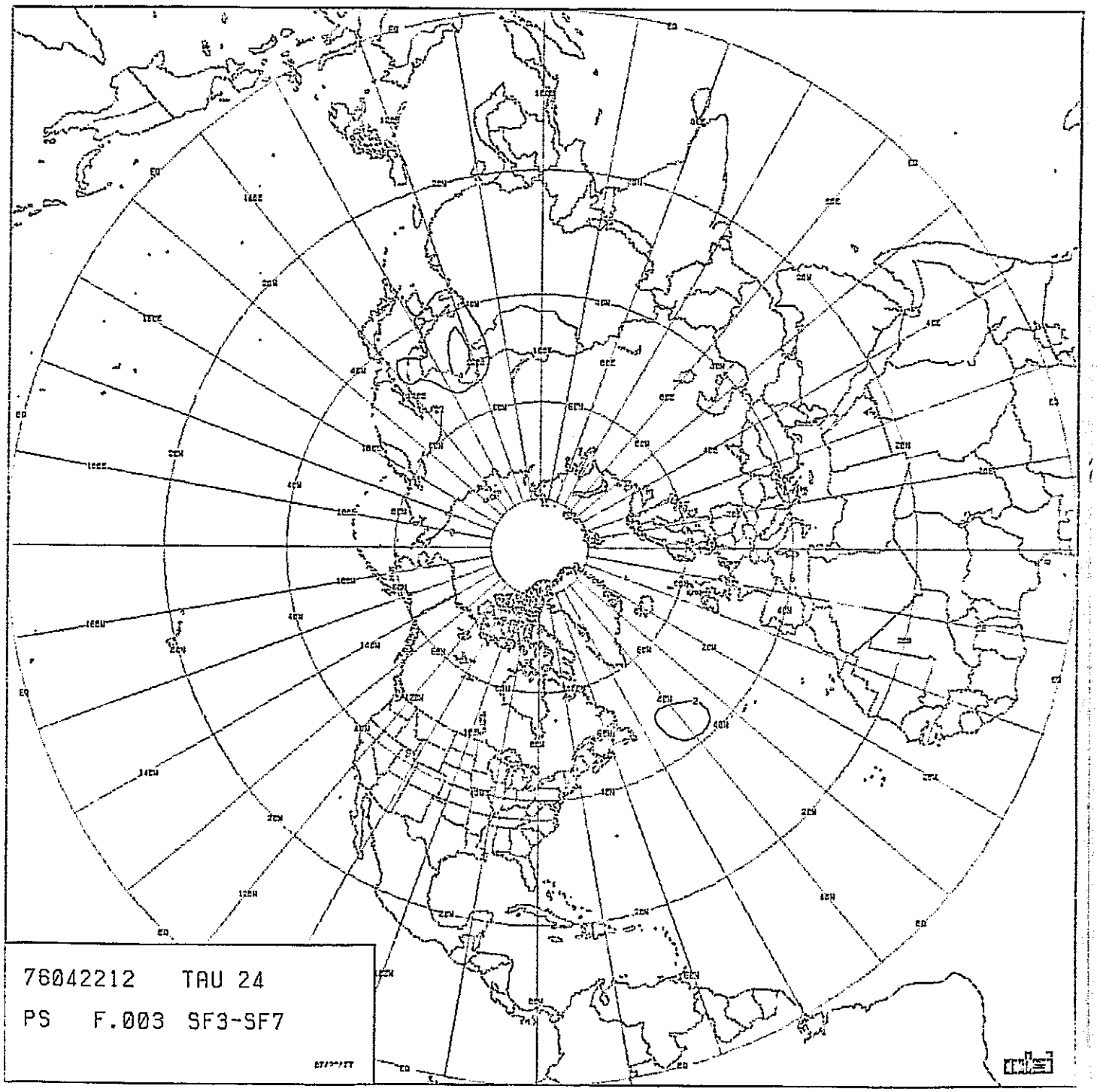

FIGURE IV-28: DIFFERENCE BETWEEN BASELINE AND SF7, SURFACE

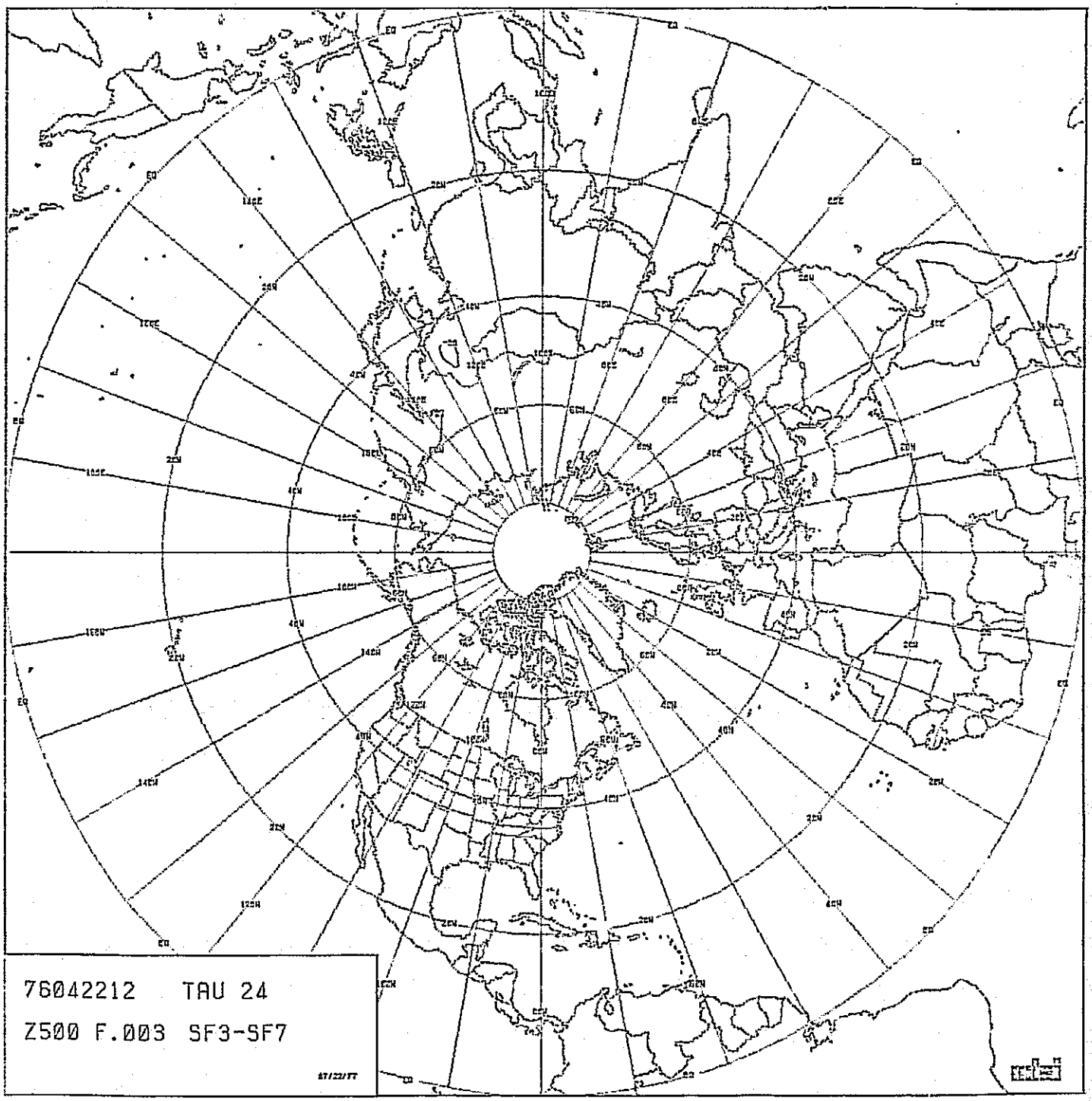

FIGURE IV-29: DIFFERENCE BETWEEN BASELINE AND SF7, 500mb

TABLE IV-9: ERROR STATISTICAL SUMMARY, SF7
(DRAG COEFFICIENT = .003).

SURFACE

FROM	TO	RMS	SD	MEAN	MAX	MIN
0	10	.710E+00	.670E+00	.237E+00	.242E+01	-.155E+01
10	20	.116E+01	.116E+01	.742E-01	.425E+01	-.280E+01
20	30	.298E+01	.280E+01	.102E+01	.920E+01	-.606E+01
30	40	.333E+01	.299E+01	.145E+01	.113E+02	-.572E+01
40	50	.378E+01	.348E+01	.148E+01	.116E+02	-.105E+02
50	60	.427E+01	.364E+01	.222E+01	.110E+02	-.116E+02
60	70	.331E+01	.280E+01	.175E+01	.763E+01	-.764E+01
70	80	.386E+01	.374E+01	.954E+00	.919E+01	-.966E+01
80	90	.241E+01	.165E+01	.176E+01	.583E+01	-.126E+01
0	90	.250E+01	.237E+01	.775E+00	.116E+02	-.116E+02

500 MB

FROM	TO	RMS	SD	MEAN	MAX	MIN
0	10	.166E+02	.147E+02	.763E+01	.546E+02	-.351E+02
10	20	.267E+02	.247E+02	.101E+02	.625E+02	-.494E+02
20	30	.229E+02	.190E+02	.129E+02	.641E+02	-.410E+02
30	40	.359E+02	.338E+02	.122E+02	.125E+03	-.116E+03
40	50	.488E+02	.488E+02	.170E-01	.110E+03	-.167E+03
50	60	.363E+02	.359E+02	-.541E+01	.718E+02	-.126E+03
60	70	.255E+02	.236E+02	-.968E+01	.542E+02	-.891E+02
70	80	.419E+02	.240E+02	-.343E+02	.692E+01	-.108E+03
80	90	.447E+02	.123E+02	-.430E+02	-.232E+02	-.692E+02
0	90	.288E+02	.282E+02	.599E+01	.125E+03	-.167E+03

J. Drag Coefficient = .00015 (SF9)

Reducing the drag coefficient by one order of magnitude does not appear to greatly decrease the quality of the forecast in 24 hours. Figure IV-30 shows only slightly larger areas of departure from the base line than was seen in the last case, but these departures are of opposite signs. At 500 mb, Figure IV-31 shows only a small area of departure from the baseline. The statistical error summary for SF9, Table IV-10, shows a generally slight increase in error at the surface and almost no difference at 500 mb in comparison with the baseline.

More striking illustrations of the effect of tampering with the drag coefficient are seen in Figures IV-32 and IV-33, which are the differences between the SF7 and SF9 runs at the surface and 500 mb, respectively. Here we can see differences of more than 8 mb at the surface and 60M at 500 mb.

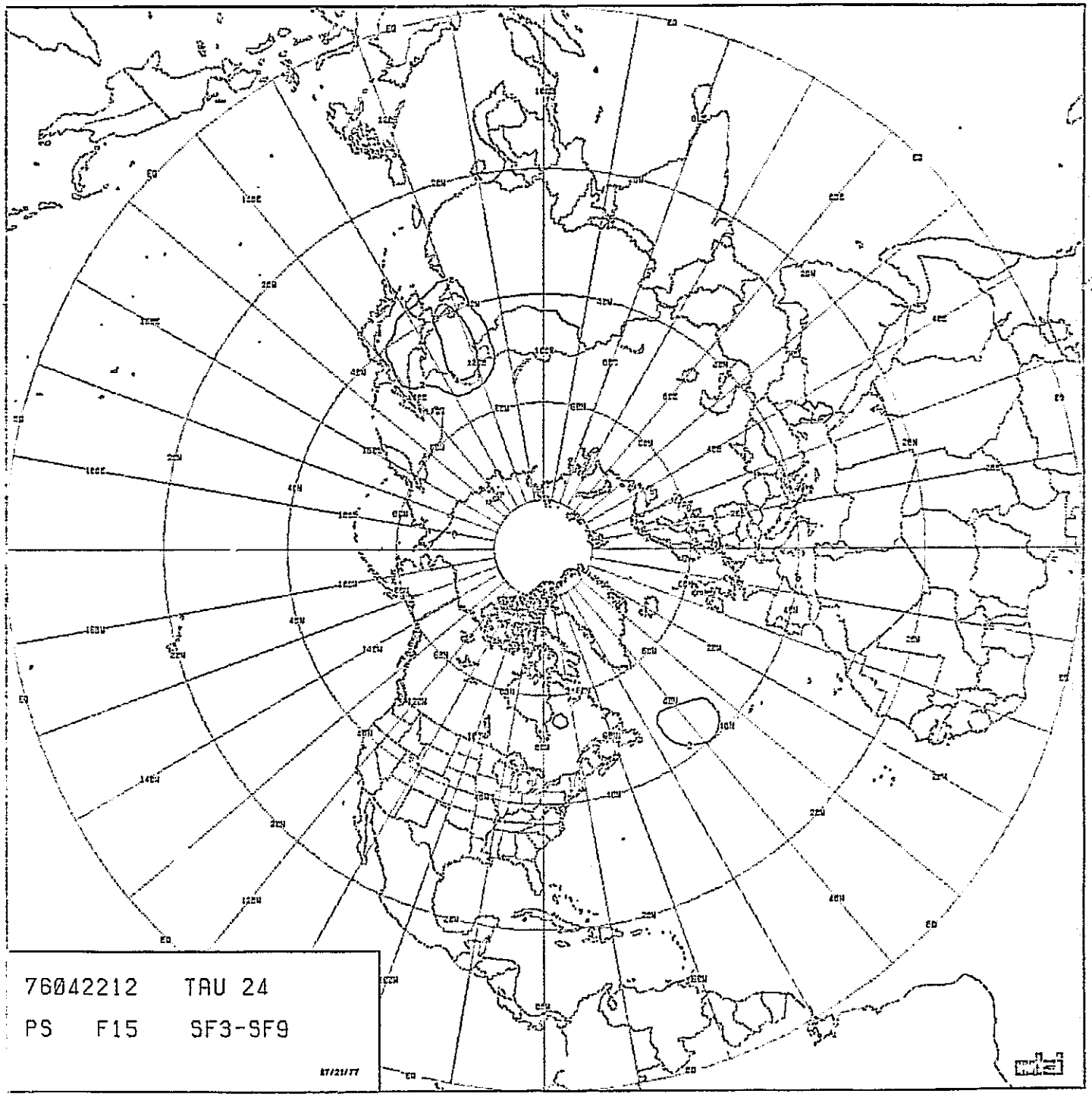

FIGURE IV-30: DIFFERENCE BETWEEN BASELINE AND SF9, SURFACE

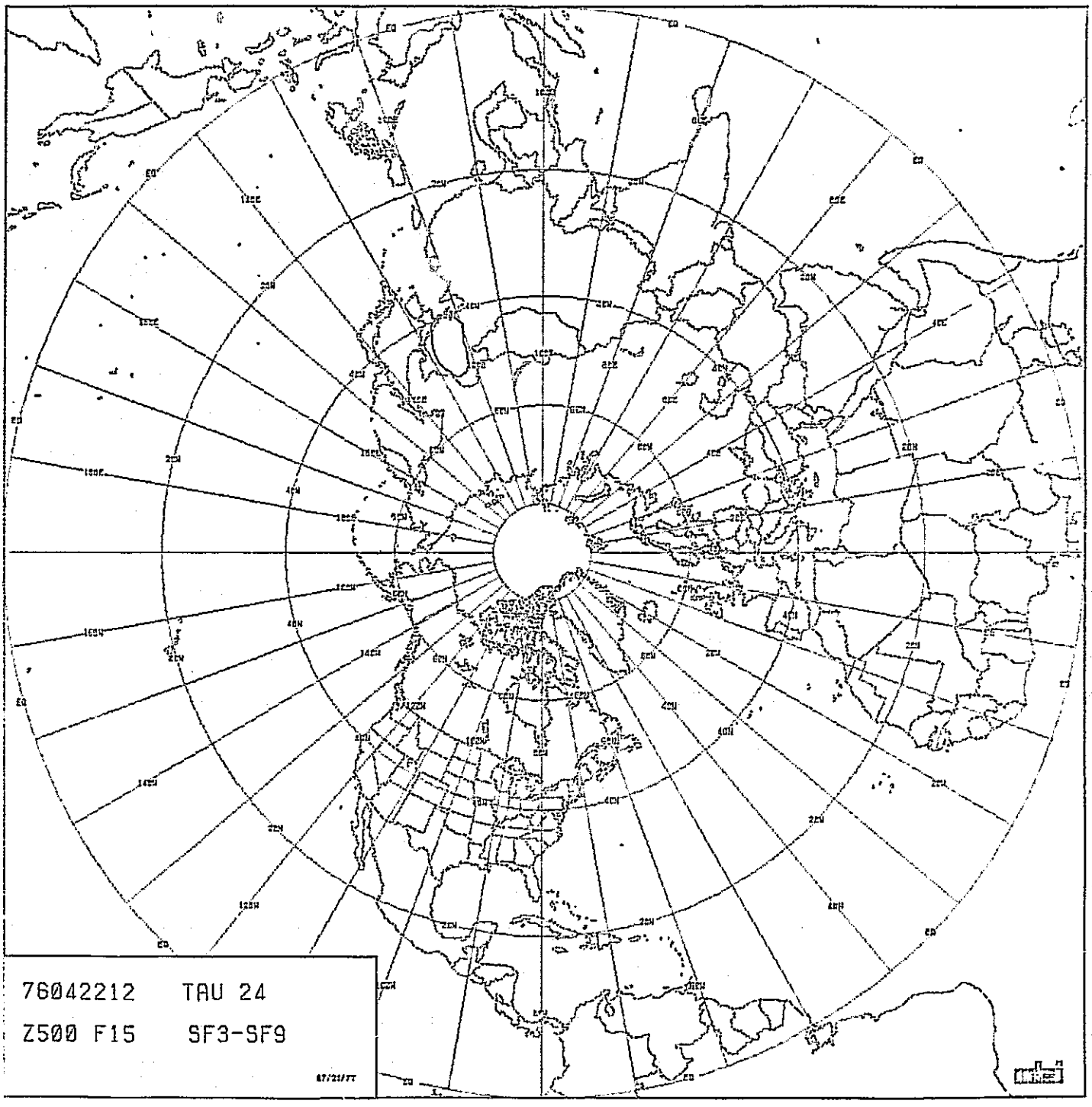

FIGURE IV-31: DIFFERENCE BETWEEN BASELINE AND SF9, 500mb

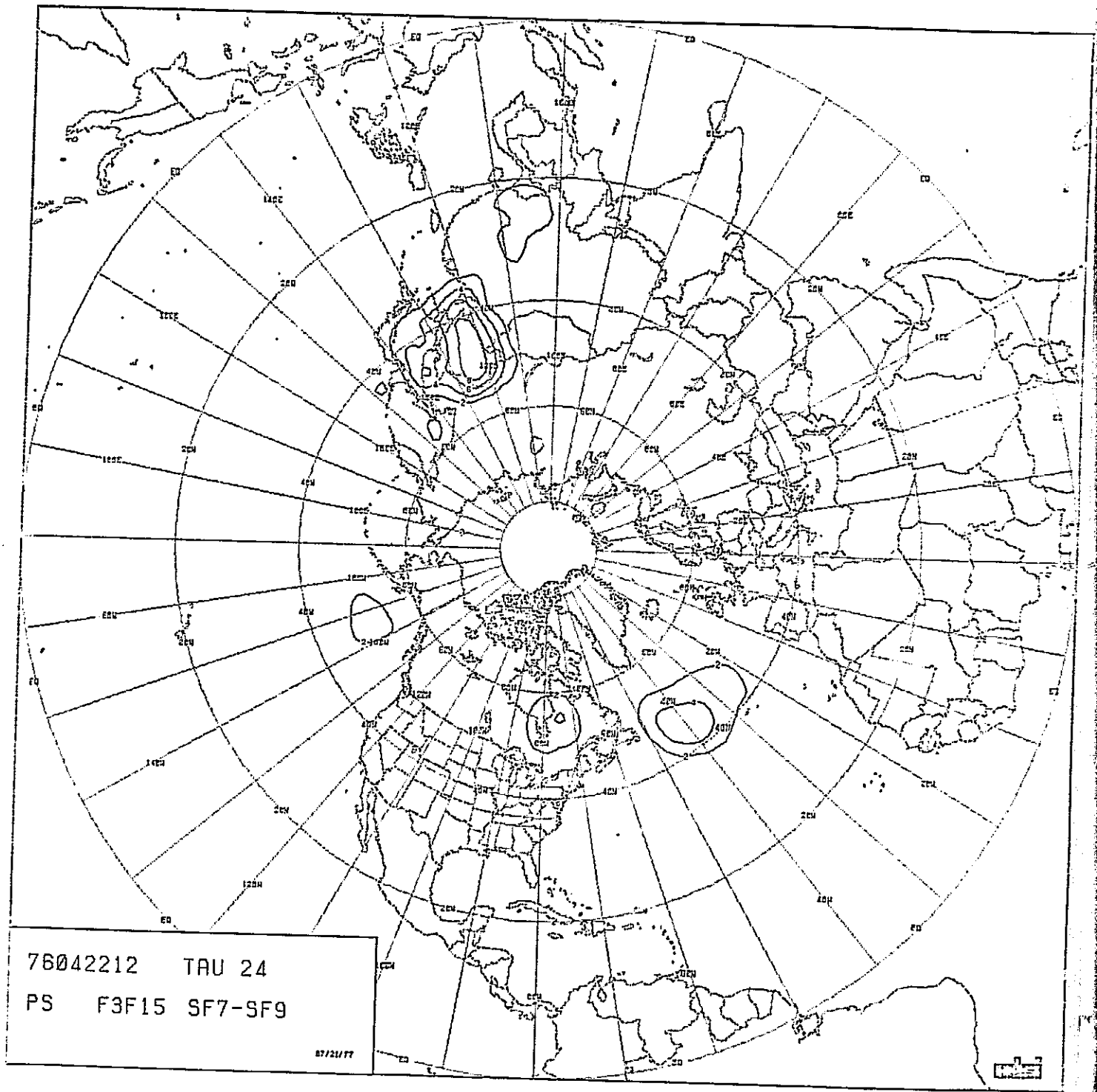

FIGURE IV-32: DIFFERENCE BETWEEN SF7 AND SF9, SURFACE

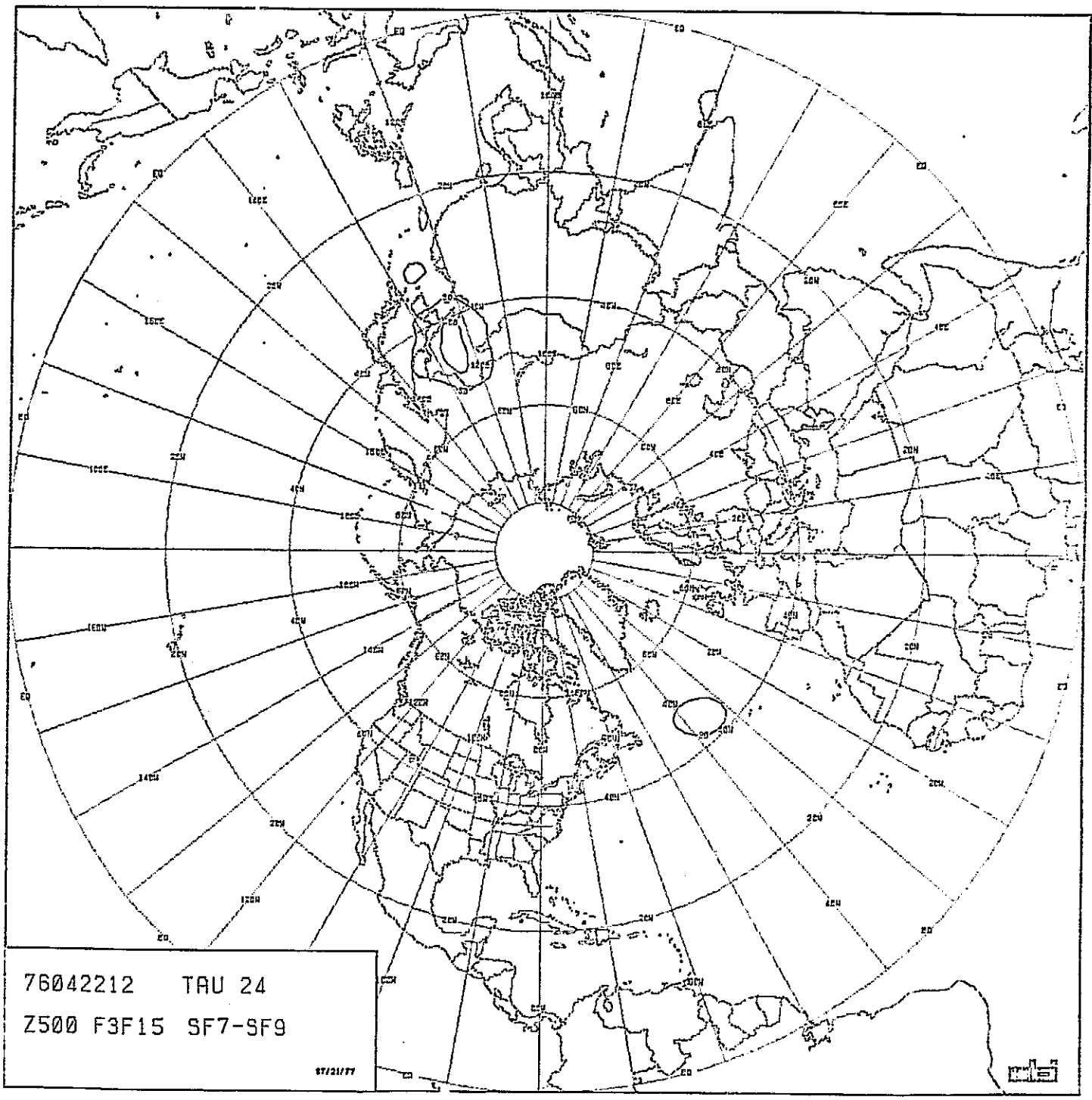

FIGURE IV-33: DIFFERENCE BETWEEN SF7 AND SF9, 500mb

TABLE IV-10: ERROR STATISTICAL SUMMARY, SF9
(DRAG COEFFICIENT = .00015).

SURFACE

FROM	TO	RMS	SD	MEAN	MAX	MIN
0	10	.719E+00	.675E+00	.221E+00	.243E+01	-.156E+01
10	20	.118E+01	.118E+01	-.419E-01	.401E+01	-.286E+01
20	30	.290E+01	.282E+01	.679E+00	.931E+01	-.565E+01
30	40	.357E+01	.319E+01	.158E+01	.112E+02	-.640E+01
40	50	.414E+01	.315E+01	.269E+01	.138E+02	-.747E+01
50	60	.455E+01	.342E+01	.300E+01	.135E+02	-.839E+01
60	70	.335E+01	.274E+01	.193E+01	.795E+01	-.686E+01
70	80	.364E+01	.344E+01	.121E+01	.867E+01	-.833E+01
80	90	.236E+01	.141E+01	.190E+01	.559E+01	-.302E+00
0	90	.259E+01	.244E+01	.871E+00	.138E+02	-.839E+01

500 MB

FROM	TO	RMS	SD	MEAN	MAX	MIN
0	10	.165E+02	.147E+02	.749E+01	.542E+02	-.354E+02
10	20	.266E+02	.248E+02	.970E+01	.622E+02	-.498E+02
20	30	.227E+02	.191E+02	.124E+02	.635E+02	-.436E+02
30	40	.380E+02	.346E+02	.156E+02	.131E+03	-.112E+03
40	50	.480E+02	.471E+02	.898E+01	.115E+03	-.160E+03
50	60	.338E+02	.338E+02	-.156E+00	.841E+02	-.116E+03
60	70	.251E+02	.238E+02	-.794E+01	.539E+02	-.839E+02
70	80	.388E+02	.219E+02	-.321E+02	.111E+02	-.997E+02
80	90	.433E+02	.114E+02	-.418E+02	-.240E+02	-.628E+02
0	90	.286E+02	.276E+02	.737E+01	.131E+03	-.160E+03

K. Flat Earth (SF13)

The elimination of terrain was detrimental principally in the lower levels. The two basic types of errors introduced at the surface, seen in Figure IV-34, are:

° The unimpeded movement of pressure systems demonstrated by the low over southern Afghanistan moving to the northwest and the central Asia high spreading in all directions. Those show up in both the surface error chart, Figure IV-36, as a series of errors through central Asia and on the baseline departure chart, Figure IV-38, in the same region.

° The lack of eddy low formations, as seen on the surface chart, off the east coast of the U.S. and east of Greenland.

The effects of the flat earth at 500 mb are generally a reflection of deviations at lower levels. SF13 at 500 mb, Figure IV-35, bears a close resemblance to the baseline. The error chart, Figure IV-37, is about the same as the baseline except for the China-USSR border area where the errors are <u>smaller</u> than those of the baseline. The amount of difference between the baseline and SF13, Figure IV-39, is about 60M in central Asia.

The improved forecast at 500 mb due to the flat earth model is undoubtedly a transitory feature. As the forecast advances beyond 24 hours, the errors at the surface will grow more rapidly and will, in turn, be reflected by increasing errors in the upper levels.

The statistical error summary for SF13, Table IV-11, shows an overall increase in errors at the surface and some decrease of errors at 500 mb.

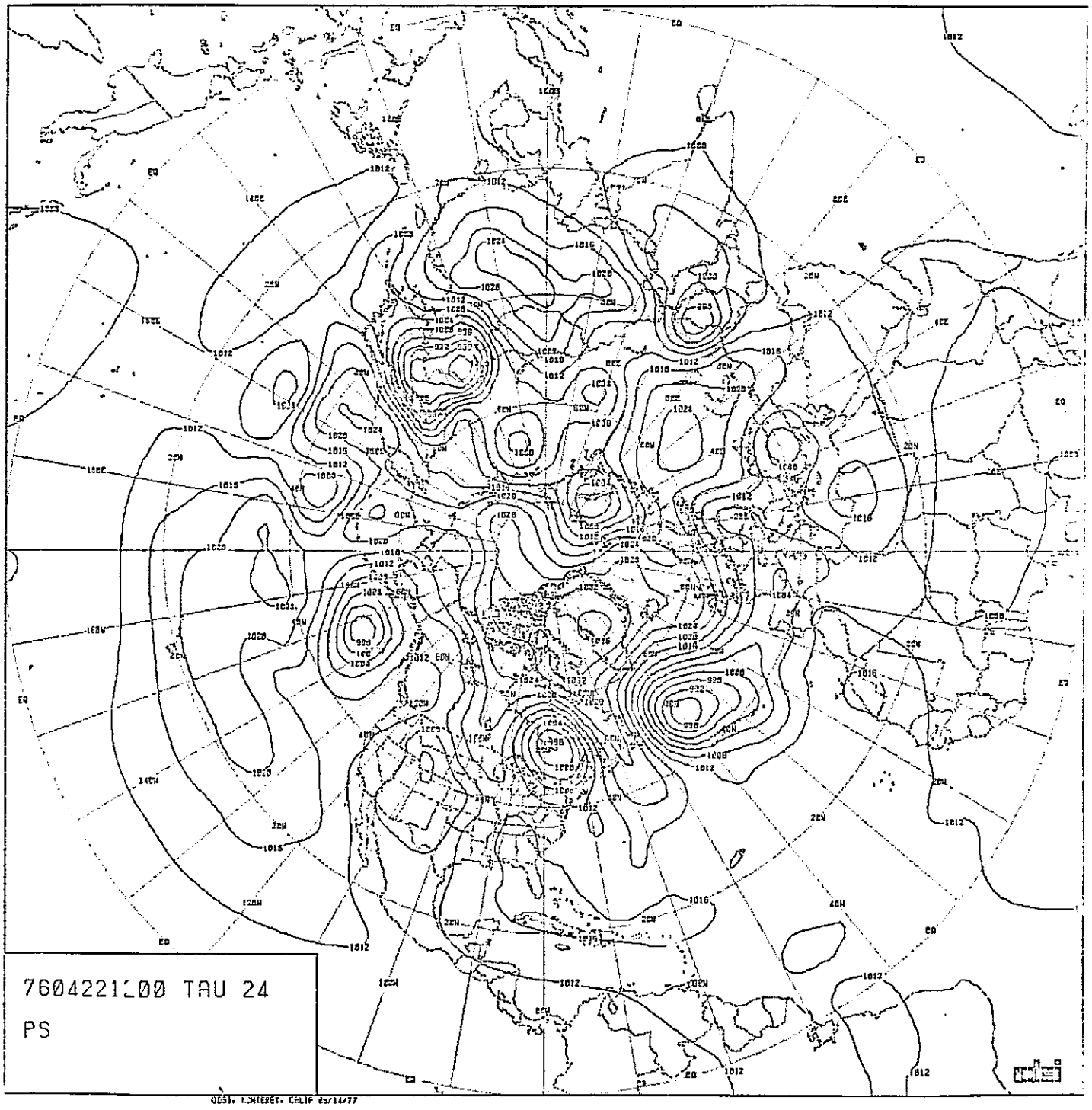

FIGURE IV-34: FORECAST, SURFACE, SF13

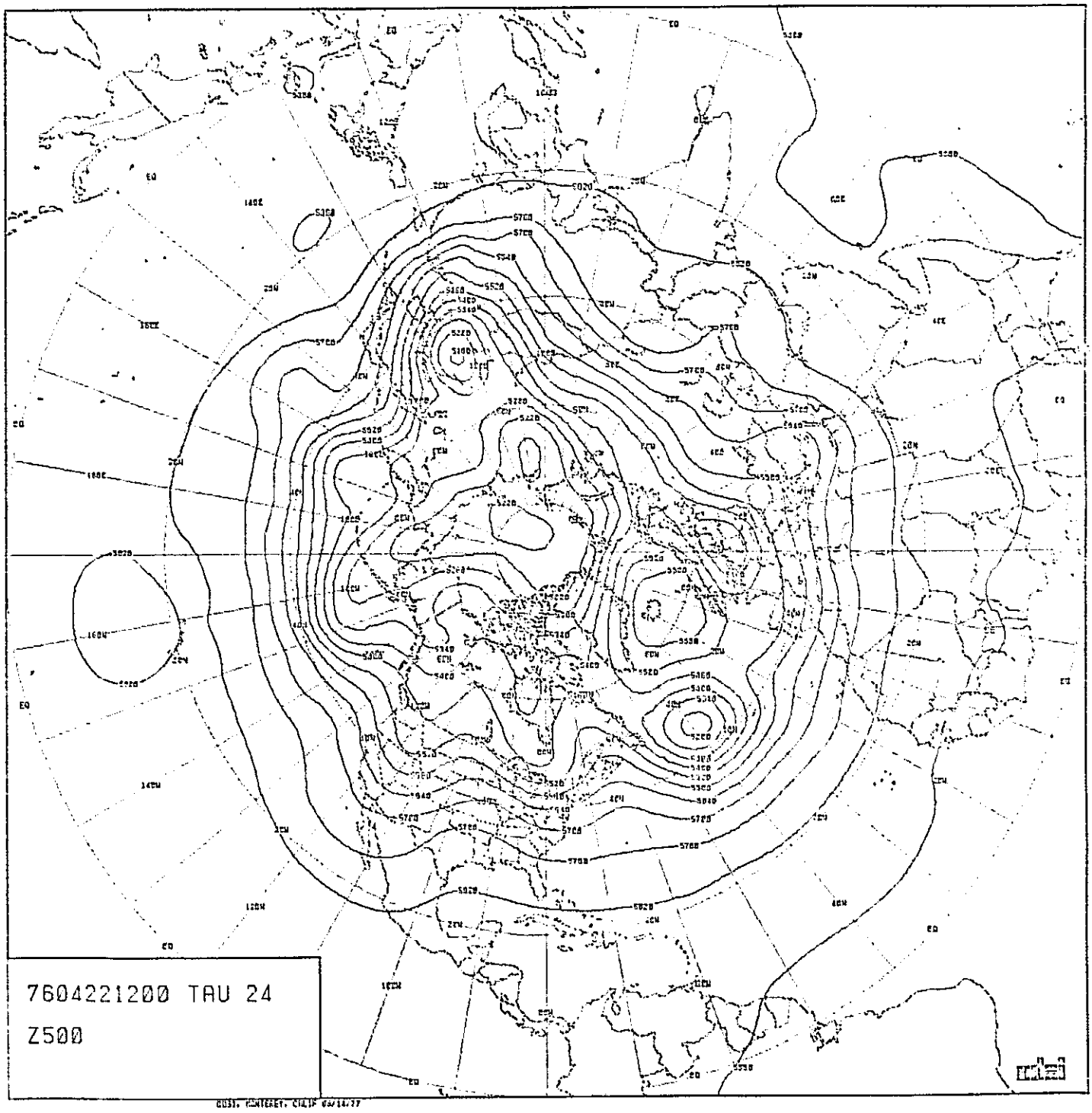

FIGURE IV-35: FORECAST, 500mb, SF13

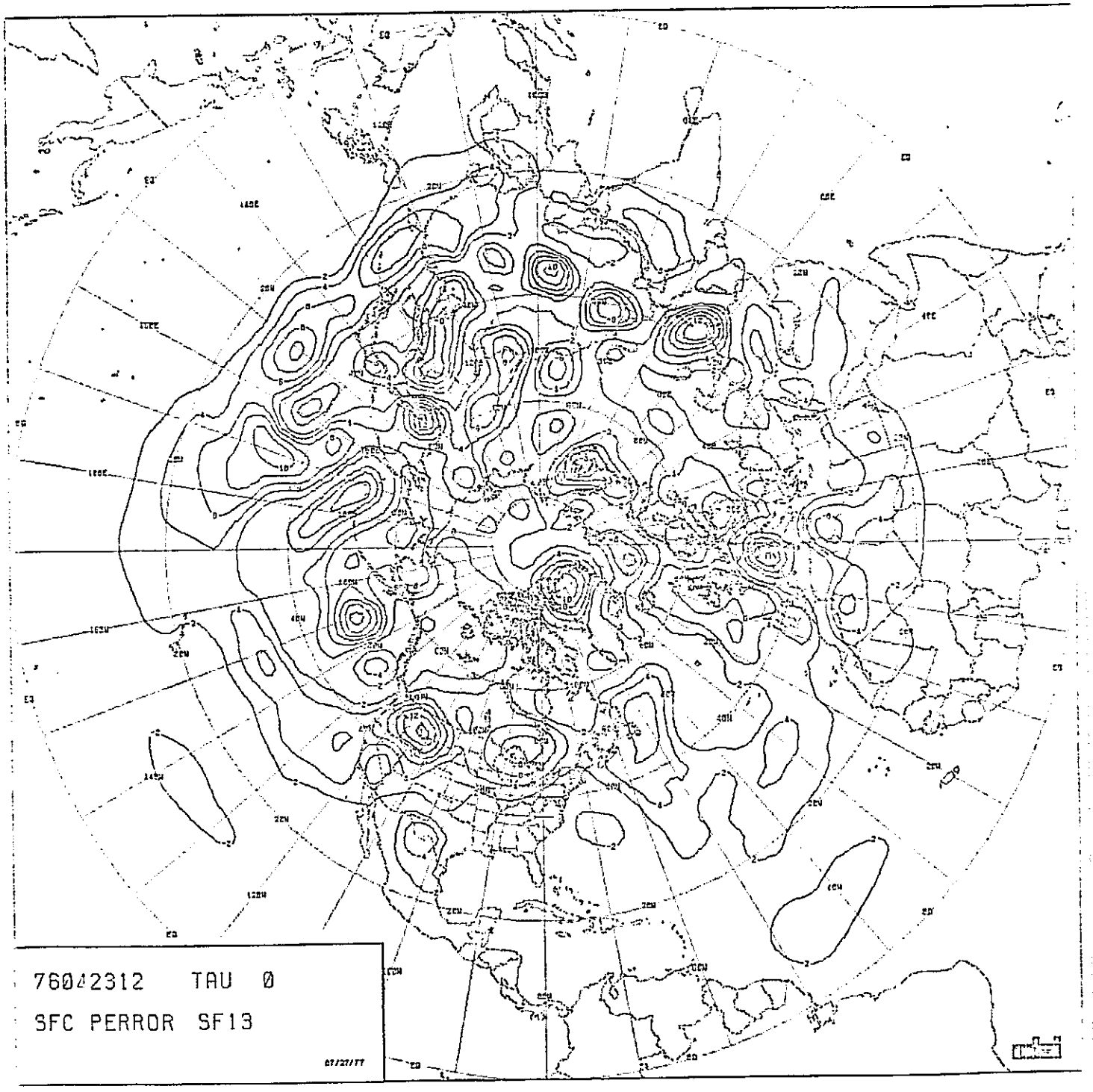

FIGURE IV-36: ERROR PATTERN, SURFACE, SF13

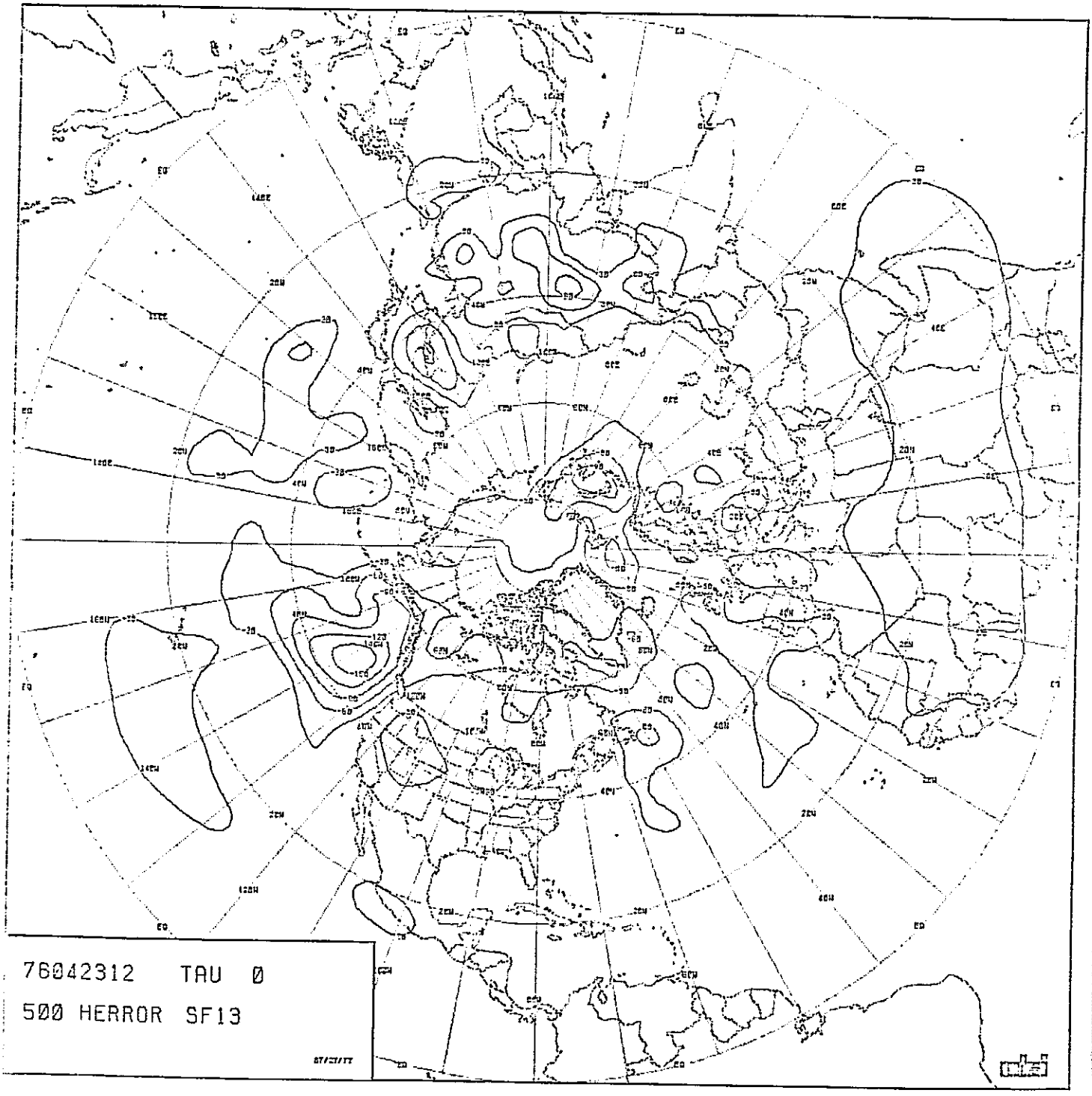

FIGURE IV-37: ERROR PATTERN, 500mb, SF13

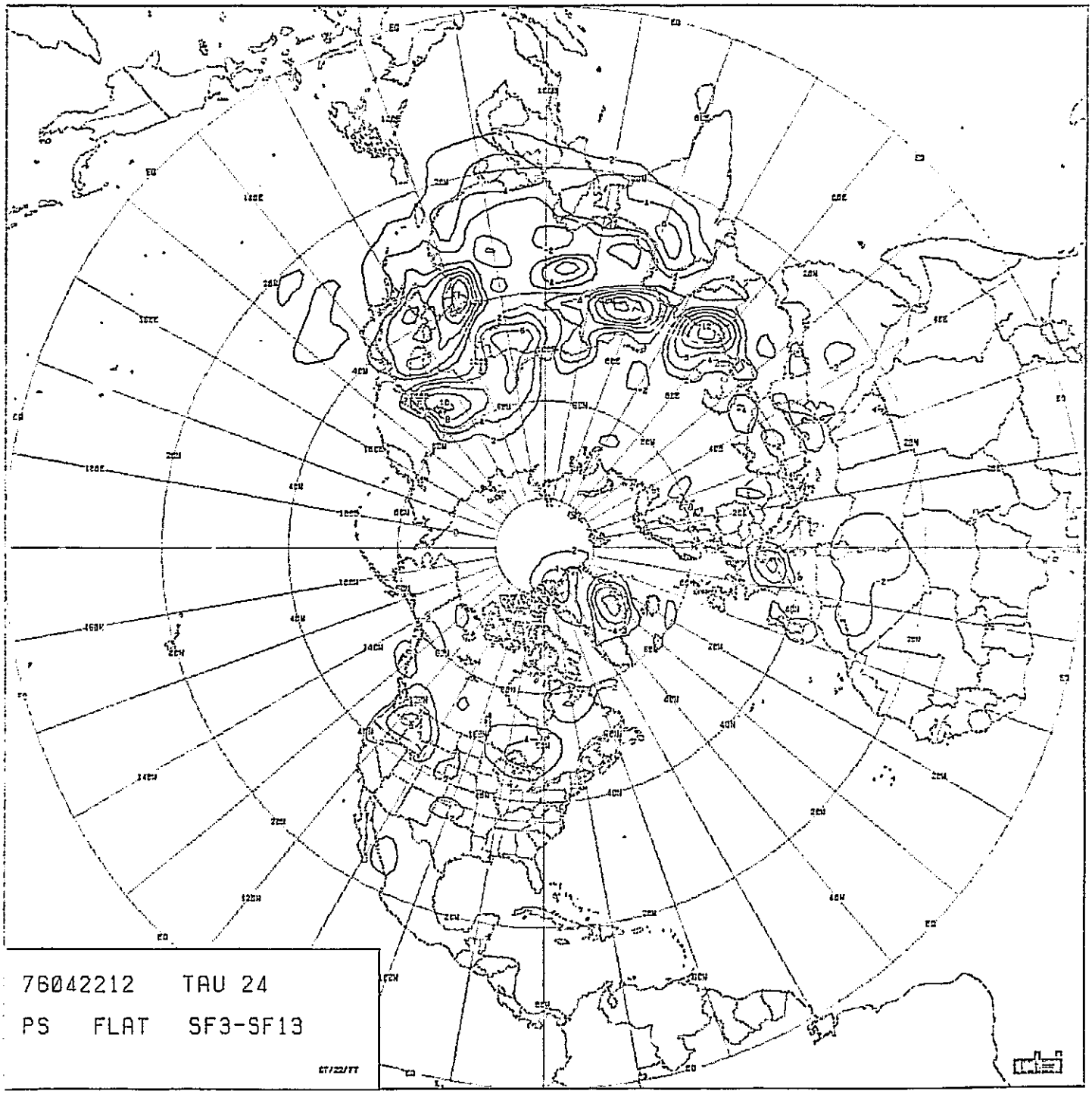

FIGURE IV-38: DIFFERENCE BETWEEN BASELINE AND SF13, SURFACE

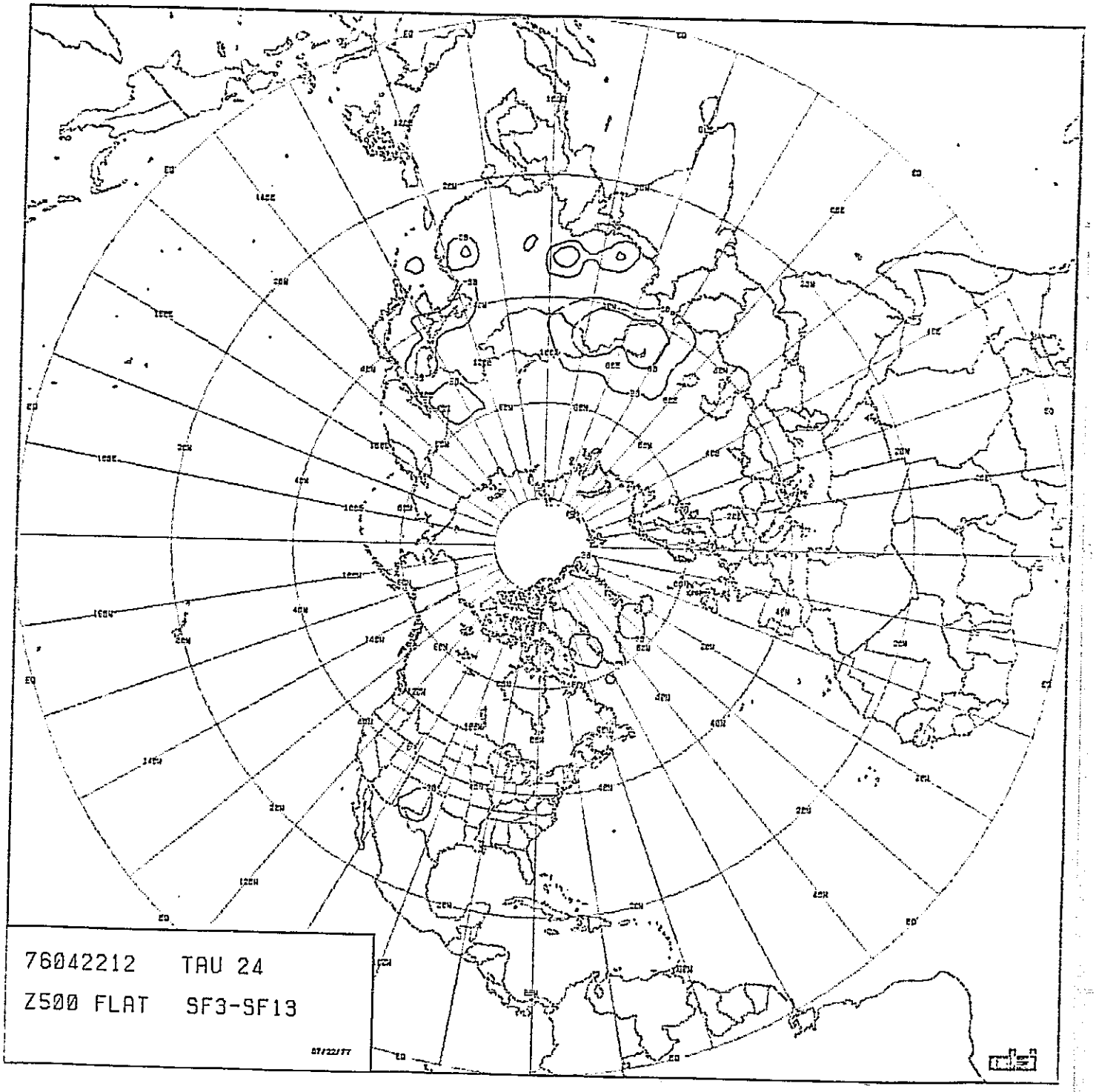

FIGURE IV-39: DIFFERENCE BETWEEN BASELINE AND SF13, 500mb

TABLE IV-11: ERROR STATISTICAL SUMMARY, SF13 (NO TERRAIN).

SURFACE

FROM	TO	RMS	SD	MEAN	MAX	MIN
0	10	.716E+00	.674E+00	.243E+00	.242E+01	-.154E+01
10	20	.127E+01	.127E+01	.108E+00	.406E+01	-.276E+01
20	30	.332E+01	.308E+01	.122E+01	.100E+02	-.610E+01
30	40	.391E+01	.365E+01	.141E+01	.135E+02	-.959E+01
40	50	.459E+01	.420E+01	.184E+01	.145E+02	-.895E+01
50	60	.435E+01	.324E+01	.290E+01	.118E+02	-.689E+01
60	70	.317E+01	.280E+01	.147E+01	.687E+01	-.780E+01
70	80	.365E+01	.356E+01	.811E+00	.102E+02	-.790E+01
80	90	.395E+01	.235E+01	.317E+01	.108E+02	.869E+00
0	90	.278E+01	.264E+01	.877E+00	.145E+02	-.959E+01

500 MB

FROM	TO	RMS	SD	MEAN	MAX	MIN
0	10	.165E+02	.146E+02	.772E+01	.543E+02	-.351E+02
10	20	.265E+02	.245E+02	.100E+02	.589E+02	-.496E+02
20	30	.221E+02	.190E+02	.112E+02	.792E+02	-.405E+02
30	40	.336E+02	.324E+02	.898E+01	.105E+03	-.116E+03
40	50	.445E+02	.442E+02	-.493E+01	.680E+02	-.165E+03
50	60	.344E+02	.327E+02	-.106E+02	.602E+02	-.127E+03
60	70	.318E+02	.273E+02	-.163E+02	.477E+02	-.901E+02
70	80	.423E+02	.218E+02	-.363E+02	-.317E+01	-.108E+03
80	90	.390E+02	.151E+02	-.359E+02	-.475E+01	-.618E+02
0	90	.278E+02	.274E+02	.438E+01	.105E+03	-.165E+03

L. No Precipitation (SF14)

The effects of "turning off" precipitation on the model are almost all in the lowest levels during the first 24 hours. This generally results in the reduction in the intensification of lows. In Figure IV-40, almost every low at the surface is less intense than in the corresponding baseline situation (see SF17 [section IV-N], following, for a comparison with the low relative humidity situation). Although this is a problem in some areas, such as the U.S. East coast low development, it tended to reduce the surface errors (Figure IV-41) as compared to the baseline. This reduction occurred because much of the baseline error was due to overly rapid system development and movement. By elimination of the precipitation mechanism, the energy of these systems was reduced, and less development and movement took place. The difference between the baseline and SF14 at the surface is seen in Figure IV-42.

Table IV-12 shows, inter alia, that for the entire northern hemisphere the RMS error is 2.42 mb for the surface SF14 vice 2.5 mb for the baseline, and that for SF14, the absolute maximum error shifted from positive to negative.

All of the above does not prove the necessity for eliminating precipitation from the model. The apparent

salubrious effects discussed above are fleeting, and as the model progresses through time, the lack of the precipitation mechanisms would lead to gross underdevelopment of systems.

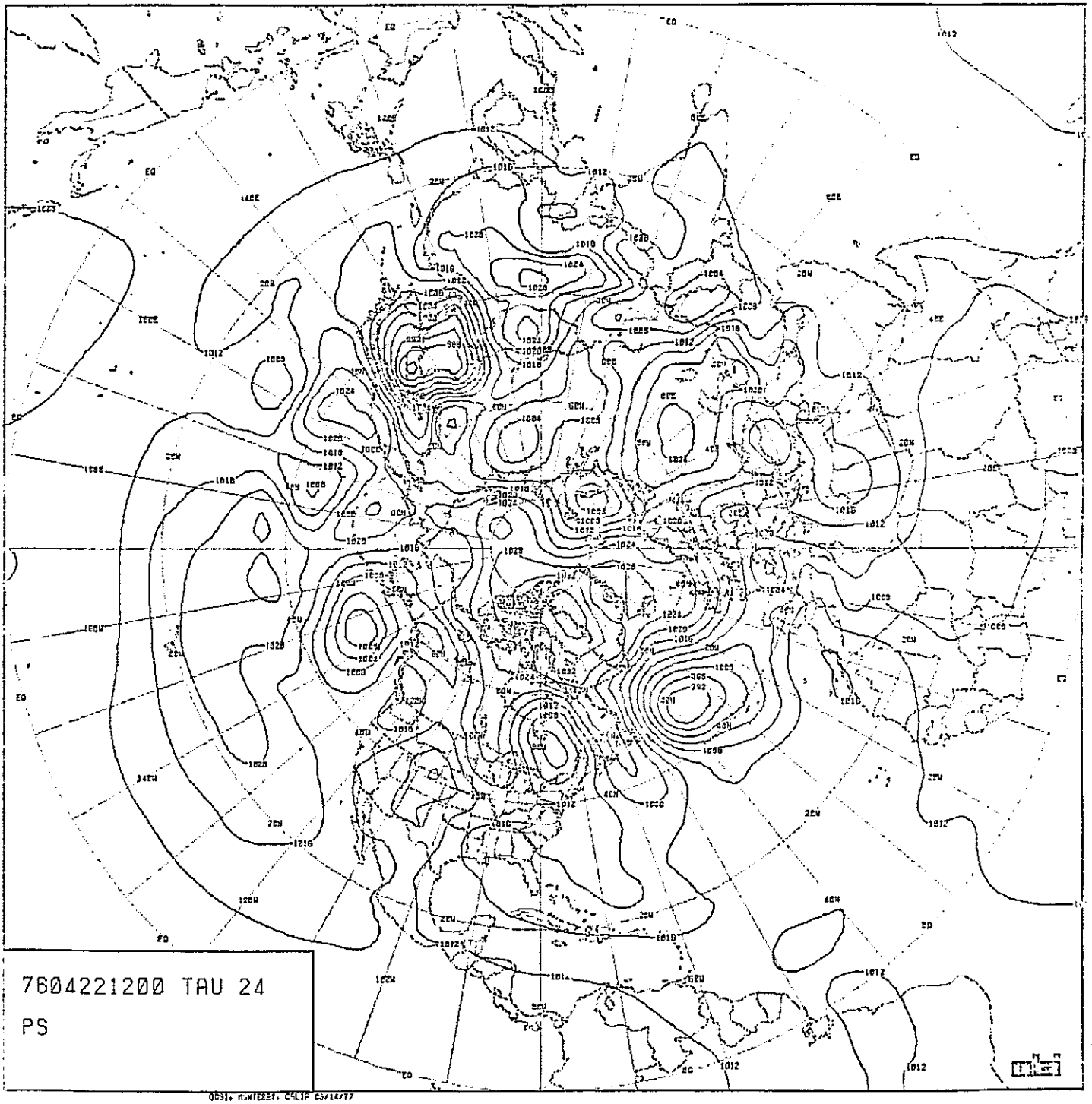

FIGURE IV-40: FORECAST, SURFACE, SF14

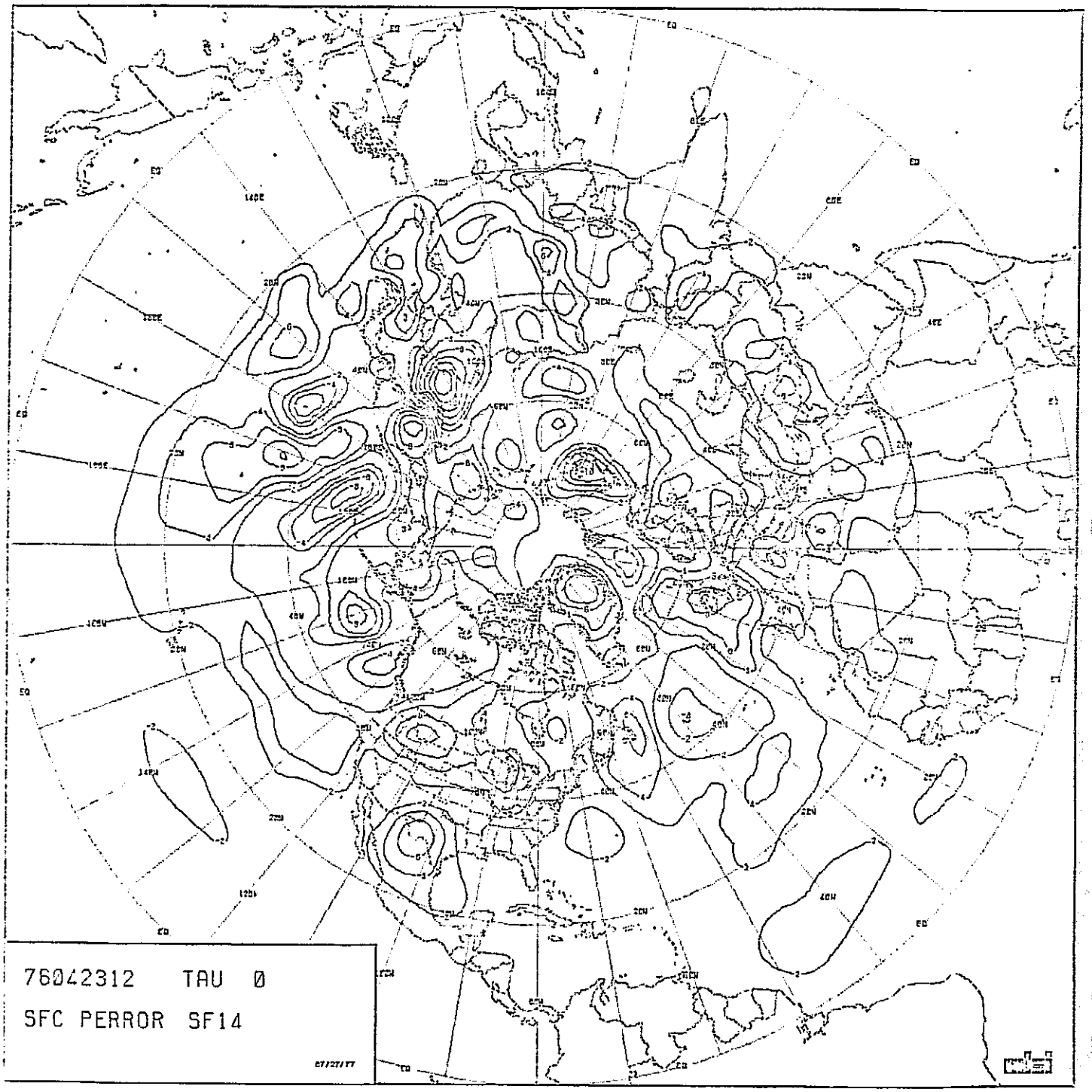

FIGURE IV-41: ERROR PATTERN, SURFACE, SF14

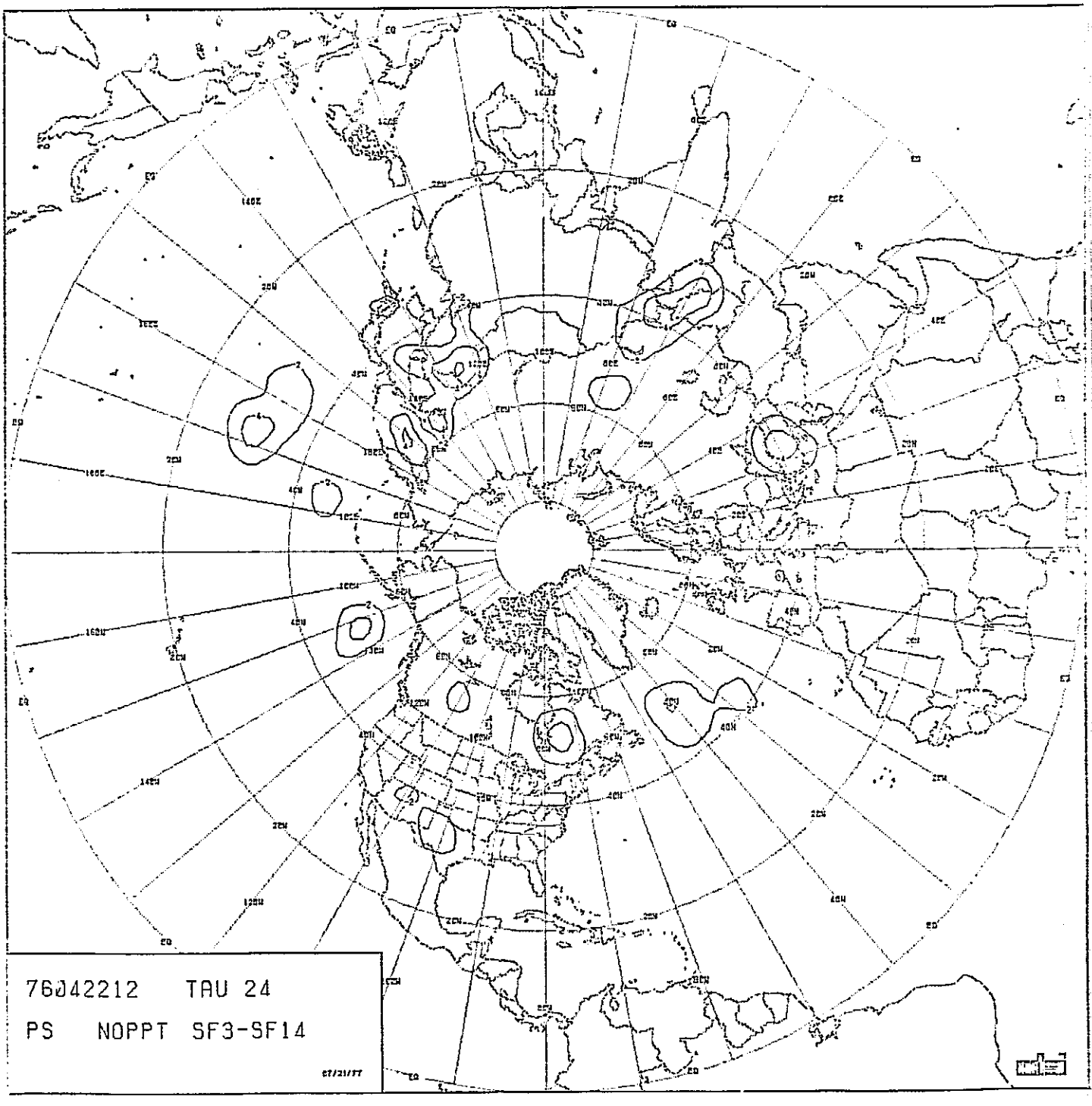

FIGURE IV-42: DIFFERENCE BETWEEN BASELINE AND SF14, SURFACE

TABLE IV-12: ERROR STATISTICAL SUMMARY, SF14 (NO PRECIPITATION).

SURFACE

FROM	TO	RMS	SD	MEAN	MAX	MIN
0	10	.718E+00	.674E+00	.248E+00	.247E+01	-.152E+01
10	20	.118E+01	.118E+01	.220E-01	.411E+01	-.282E+01
20	30	.276E+01	.272E+01	.467E+00	.779E+01	-.775E+01
30	40	.311E+01	.306E+01	.543E+00	.101E+02	-.760E+01
40	50	.357E+01	.343E+01	.999E+00	.889E+01	-.125E+02
50	60	.432E+01	.381E+01	.203E+01	.102E+02	-.131E+02
60	70	.351E+01	.288E+01	.200E+01	.801E+01	-.717E+01
70	80	.390E+01	.370E+01	.123E+01	.933E+01	-.937E+01
80	90	.262E+01	.159E+01	.208E+01	.609E+01	-.788E+00
0	90	.242E+01	.236E+01	.545E+00	.102E+02	-.131E+02

500 MB

FROM	TO	RMS	SD	MEAN	MAX	MIN
0	10	.166E+02	.147E+02	.774E+01	.551E+02	-.348E+02
10	20	.270E+02	.249E+02	.105E+02	.629E+02	-.492E+02
20	30	.242E+02	.192E+02	.148E+02	.644E+02	-.412E+02
30	40	.373E+02	.329E+02	.176E+02	.129E+03	-.109E+03
40	50	.470E+02	.461E+02	.908E+01	.110E+03	-.155E+03
50	60	.329E+02	.327E+02	.362E+01	.736E+02	-.108E+03
60	70	.244E+02	.240E+02	-.403E+01	.578E+02	-.822E+02
70	80	.367E+02	.224E+02	-.290E+02	.125E+02	-.975E+02
80	90	.406E+02	.117E+02	-.389E+02	-.201E+02	-.621E+02
0	90	.285E+02	.271E+02	.873E+01	.129E+03	-.155E+03

M. Balance Wind Initialization (SF16)

The initialization of the winds by solution of the balance equation rather than by the analysis of wind fields produced a meteorologically good forecast that resembles the baseline in most respects. The one notable exception at the surface was in the development and movement of the East Asia low, as seen in Figure IV-43. SF16 avoided the false development of the trough west of Kamchatka and thereby eliminated the error in that area. It failed, however, to move the main center of the low sufficiently eastward which lead to a new area of error as seen in Figure IV-44. Figure IV-45 shows that there are only slight differences between the baseline and SF16 elsewhere at the surface.

At 500 mb, Figure IV-46, the departures from the baseline are even more subtle and tend to be associated with the East Asia low position and intensity as well as the slope of the trough south of Korea. The error pattern, Figure IV-47, shows some variations from the baseline in that the errors are less severe over China and slightly greater south of Kamchatka and over Korea. This variation shows up on Figure IV-48.

Although the summary of errors for SF16 (Table IV-13) shows a greater degree of error than the baseline, the difference is not significant.

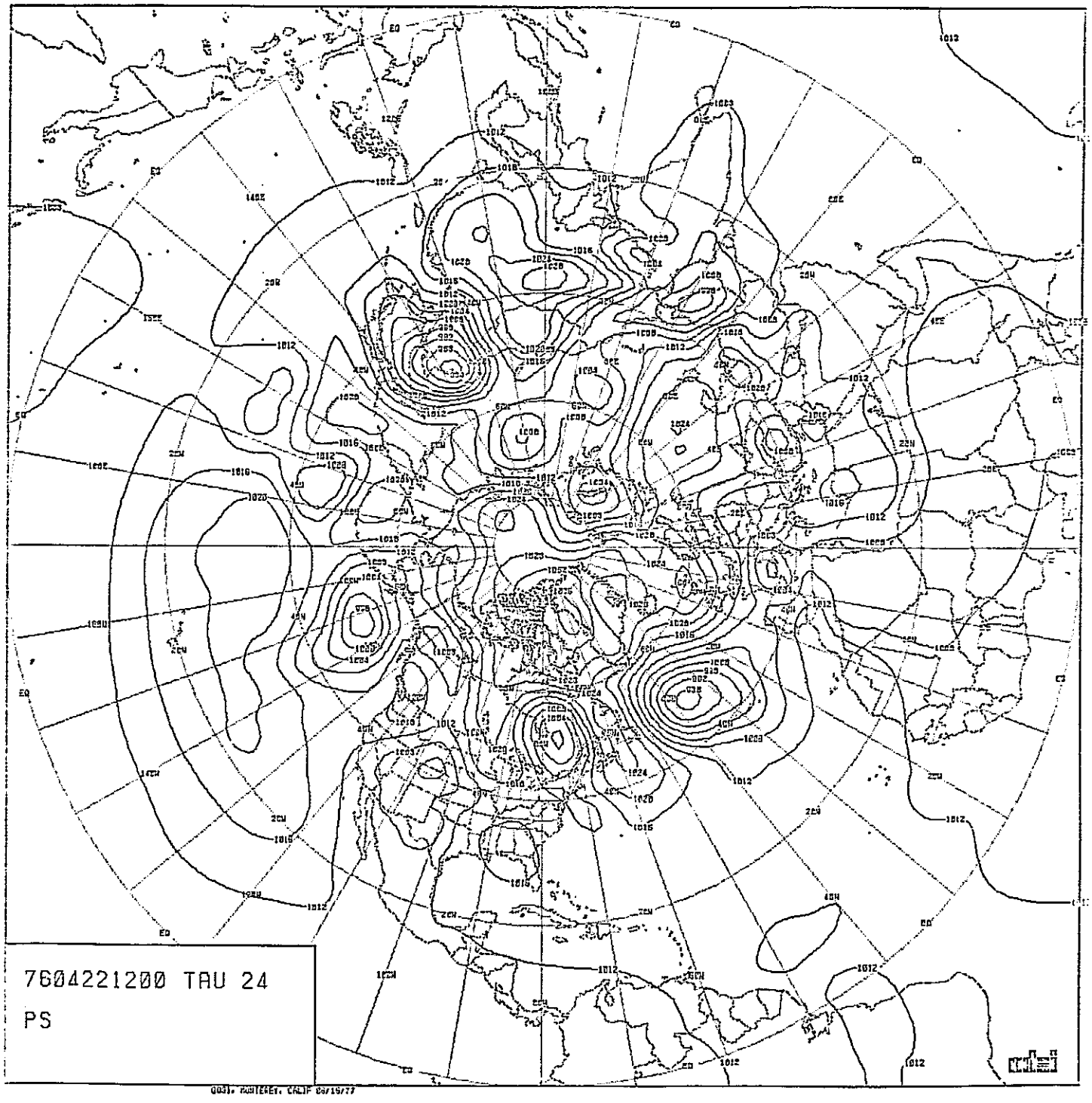

FIGURE IV-43: FORECAST, SURFACE, SF16

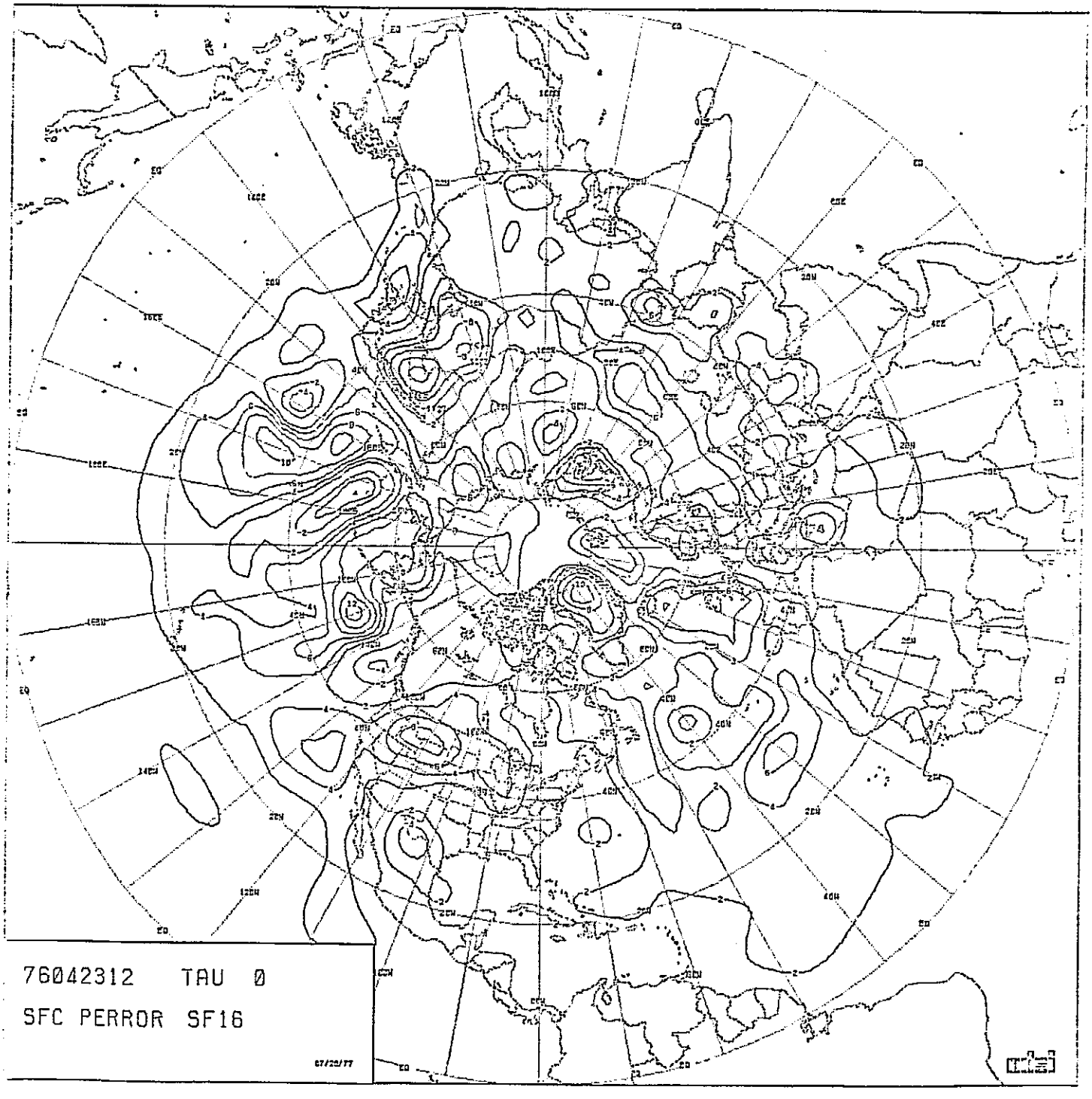

FIGURE IV-44: ERROR PATTERN, SURFACE, SF16

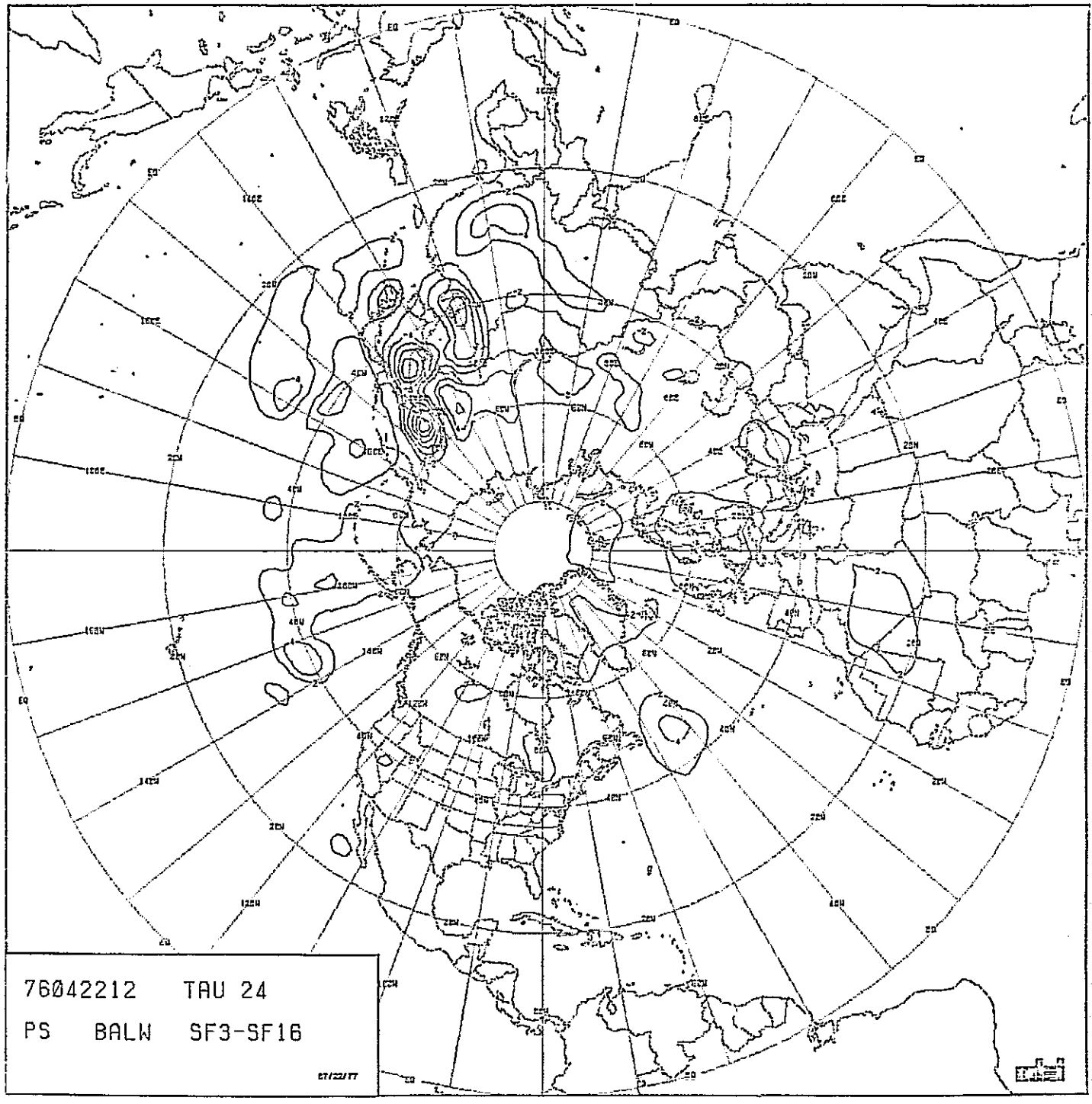

FIGURE IV-45: DIFFERENCE BETWEEN BASELINE AND SF16, SURFACE

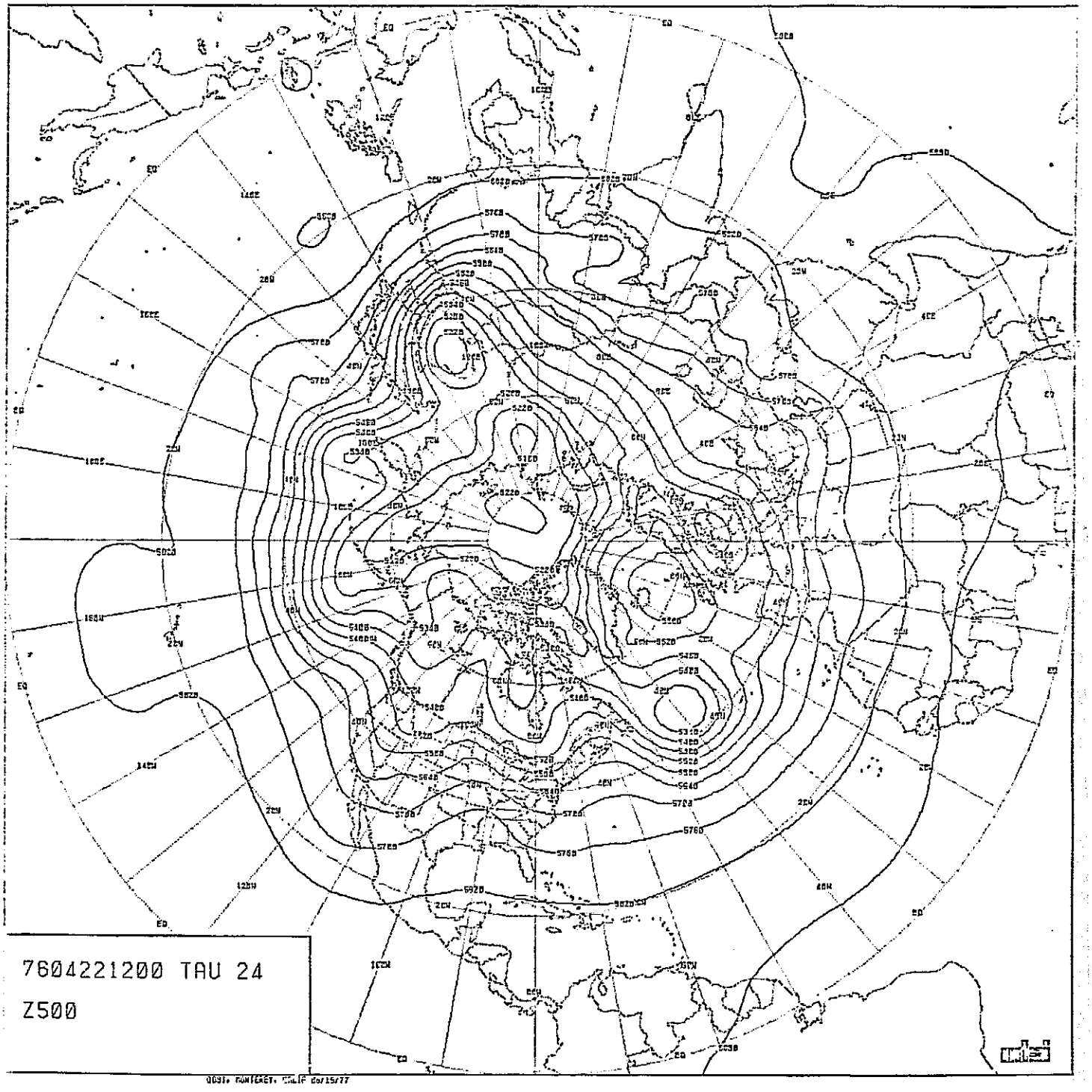

FIGURE IV-46: FORECAST, 500mb, SF16

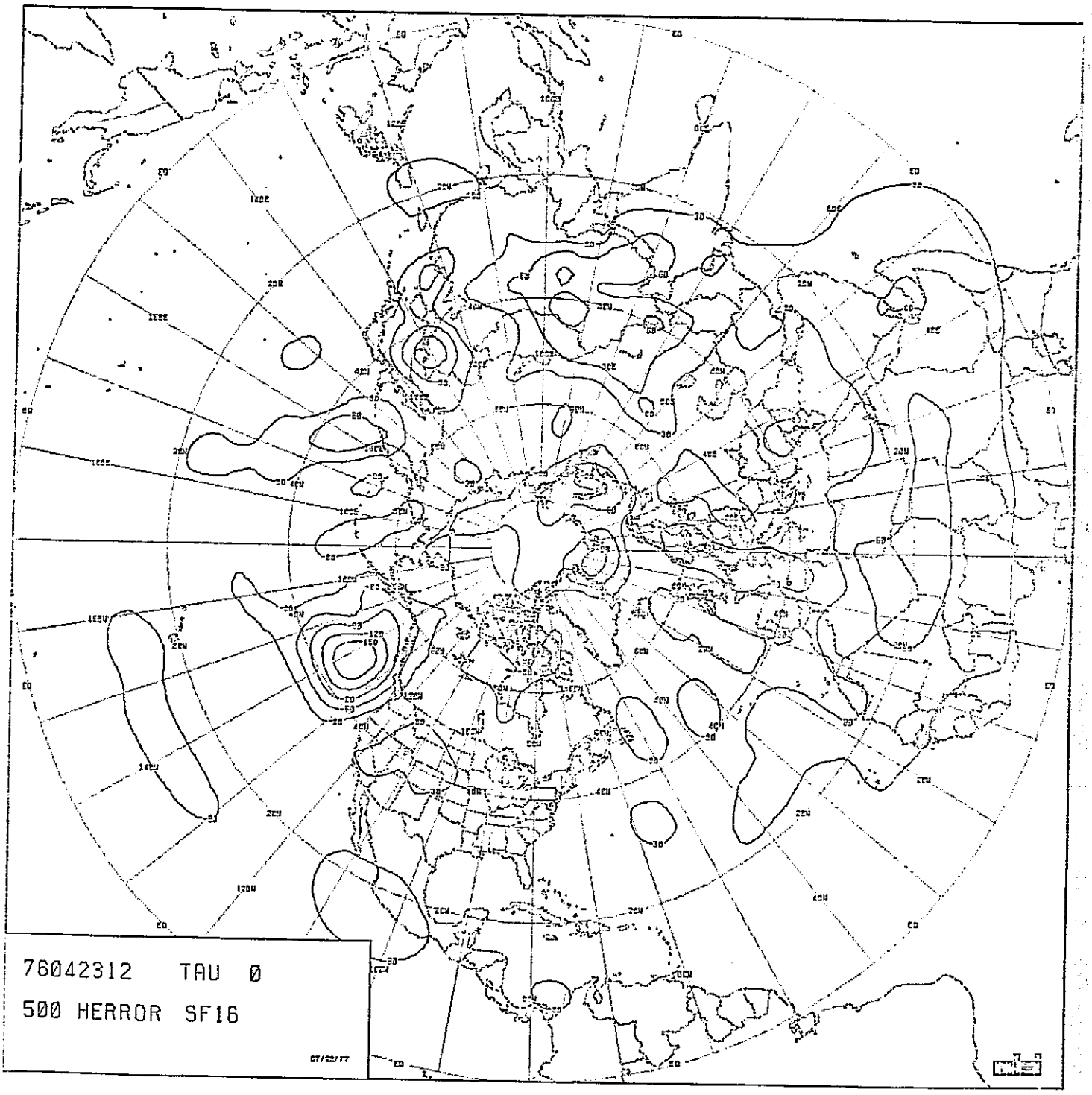

FIGURE IV-47: ERROR PATTERN, 500mb, SF16

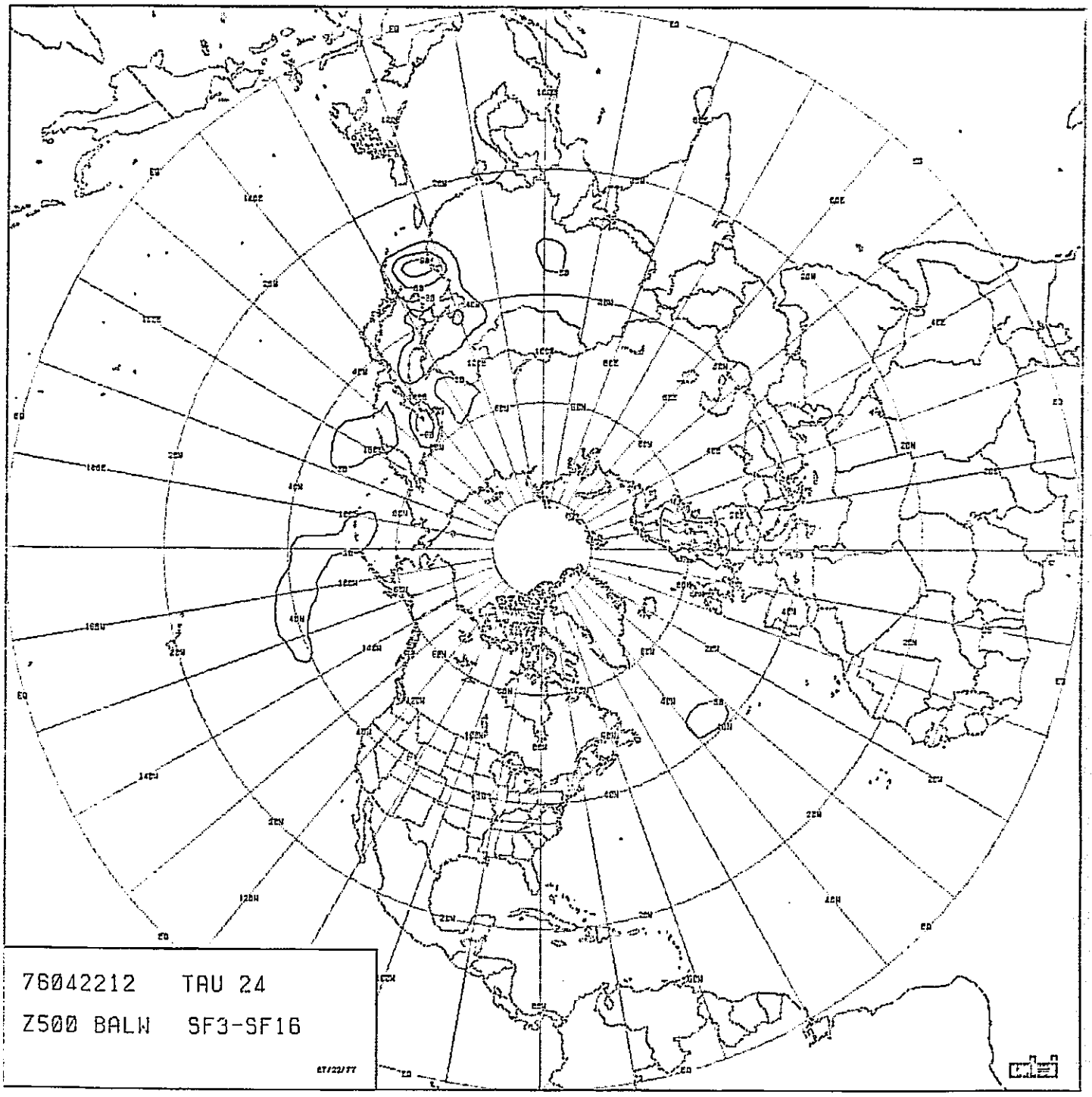

FIGURE IV-48: DIFFERENCE BETWEEN BASELINE AND SF16, 500mb

TABLE IV-13: ERROR STATISTICAL SUMMARY, SF16 (BALANCED WINDS).

SURFACE

FROM	TO	RMS	SD	MEAN	MAX	MIN
0	10	.701E+00	.635E+00	.297E+00	.256E+01	-.121E+01
10	20	.123E+01	.111E+01	.520E+00	.347E+01	-.243E+01
20	30	.259E+01	.232E+01	.115E+01	.913E+01	-.496E+01
30	40	.342E+01	.305E+01	.154E+01	.109E+02	-.616E+01
40	50	.433E+01	.399E+01	.168E+01	.127E+02	-.105E+02
50	60	.413E+01	.310E+01	.273E+01	.112E+02	-.554E+01
60	70	.367E+01	.294E+01	.220E+01	.952E+01	-.704E+01
70	80	.412E+01	.402E+01	.901E+00	.111E+02	-.863E+01
80	90	.248E+01	.214E+01	.126E+01	.561E+01	-.321E+01
0	90	.254E+01	.235E+01	.982E+00	.127E+02	-.105E+02

500 MB

FROM	TO	RMS	SD	MEAN	MAX	MIN
0	10	.169E+02	.148E+02	.815E+01	.604E+02	-.263E+02
10	20	.305E+02	.254E+02	.169E+02	.738E+02	-.380E+02
20	30	.295E+02	.213E+02	.204E+02	.812E+02	-.412E+02
30	40	.339E+02	.311E+02	.134E+02	.955E+02	-.903E+02
40	50	.508E+02	.507E+02	.263E+01	.101E+03	-.174E+03
50	60	.362E+02	.362E+02	.138E+01	.691E+02	-.130E+03
60	70	.255E+02	.247E+02	-.608E+01	.409E+02	-.768E+02
70	80	.438E+02	.258E+02	-.353E+02	.129E+02	-.104E+03
80	90	.482E+02	.158E+02	-.456E+02	-.949E+01	-.776E+02
0	90	.307E+02	.291E+02	.968E+01	.101E+03	-.174E+03

N. Relative Humidity at 25% (SF17)

Rather than determine the initial relative humidity on the basis of system intensity, SF17 set the relative humidity at 25% over the entire map at the three lowest levels.

The effect of this initialization was noticed primarily at the surface since the normal initial condition at the highest moisture level is of about the 25% magnitude. If the forecast extended much beyond 24 hours, however, changes in the upper levels would have become evident.

The majority of the errors in the baseline were due to a combination of incorrect central pressures and system locations. SF17 did not greatly change system location but had an inhibiting effect upon developing systems, as can be seen in Figure IV-49 where the central pressures of the Gulf of Alaska low and the East Asia low are both about 4 mb higher than in the baseline. This can also be seen in Figure IV-50 by the reduced error in these locations, and in Figure IV-51 where the difference between the baseline and SF17 is at least 4 mb in several locations. These reductions in error are due principally to a loosening of gradient rather than better forecasts.

The differences between the baseline and SF17 at 500 mb are generally less than 30M. The statistical error summary for SF17, Table IV-14, shows a slight reduction in the overall RMS and a shift of the absolute maximum to the negative.

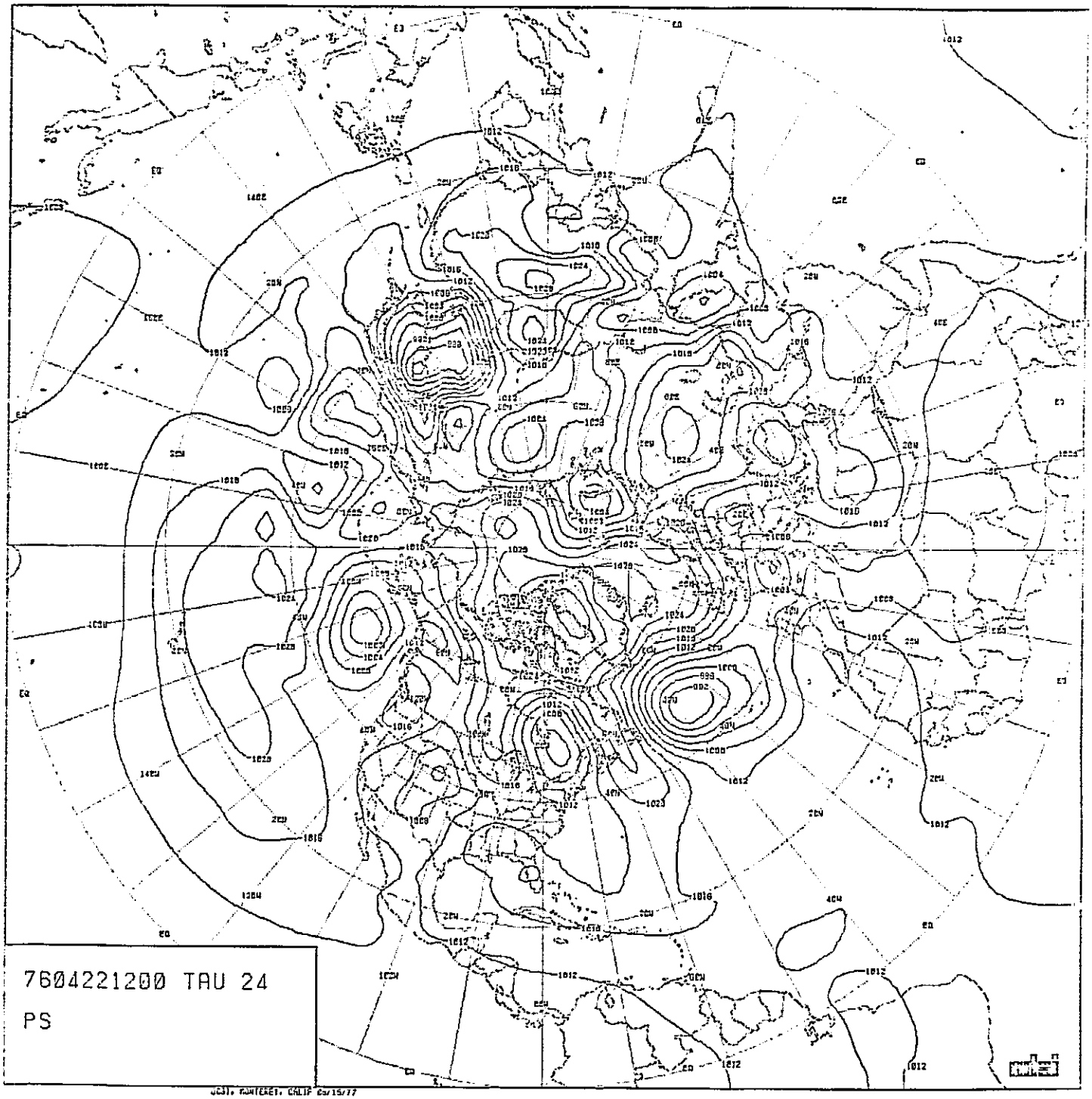

FIGURE IV-49: FORECAST, SURFACE, SF17

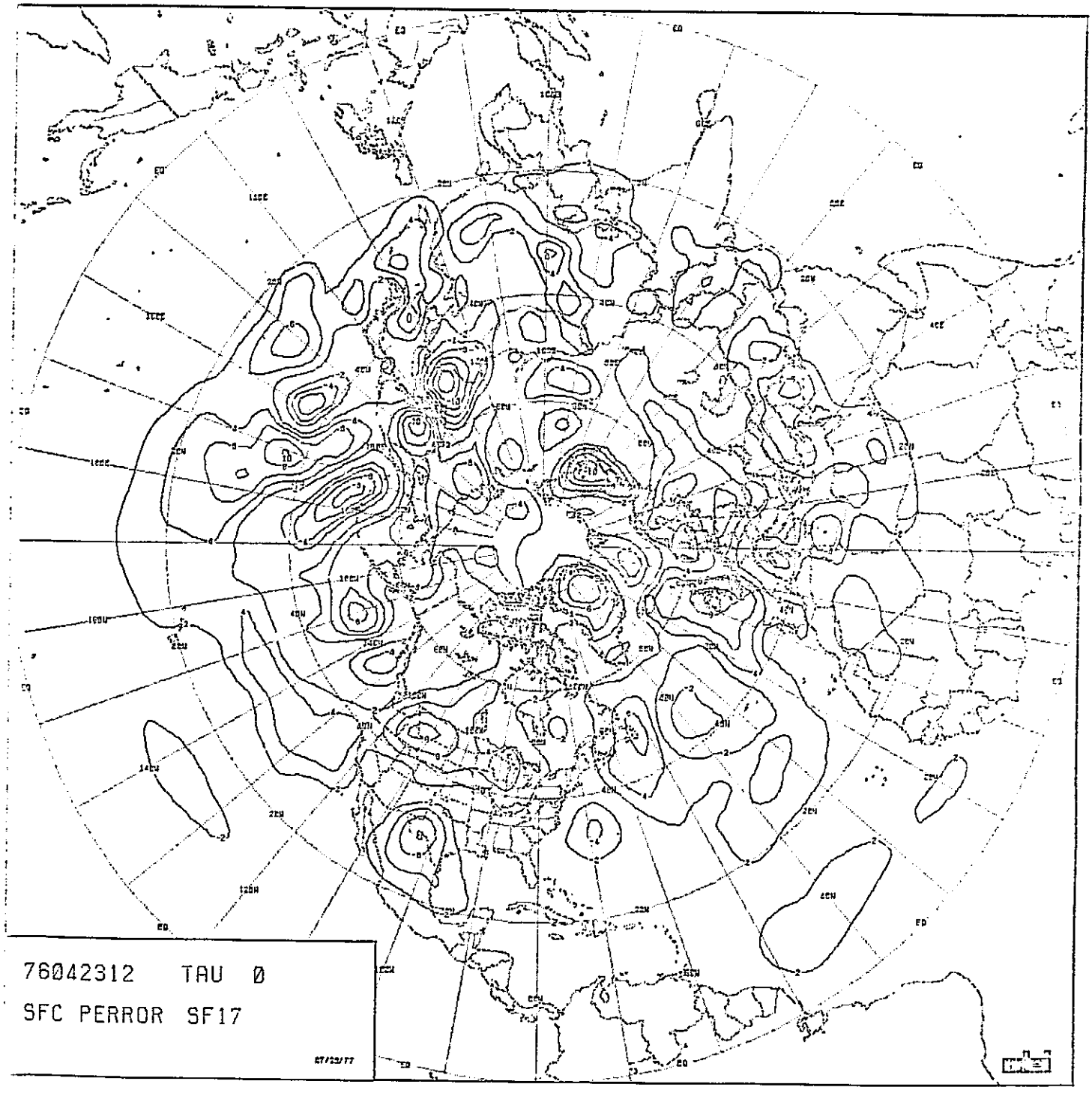

FIGURE IV-50: ERROR PATTERN, SURFACE, SF17

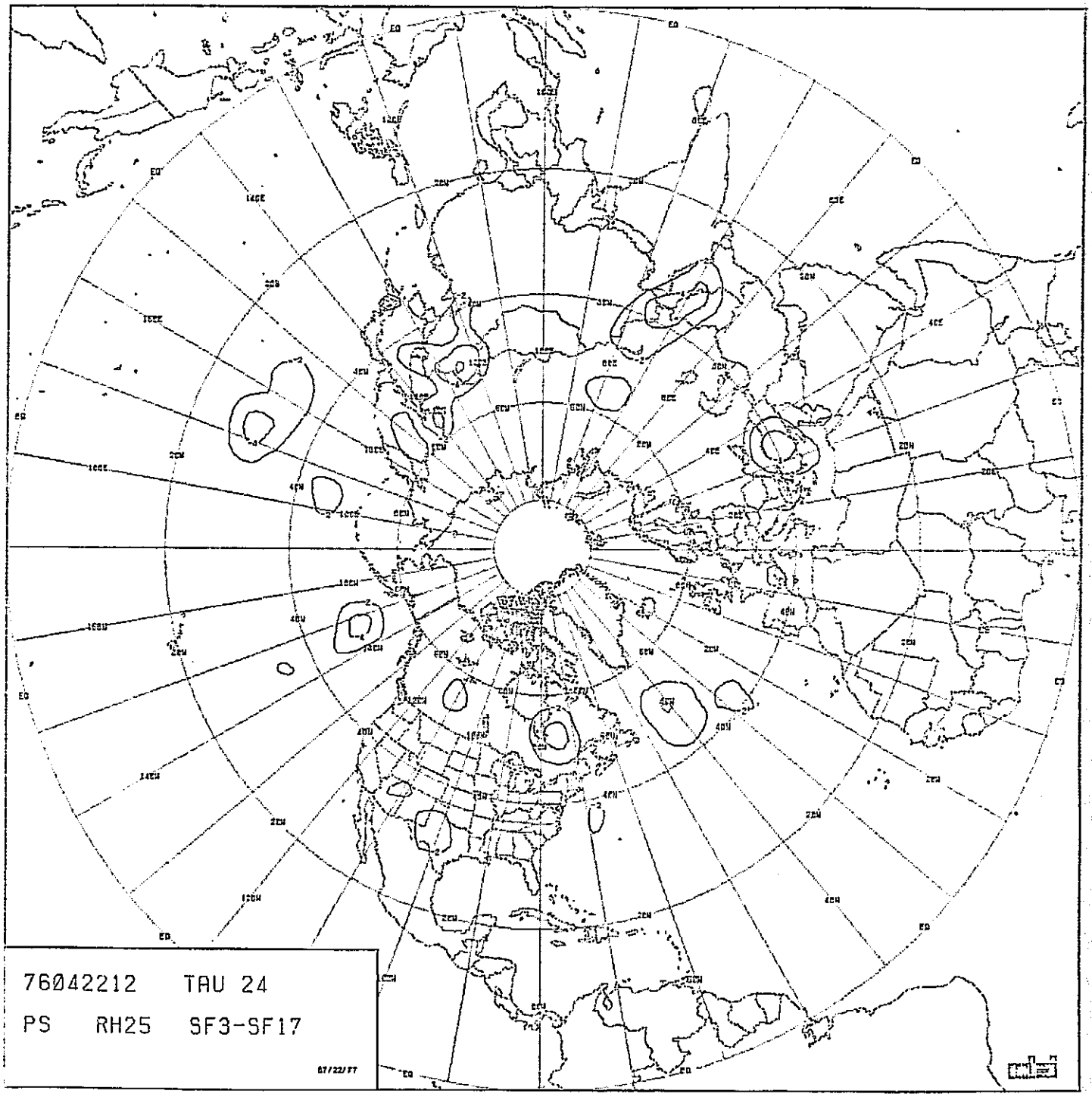

FIGURE IV-51: DIFFERENCE BETWEEN BASELINE AND SF17, SURFACE

TABLE IV-14: ERROR STATISTICAL SUMMARY, SF17
(RELATIVE HUMIDITY = 25%).

SURFACE

FROM	TO	RMS	SD	MEAN	MAX	MIN
0	10	.717E+00	.673E+00	.247E+00	.246E+01	-.153E+01
10	20	.118E+01	.118E+01	.155E-01	.409E+01	-.285E+01
20	30	.278E+01	.274E+01	.486E+00	.793E+01	-.812E+01
30	40	.309E+01	.303E+01	.585E+00	.102E+02	-.721E+01
40	50	.359E+01	.343E+01	.104E+01	.874E+01	-.123E+02
50	60	.430E+01	.378E+01	.205E+01	.105E+02	-.127E+02
60	70	.350E+01	.287E+01	.201E+01	.799E+01	-.712E+01
70	80	.388E+01	.369E+01	.121E+01	.934E+01	-.940E+01
80	90	.262E+01	.159E+01	.208E+01	.606E+01	-.855E+00
0	90	.242E+01	.236E+01	.555E+00	.105E+02	-.127E+02

500 MB

FROM	TO	RMS	SD	MEAN	MAX	MIN
0	10	.166E+02	.147E+02	.773E+01	.551E+02	-.348E+02
10	20	.270E+02	.249E+02	.105E+02	.630E+02	-.492E+02
20	30	.243E+02	.193E+02	.148E+02	.649E+02	-.414E+02
30	40	.373E+02	.329E+02	.176E+02	.128E+03	-.109E+03
40	50	.471E+02	.463E+02	.897E+01	.110E+03	-.156E+03
50	60	.328E+02	.326E+02	.346E+01	.741E+02	-.108E+03
60	70	.245E+02	.241E+02	-.419E+01	.583E+02	-.823E+02
70	80	.367E+02	.224E+02	-.291E+02	.125E+02	-.973E+02
80	90	.408E+02	.118E+02	-.390E+02	-.209E+02	-.622E+02
0	90	.285E+02	.272E+02	.868E+01	.128E+03	-.156E+03

O. Relative Humidity at 75% (SF18)

The over-specification of initial relative humidity in SF18 introduced large errors in two surface locations (see Figure IV-52). The East Asian low, which is undergoing rapid development and movement, has these processes accelerated. Where there is some overdevelopment of troughs to the east and north of this system in the baseline, SF18 has a 975 mb low form in the east and a 1000 mb low form to the north. The other location is over North Africa. What was merely a trough over Tunisia on the baseline became a 1000-mb low when excessive moisture was introduced.

Figure IV-53 shows surface error patterns for SF18. Most of the errors are greater than for the baseline, but a few selected systems, such as the Gulf of Alaska low, show a decrease in error. The difference between the baseline and SF18 at the surface, Figure IV-54, clearly shows the selectivity of the departure from baseline. The differences between the baseline and SF18 at 500 mb were generally less than 30M.

As would be expected, the error summary, Table IV-15, shows fairly sizeable increases in error at the surface.

One should note that overspecifying the amount of moisture, especially in rapidly developing systems, can greatly affect the model forecast.

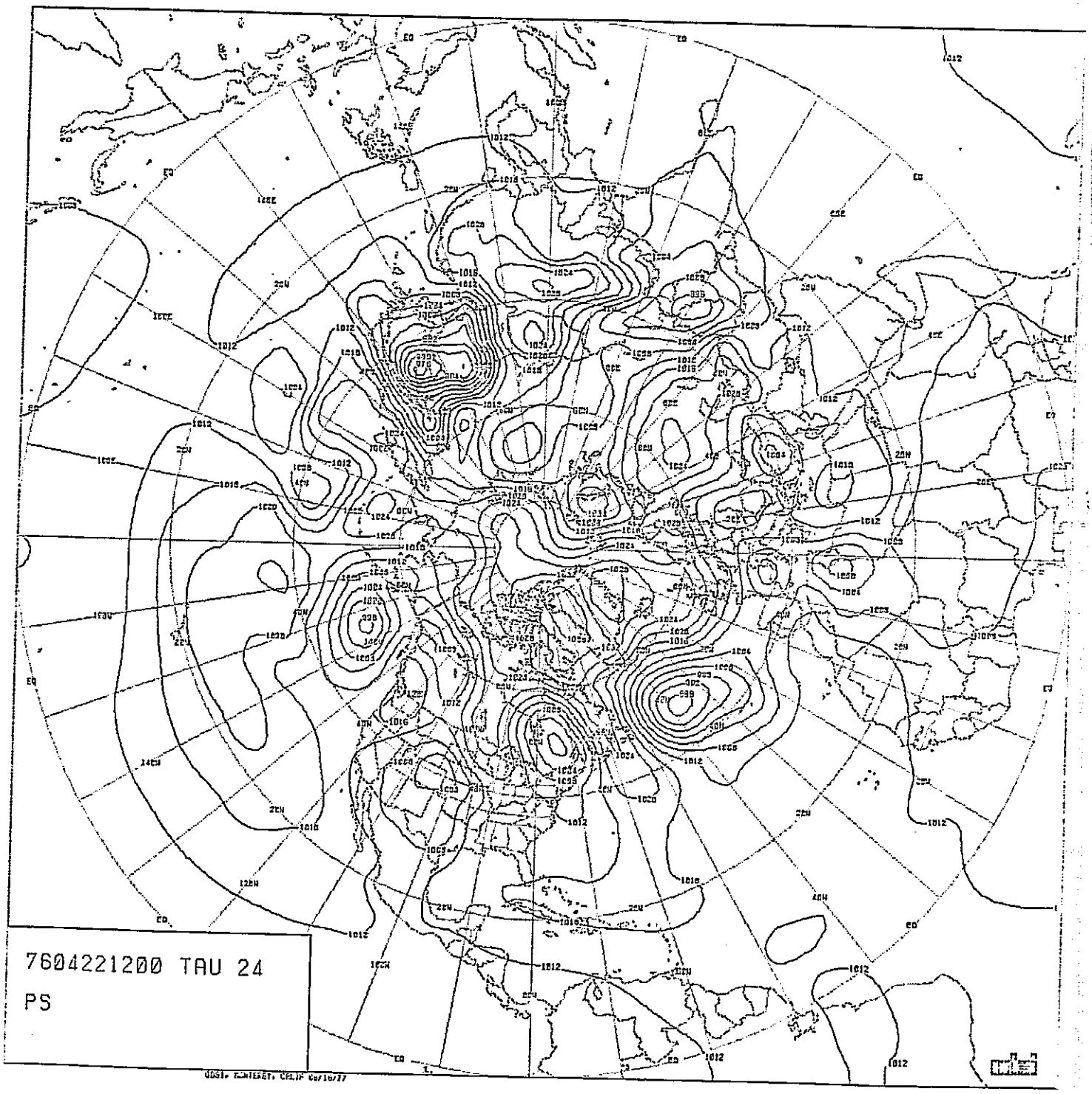

FIGURE IV-52: FORECAST, SURFACE, SF18

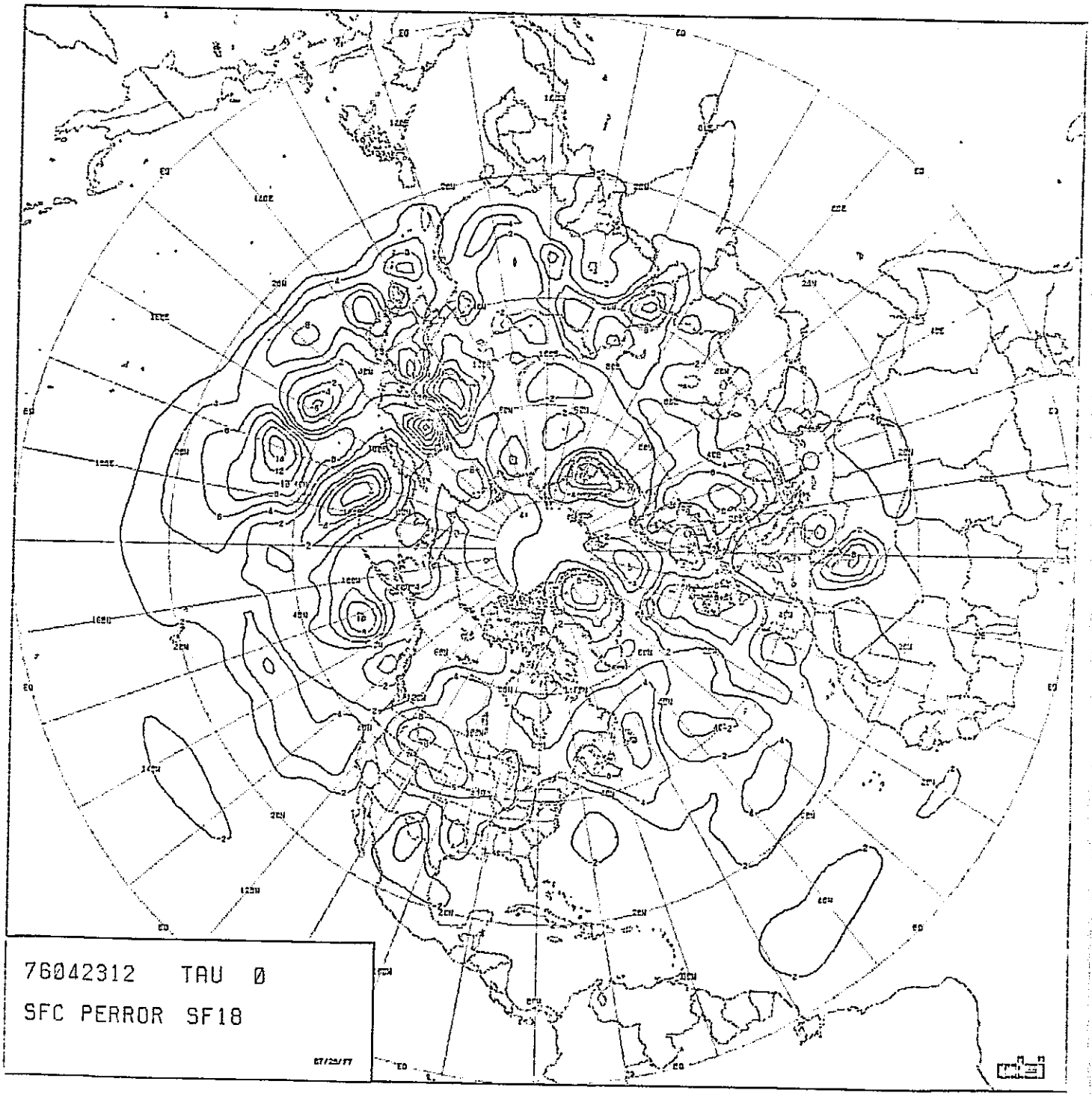

FIGURE IV-53: ERROR PATTERN, SURFACE, SF18

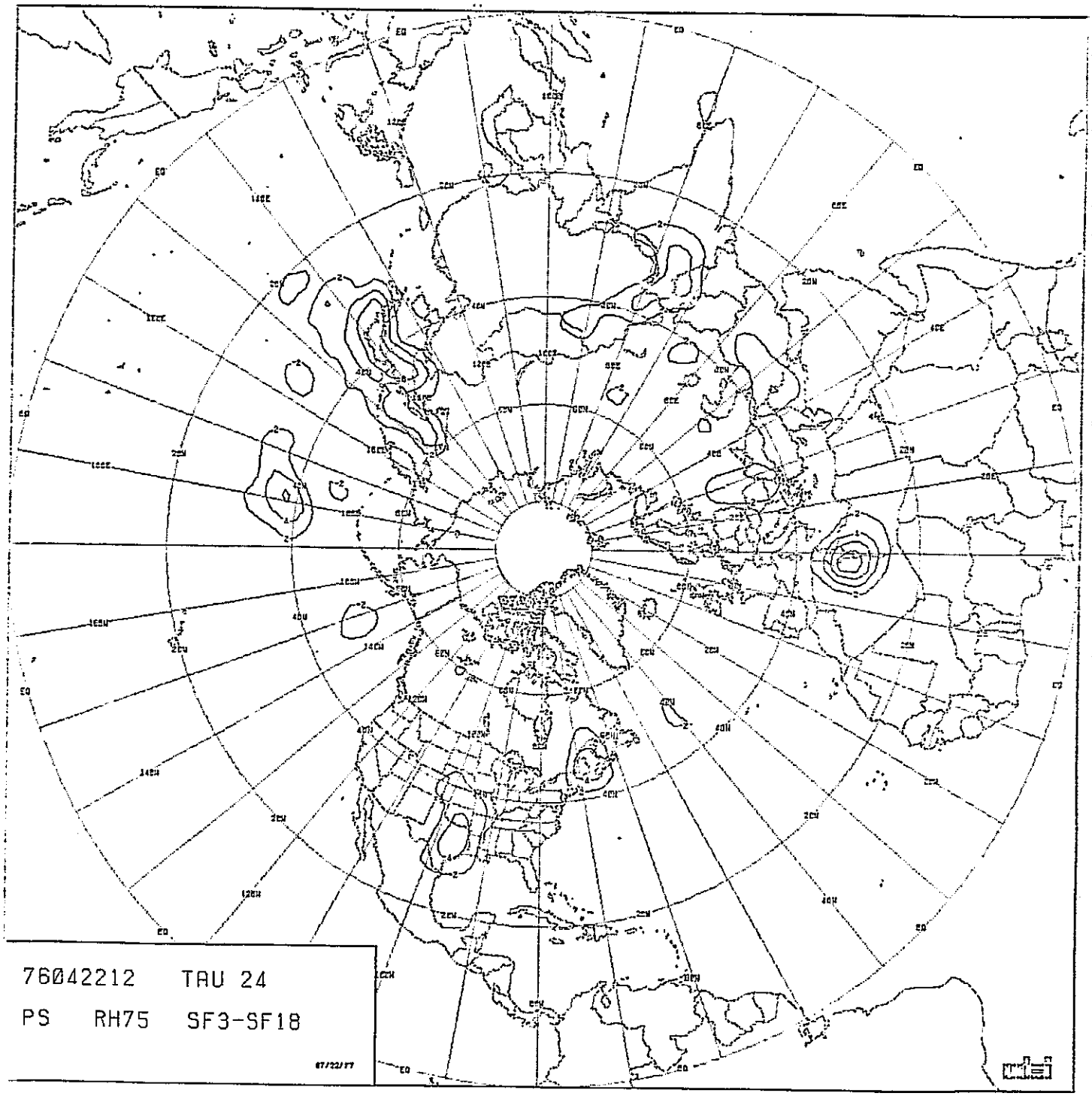

FIGURE IV-54: DIFFERENCE BETWEEN BASELINE AND SF18, SURFACE

TABLE IV-15: ERROR STATISTICAL SUMMARY, SF18
(RELATIVE HUMIDITY = 75%).

SURFACE

FROM	TO	RMS	SD	MEAN	MAX	MIN
0	10	.706E+00	.673E+00	.214E+00	.241E+01	-.162E+01
10	20	.116E+01	.116E+01	.216E-01	.423E+01	-.292E+01
20	30	.294E+01	.269E+01	.117E+01	.983E+01	-.483E+01
30	40	.406E+01	.333E+01	.232E+01	.146E+02	-.578E+01
40	50	.410E+01	.324E+01	.251E+01	.972E+01	-.935E+01
50	60	.440E+01	.365E+01	.246E+01	.170E+02	-.941E+01
60	70	.322E+01	.276E+01	.167E+01	.730E+01	-.721E+01
70	80	.369E+01	.360E+01	.783E+00	.884E+01	-.924E+01
80	90	.227E+01	.155E+01	.166E+01	.557E+01	-.119E+01
0	90	.265E+01	.247E+01	.972E+00	.170E+02	-.941E+01

500 MB

FROM	TO	RMS	SD	MEAN	MAX	MIN
0	10	.164E+02	.147E+02	.741E+01	.538E+02	-.356E+02
10	20	.265E+02	.249E+02	.915E+01	.625E+02	-.501E+02
20	30	.226E+02	.196E+02	.113E+02	.636E+02	-.487E+02
30	40	.364E+02	.345E+02	.114E+02	.117E+03	-.112E+03
40	50	.477E+02	.476E+02	.325E+01	.109E+03	-.164E+03
50	60	.347E+02	.346E+02	-.334E+01	.109E+03	-.119E+03
60	70	.257E+02	.238E+02	-.963E+01	.534E+02	-.669E+02
70	80	.402E+02	.222E+02	-.335E+02	.911E+01	-.102E+03
80	90	.441E+02	.115E+02	-.426E+02	-.242E+02	-.650E+02
0	90	.284E+02	.278E+02	.580E+01	.117E+03	-.164E+03

P. Modified Truncation/No Terrain Tapering (SF19)

SF19 was run with two computational devices modified. One modification was to reduce the truncation tendency linearly from 1 to .5 between 20°N and 5°N and then have a constant .5 south of 5°N. The other modification is to retain the full (smoothed) terrain heights up to the map borders.

Not surprisingly, SF19 produced large areas of undesirable patterns. Figure IV-55 shows that at the surface these are evident south of 20°N. Figure IV-56 shows that these patterns introduced errors as large as 12 mb.

In spite of the fact that the devices were only modified south of 20°N, the departure from the baseline extended north of 60°N in 24 hours as is evident in Figure IV-57. In 72 hours, the entire domain would be strongly disturbed by these modifications.

At 500 mb, Figure IV-58, some irregularities are observed below 20°N that do not appear to be as intense as those seen at the surface. Figure IV-59 illustrates that these errors are not much more than 60M greater than the errors of the baseline. This slight departure is even more readily apparent in Figure IV-60.

Although both truncation and terrain modifications were introduced to SF19, it appears that the truncation factor was far more critical. This is assumed by the facts that: terrain

does not influence greatly the upper levels but in SF19 the 500 mb is affected; the area below 20°N is predominantly sea level; and areas over land do not appear to be more adversely affected than do the ocean areas.

In Table IV-16, the RMS errors are greater than the baseline at the surface at every latitude band. At 500 mb, it exceeds the baseline up to 60°N.

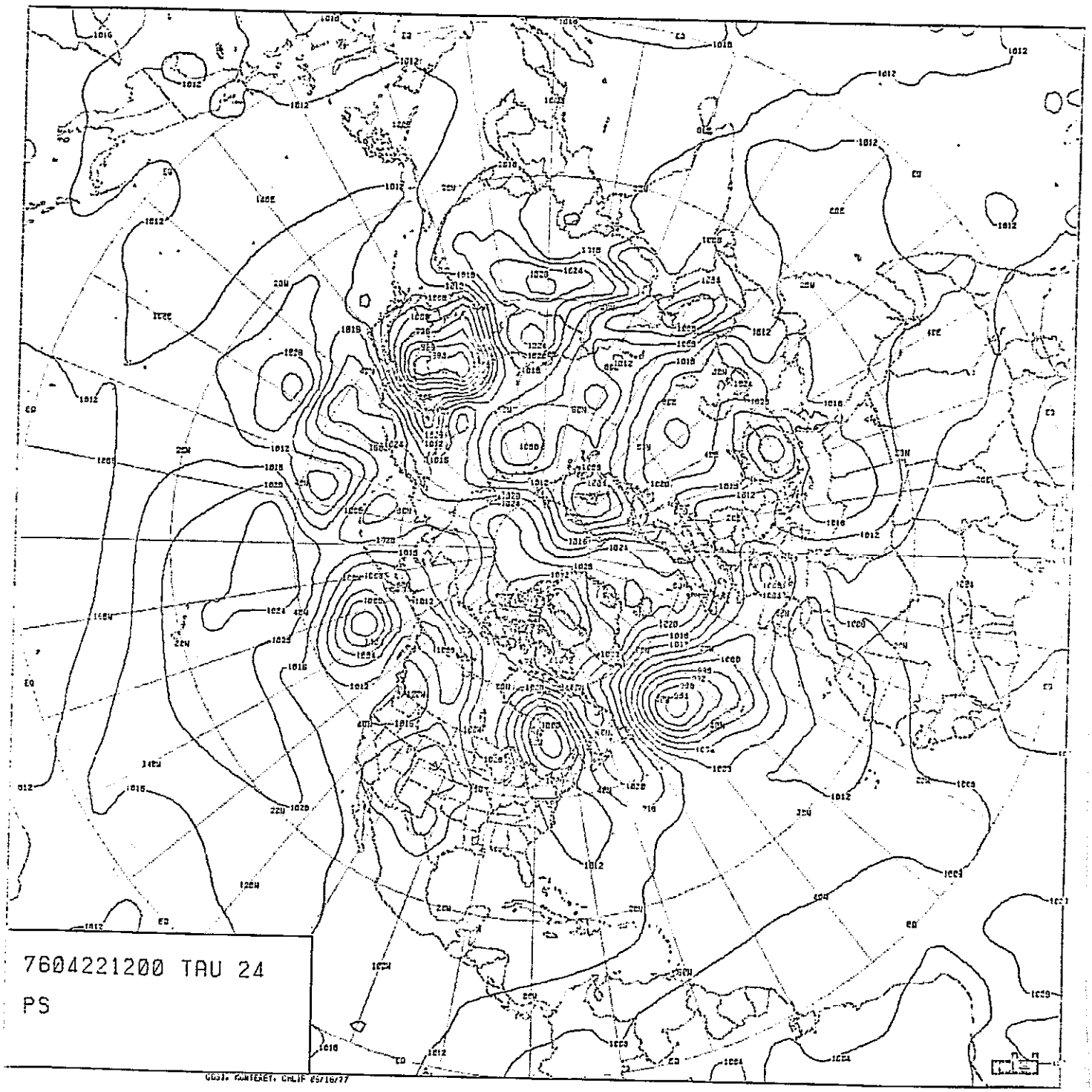

FIGURE IV-55: FORECAST, SURFACE, SF19

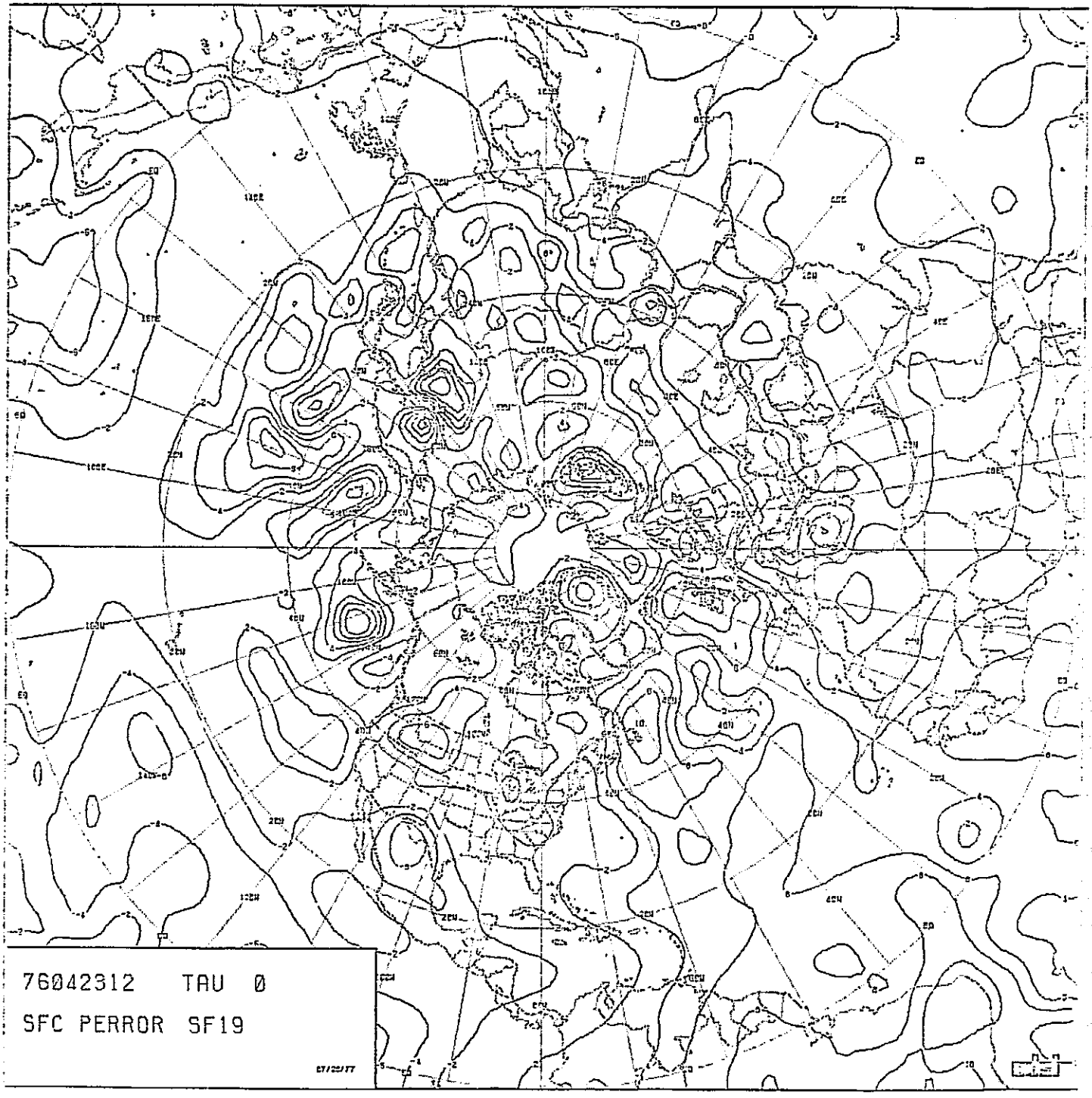

FIGURE IV-56: ERROR PATTERN, SURFACE, SF19

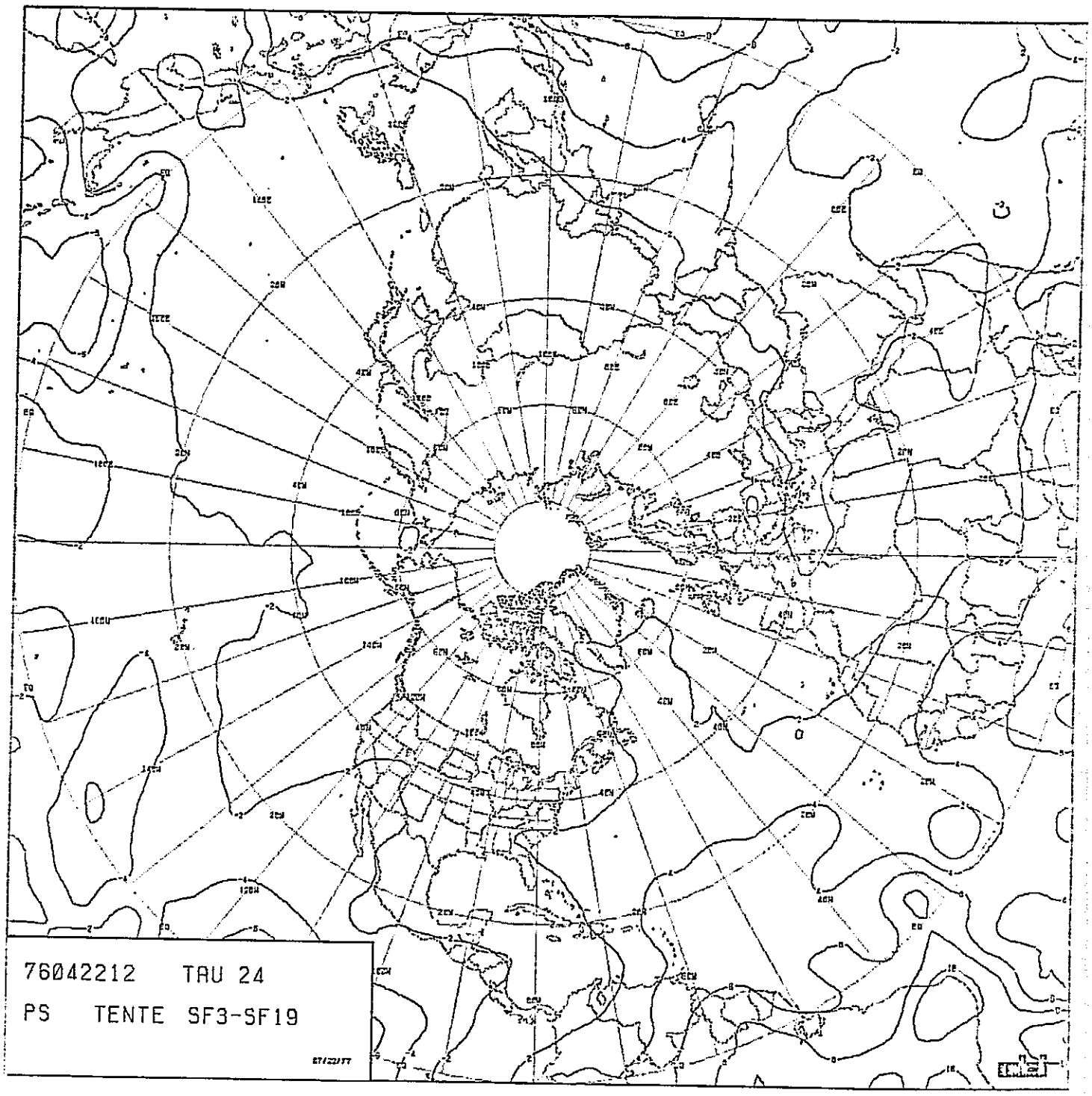

FIGURE IV-57: DIFFERENCE BETWEEN BASELINE AND SF19, SURFACE

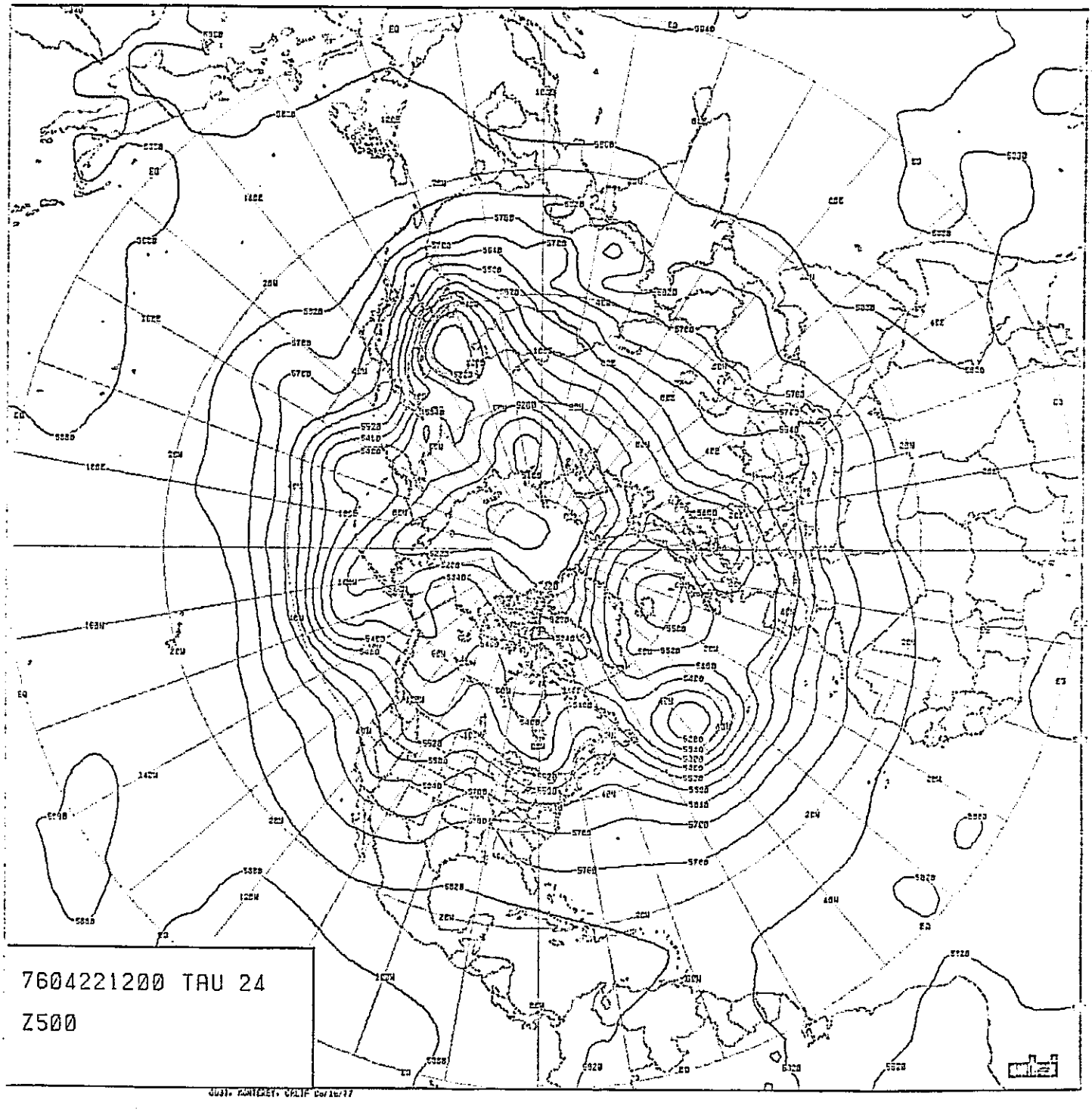

FIGURE IV-58: FORECAST, 500mb, SF19

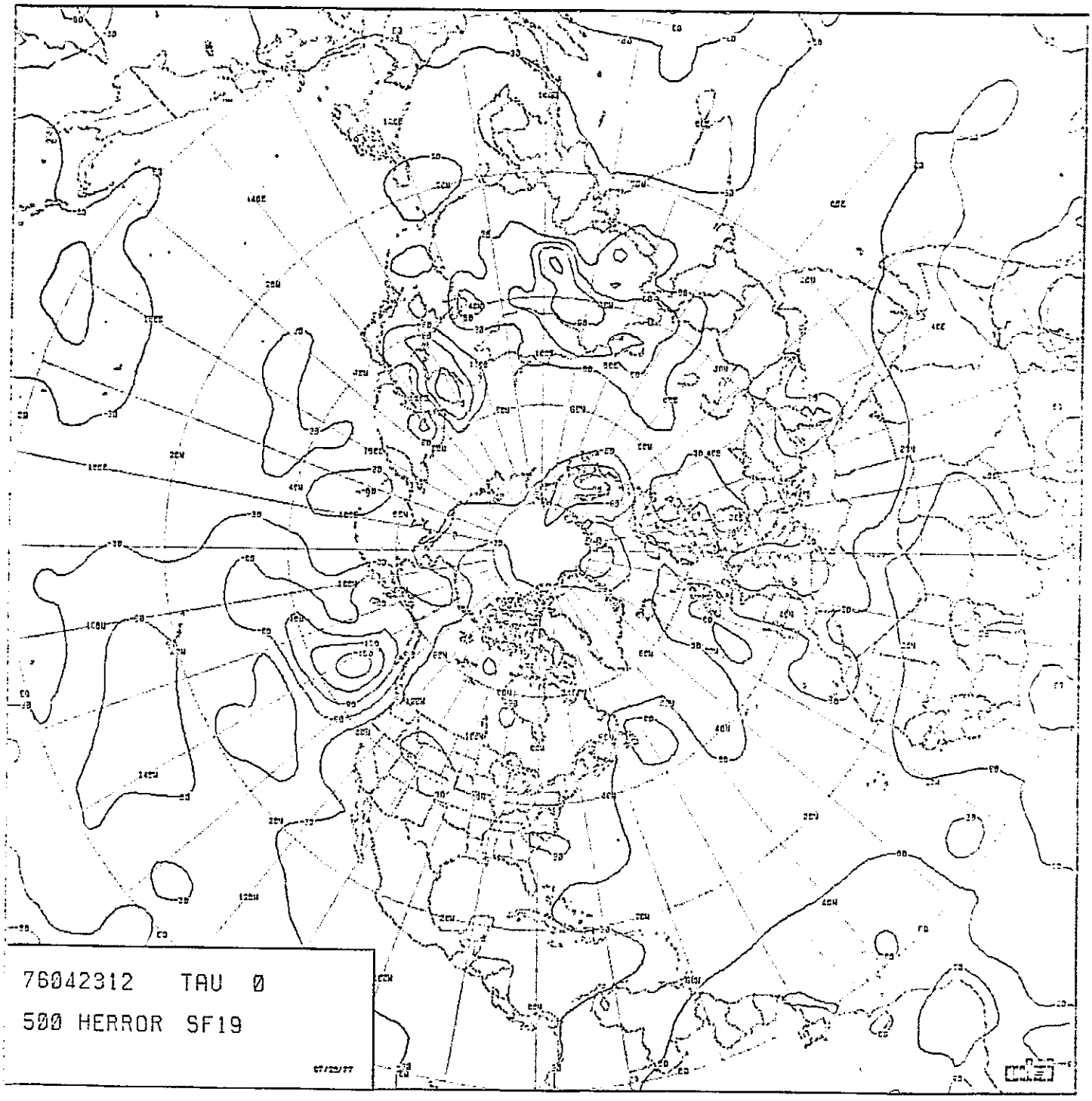

FIGURE IV-59: ERROR PATTERN, 500mb, SF19

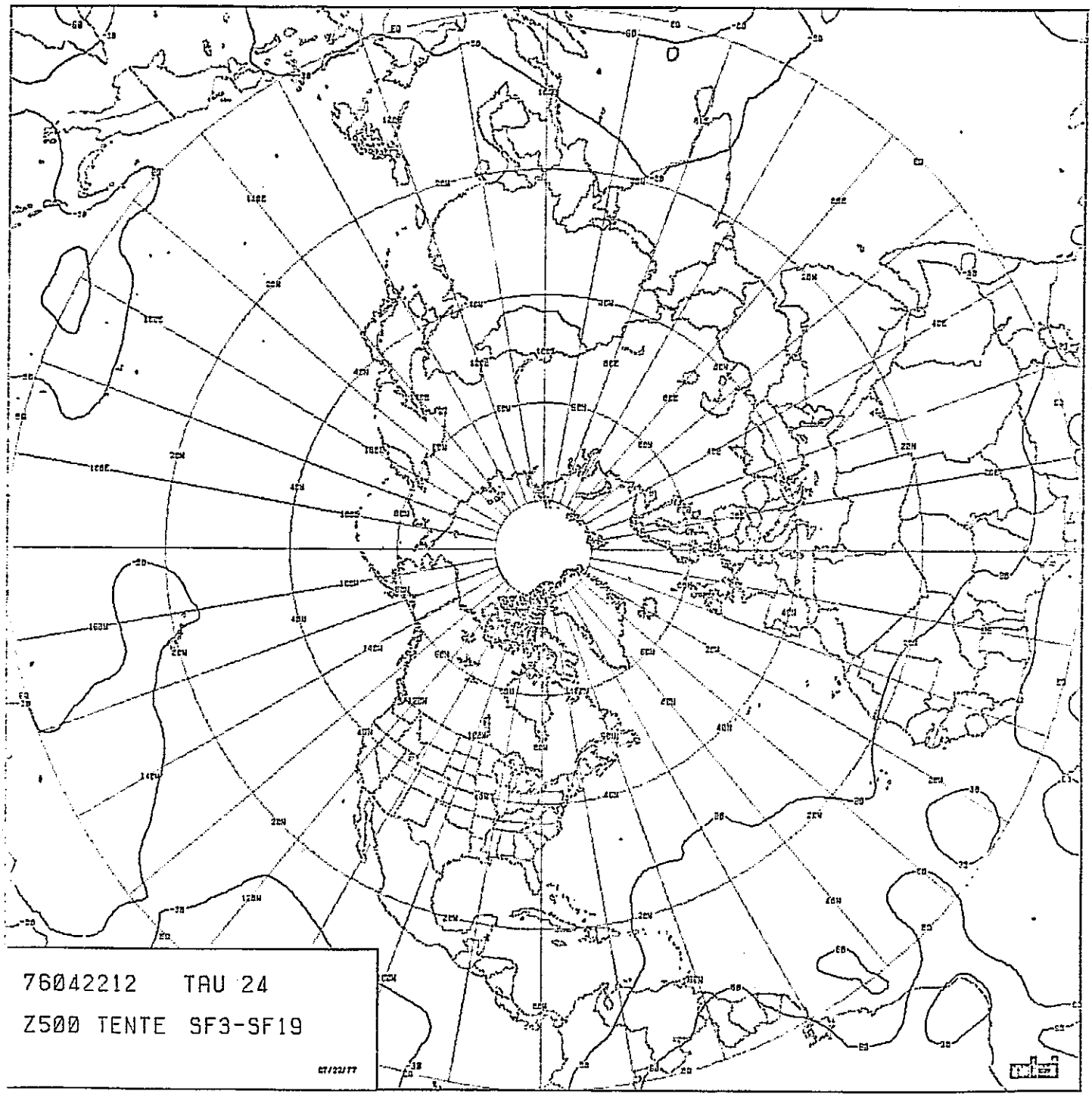

FIGURE IV-60: DIFFERENCE BETWEEN BASELINE AND SF19, 500 mb

TABLE IV-16: ERROR STATISTICAL SUMMARY, SF19 (MODIFIED TRUNCATION/TERRAIN TAPERING).

SURFACE

FROM	TO	RMS	SD	MEAN	MAX	MIN
0	10	.438E+01	.434E+01	-.524E+00	.954E+01	-.838E+01
10	20	.332E+01	.328E+01	-.546E+00	.658E+01	-.653E+01
20	30	.366E+01	.363E+01	.484E+00	.799E+01	-.755E+01
30	40	.373E+01	.360E+01	.980E+00	.106E+02	-.815E+01
40	50	.385E+01	.346E+01	.169E+01	.111E+02	-.914E+01
50	60	.461E+01	.374E+01	.271E+01	.115E+02	-.112E+02
60	70	.336E+01	.254E+01	.220E+01	.869E+01	-.641E+01
70	80	.376E+01	.350E+01	.137E+01	.982E+01	-.823E+01
80	90	.241E+01	.149E+01	.189E+01	.589E+01	-.661E+00
0	90	.389E+01	.387E+01	.355E+00	.115E+02	-.112E+02

500 MB

FROM	TO	RMS	SD	MEAN	MAX	MIN
0	10	.462E+02	.460E+02	.434E+01	.953E+02	-.763E+02
10	20	.421E+02	.415E+02	.751E+01	.914E+02	-.833E+02
20	30	.307E+02	.295E+02	.829E+01	.719E+02	-.663E+02
30	40	.397E+02	.389E+02	.791E+01	.120E+03	-.115E+03
40	50	.495E+02	.495E+02	.128E+01	.110E+03	-.163E+03
50	60	.378E+02	.378E+02	-.187E+01	.691E+02	-.119E+03
60	70	.241E+02	.234E+02	-.571E+01	.603E+02	-.812E+02
70	80	.385E+02	.228E+02	-.310E+02	.842E+01	-.978E+02
80	90	.437E+02	.108E+02	-.424E+02	-.265E+02	-.610E+02
0	90	.414E+02	.412E+02	.382E+01	.120E+03	-.163E+03

Q. Multiple Modification (SF11)

The previous studies generally resulted in subtle changes in the forecast. In addition to those, it was instructive to demonstrate the effect of the modification of several devices simultaneously. In SF11, the coefficients for temperature and momentum diffusion, as well as for surface drag and pressure smoothing, were set to zero. In addition, the precipitation and heating processes were eliminated. This would be an adiabatic, frictionless version of the standard model.

In 24 hours, the damage to the forecast was drastic. At the surface, Figure IV-61, most of the systems are recognizable but all have undergone excessive development. The pattern of Figure IV-62 has errors in excess of 20 mb and almost without exception there are large departures from the baseline in Figure IV-63.

At 500 mb, Figure IV-64, systems have assumed non-meteorological gradients and shapes. While some of the errors in Figure IV-65 resemble those of the baseline, there are new regions with large errors. Figure IV-66 shows the departure from the baseline to be largely confined to Asia although other departures exist.

Table IV-17 indicates large errors associated with SF11. The maximum errors were 40 mb at the surface and 414M at 500 mb, while the baseline was 12.7 mb and 163M at those levels.

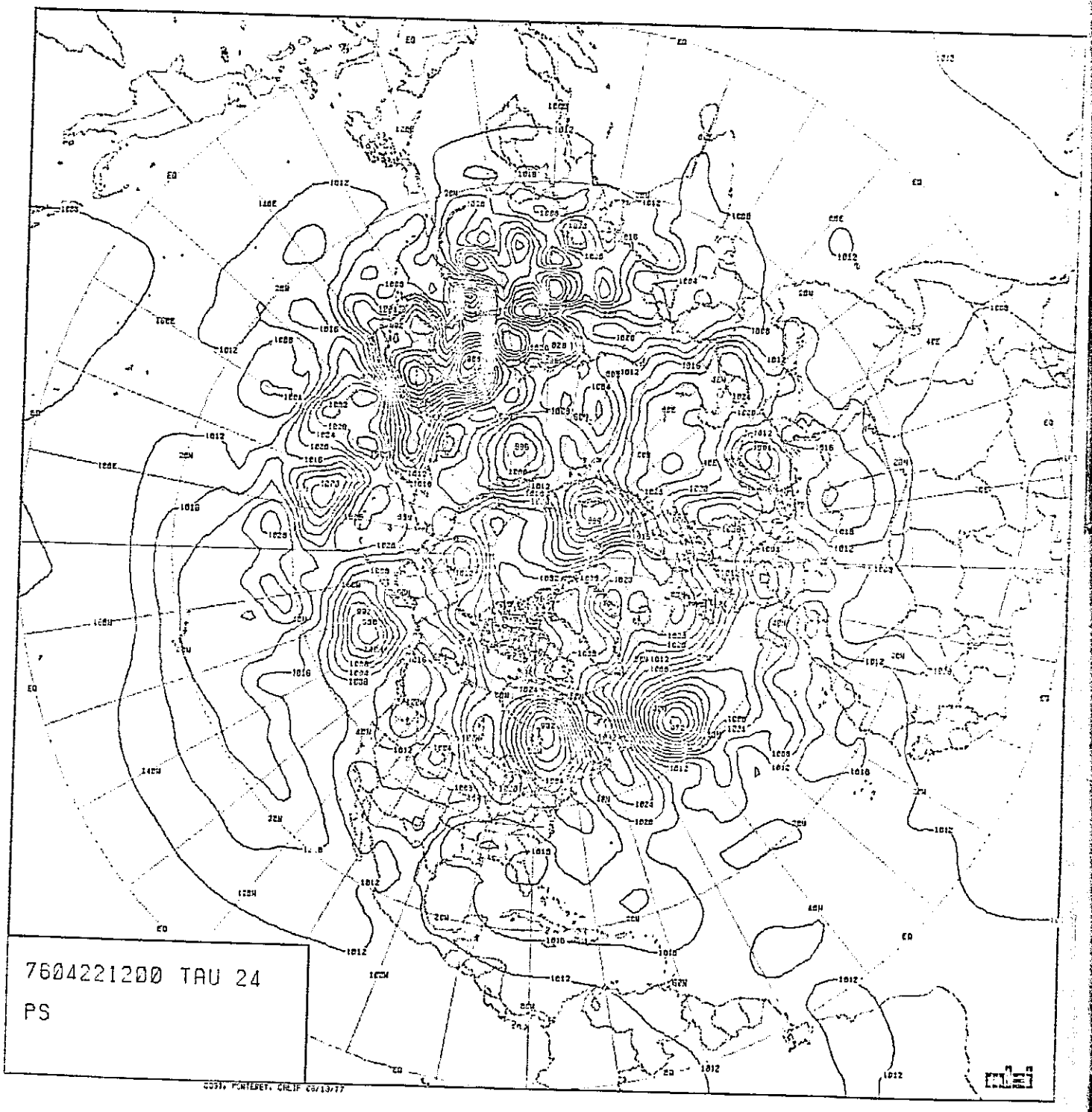

FIGURE IV-61: FORECAST, SURFACE, SF11

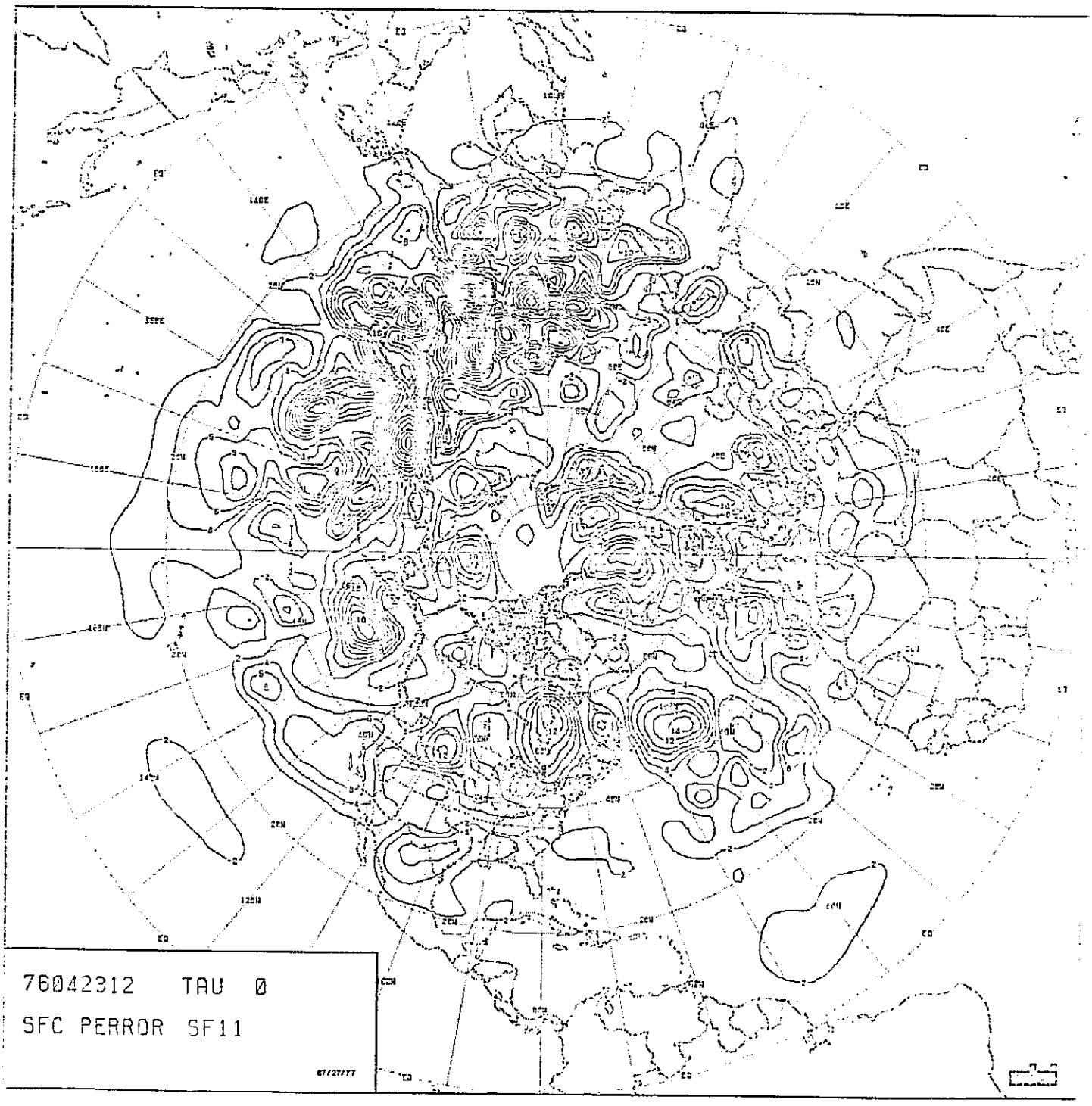

FIGURE IV-62: ERROR PATTERN, SURFACE, SF11

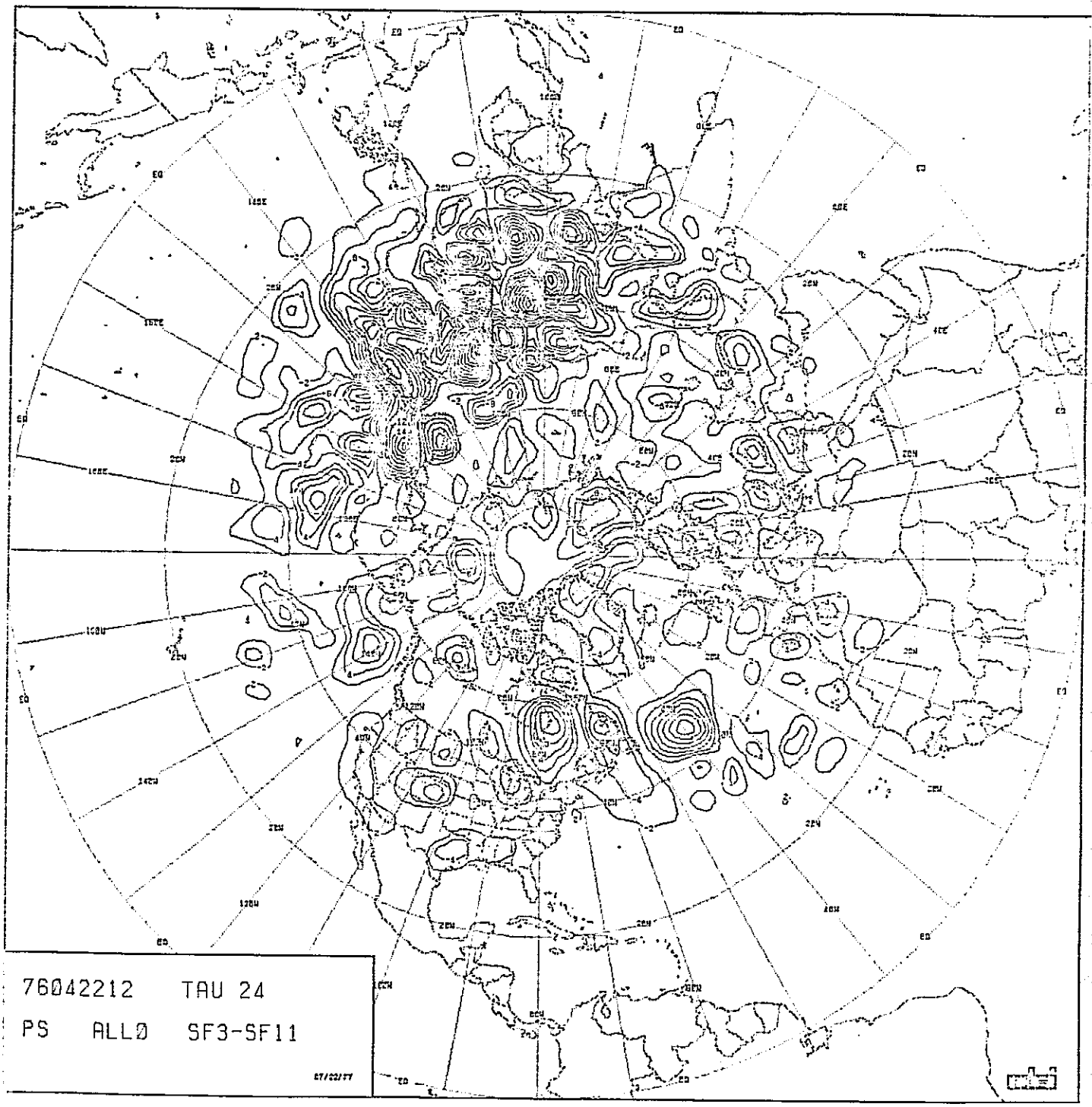

FIGURE IV-63: DIFFERENCE BETWEEN BASELINE AND SF11, SURFACE

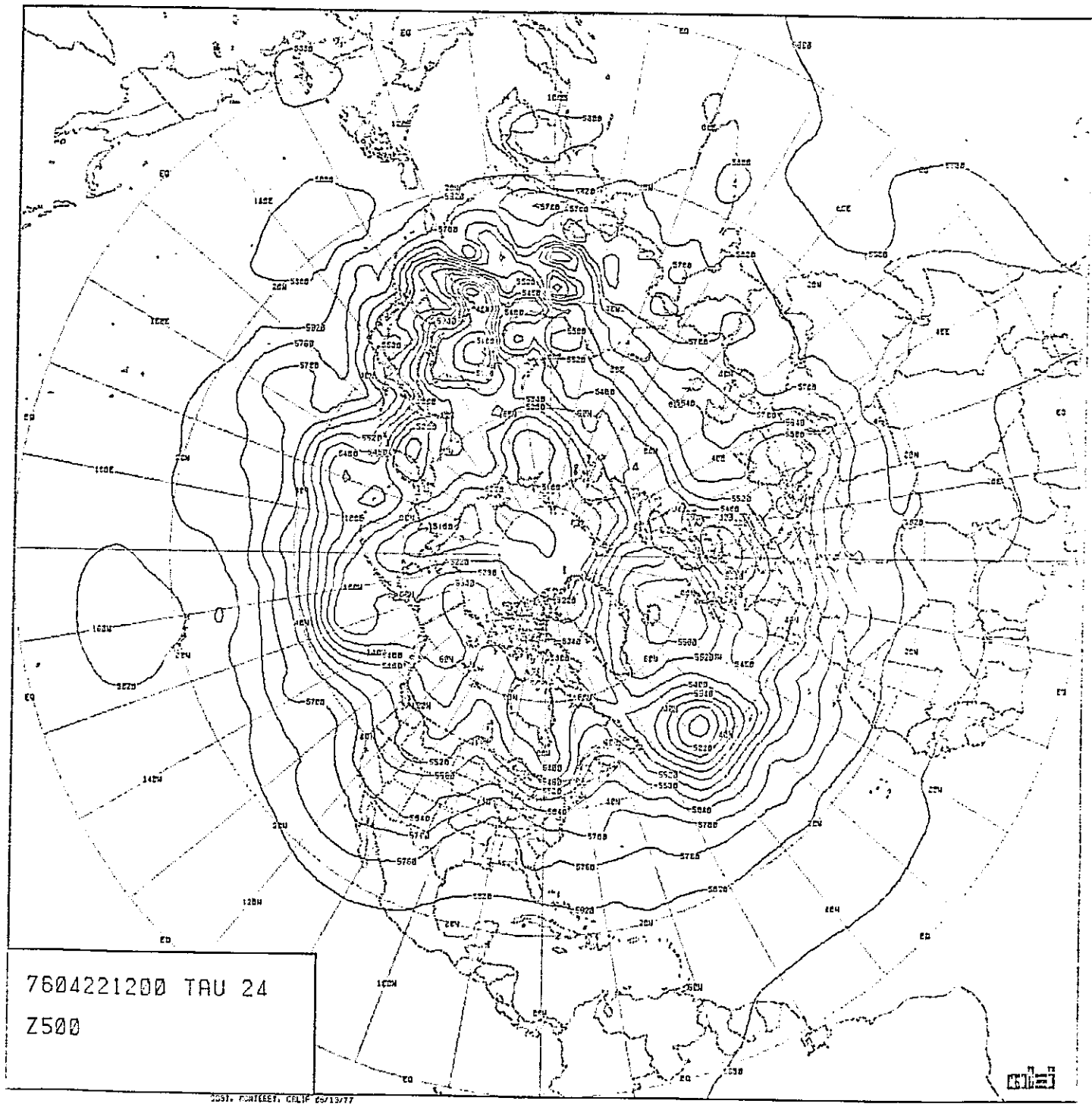

FIGURE IV- 64: FORECAST, 500mb, SF11

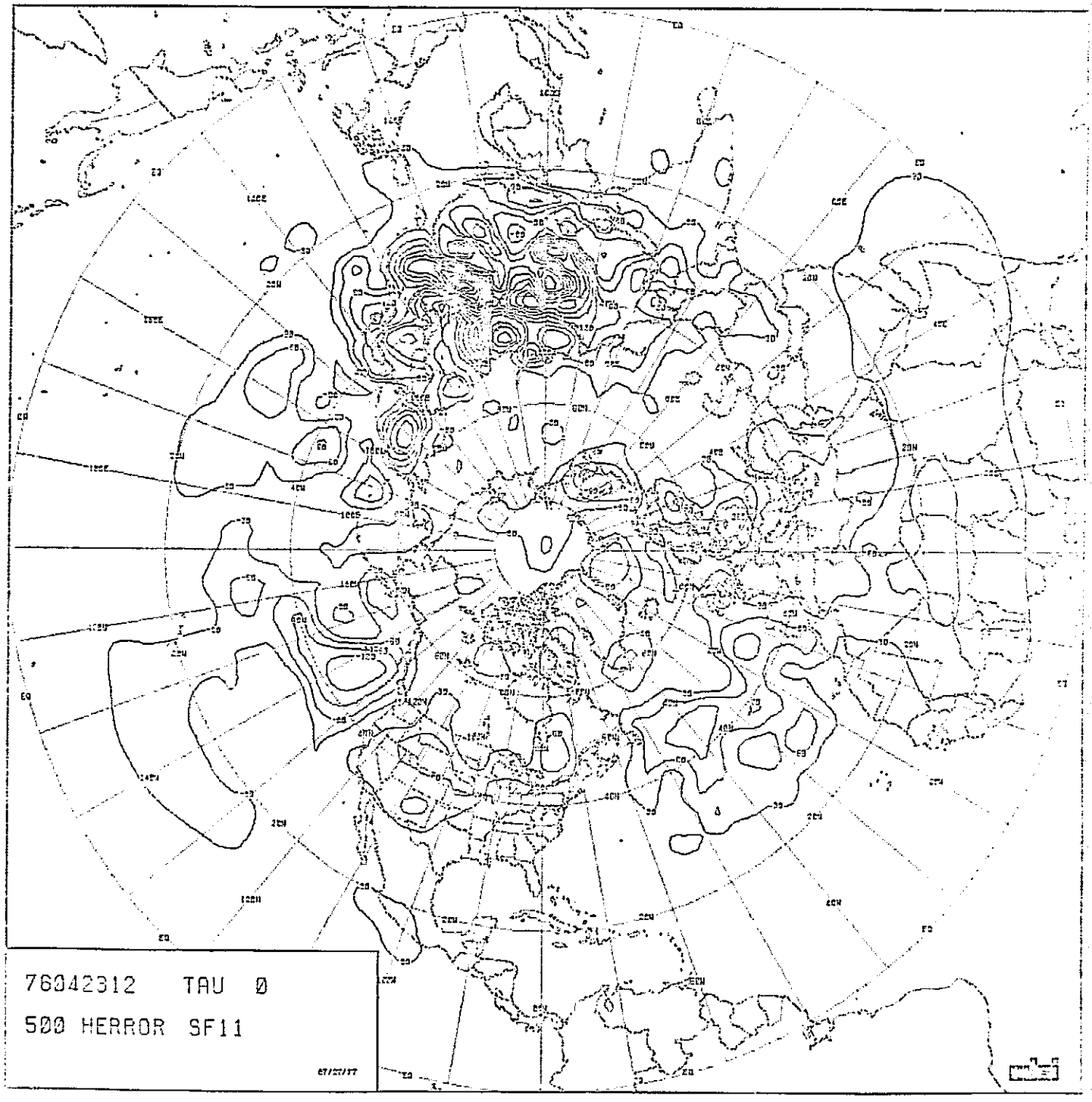

FIGURE IV-65: ERROR PATTERN, 500 mb, SF11

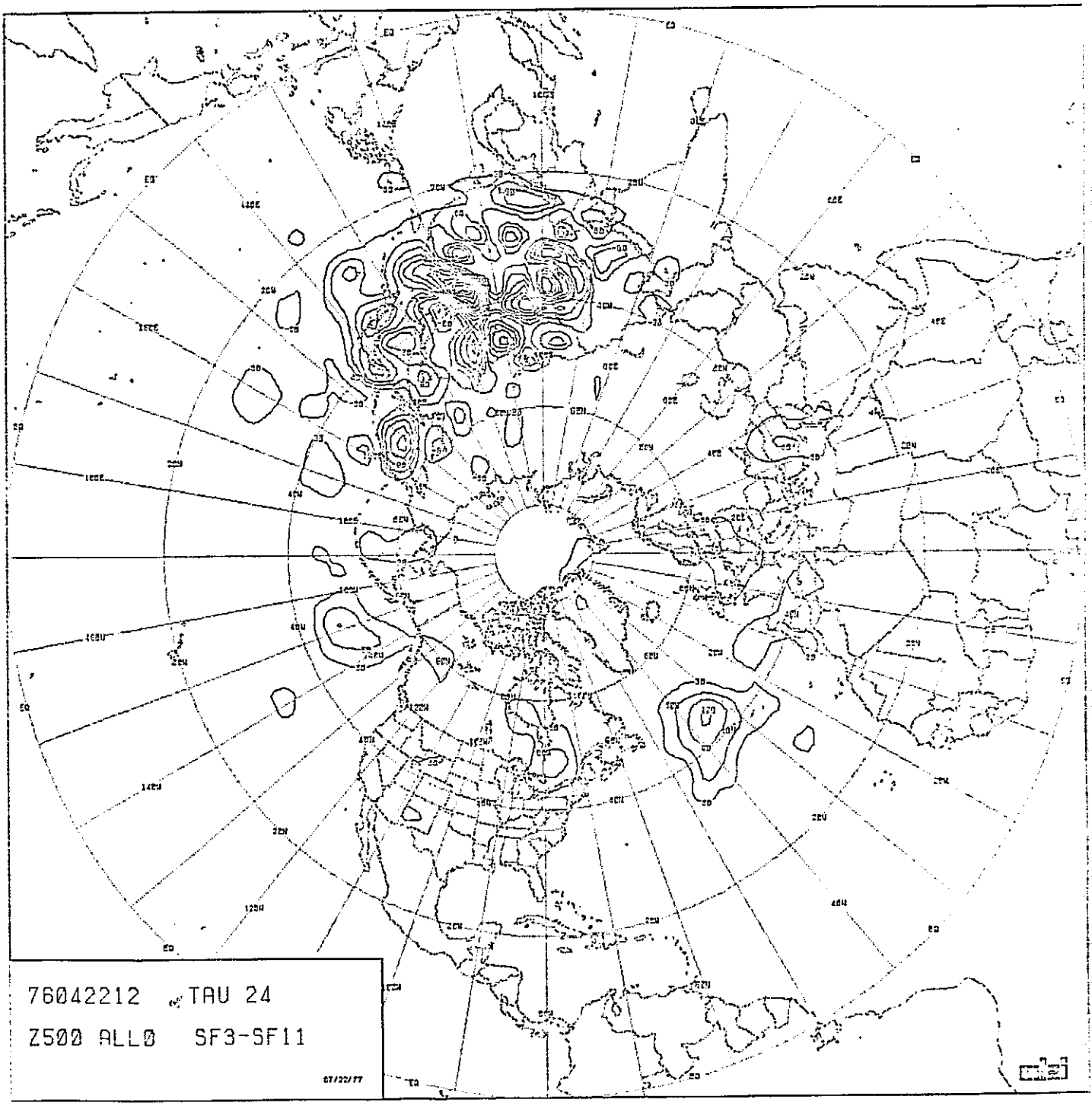

FIGURE IV-66: DIFFERENCE BETWEEN BASELINE AND SF11, 500mb

TABLE IV-17: ERROR STATISTICAL SUMMARY, SF11
(MULTIPLE MODIFICATIONS).

SURFACE

FROM	TO	RMS	SD	MEAN	MAX	MIN
0	10	.727E+00	.700E+00	.196E+00	.256E+01	-.152E+01
10	20	.144E+01	.144E+01	-.106E+00	.469E+01	-.404E+01
20	30	.387E+01	.381E+01	.657E+00	.129E+02	-.141E+02
30	40	.634E+01	.621E+01	.125E+01	.400E+02	-.176E+02
40	50	.654E+01	.595E+01	.295E+01	.225E+02	-.151E+02
50	60	.625E+01	.552E+01	.292E+01	.255E+02	-.105E+02
60	70	.391E+01	.343E+01	.188E+01	.926E+01	-.792E+01
70	80	.449E+01	.436E+01	.105E+01	.977E+01	-.955E+01
80	90	.215E+01	.206E+01	.642E+00	.622E+01	-.388E+01
0	90	.384E+01	.375E+01	.811E+00	.400E+02	-.176E+02

500 MB

FROM	TO	RMS	SD	MEAN	MAX	MIN
0	10	.162E+02	.146E+02	.699E+01	.557E+02	-.345E+02
10	20	.279E+02	.266E+02	.833E+01	.701E+02	-.486E+02
20	30	.355E+02	.299E+02	.191E+02	.162E+03	-.620E+02
30	40	.704E+02	.632E+02	.308E+02	.414E+03	-.115E+03
40	50	.637E+02	.564E+02	.255E+02	.262E+03	-.146E+03
50	60	.427E+02	.411E+02	.114E+02	.170E+03	-.955E+02
60	70	.288E+02	.286E+02	-.349E+01	.684E+02	-.875E+02
70	80	.381E+02	.255E+02	-.283E+02	.361E+02	-.108E+03
80	90	.337E+02	.186E+02	-.281E+02	-.538E+00	-.647E+02
0	90	.392E+02	.372E+02	.122E+02	.414E+03	-.146E+03

R. No Heating (SF20)

In the final run of the model, the processes that generate heating contributions every hour were eliminated. The departure of this run from the baseline was negligible. The greatest departure from the baseline was less than .5 mb at the surface and 1.5M at 500 mbs.

V. COMPARATIVE PERFORMANCE: ENERGETICS, PRECIPITATION AND STORM INTENSITY

Characteristics, effects, devices, and/or coefficients peculiar to the standard forecast model (SF-3) were altered, singly or in combination, in order to determine the relative impacts on a one-day forecast. Once presented, these impacts can be ordered and discussed.

A. Energetics

The effects of each model alteration on 24-hour forecasts of layer-mean kinetic energy and square vorticity are tabulated and described.

1. Temporal Filtering

Tables V-1 and V-2 show the effect of temporal filtering on forecast changes of mean kinetic energy and mean square vorticity, respectively. In both, the impact is shown to be negligible.

2. Radiation

Tables V-3 and V-4 show the effect of radiation calculations on forecast changes of mean kinetic energy and mean square vorticity, respectively. In both, the impact is negligible.

3. Vertical Resolution

Tables V-5 and V-6 show the effect of doubling the vertical resolution (from five to ten layers) on forecast changes of mean kinetic energy and mean square vorticity, respectively. In both cases, doubling the resolution leads to greater losses in low levels and to greater gains at high levels.

4. Temperature Diffusion

Tables V-7 and V-8 show the effect of temperature diffusion on forecast changes of mean kinetic energy and mean square vorticity, respectively. The coefficient (TDK) was reduced by an order of magnitude (from the standard model). This led to increases in forecast KE of about 5%, generally. The impact on square vorticity varied with level, with maximum impact near the Sigma=0.3 level (strongest winds).

5. Initial Winds

Tables V-9 and V-10 show the effect of a variation in the initial wind specification on forecast changes of mean kinetic energy and mean square vorticity, respectively. The standard model used analyzed winds. Run SF--16 was initialized

with non-divergent winds obtained through solution of the non-linear balance equation. In general, the balanced winds produced smaller increases (or larger decreases) in predicted KE and SV.

6. Precipitation

Tables V-11 and V-12 show the effect of precipitation on forecast changes on mean kinetic energy and mean square vorticity, respectively. As expected, smaller increases (or larger decreases) in predicted KE and SV are indicated in the moisture-bearing levels.

7. Initial Moisture Specification

Tables V-13 and V-14 show the effect of variations in the initial moisture specification on forecast changes of mean kinetic energy and mean square vorticity, respectively. Examine Runs SF-17 and SF-18, first. There is a difference of 50% in the initial relative humidities. The greater RH produced larger increases (smaller decreases) in KE and SV, generally. The effect seems to attenuate with altitude (level), but there are exceptions. The 28% difference in SV at Sigma=0.3 level is anomalous. Next, note that the actual run (SF-3) seems to indicate that its (initial) humidity condition was bounded by these extreme conditions, mainly.

8. Mountains

Tables V-15 and V-16 show the effect of mountains on forecast changes in mean kinetic energy and mean square vorticity, respectively. Clearly, mountains lead to larger increases in both KE and SV, mainly as a consequence of increased latent heating. The effect seems to attenuate with height through the moisture-bearing layers. Minor alterations to the mountains (Run SF-19) in the low latitudes had minor effect (there is no precipitation south of about 25°N in these models).

9. Pressure Smoothing

Tables V-17 and V-18 show the effect of variation in the non-linear pressure-smoothing coefficient (SM) on forecast changes of mean kinetic energy and mean square vorticity, respectively. This effect is rather large, and it decreases with height. The KE and SV forecast changes are larger positive (smaller negative) as SM is reduced in magnitude.

10. Momentum Diffusion

Tables V-19 and V-20 show the effect of momentum diffusion on forecast changes in mean kinetic energy and mean square vorticity, respectively. In Run SF-2, the coefficient

(DK) was reduced by an order of magnitude. This led to large increases in the forecast changes in KE and SV. Indeed, when the term is caused to vanish (Run SF-10), extremely large increases result. The term is obviously needed to maintain reasonable levels of KE and SV, but not so strong that net decreases result (Run SF-1).

11. Surface Friction

Tables V-21 and V-22 show the effect of friction on forecast changes in mean kinetic energy and mean square vorticity, respectively. Note that the tests were conducted for two magnitudes of pressure smoothing.

In general, the two-fold increase in friction led to smaller increases (larger decreases) in forecast KE and SV. At Sigma=0.9, the KE difference is 14.6 when SM=0.01 and 11.1 when SM=0.02. At Sigma=0.9, the SV difference is 19.3 when SM=0.01 and 14.4 when SM=0.02. Thus, the 100% variation in friction produces different results when an important discretionary procedure such as pressure smoothing is operative.

B. Storm Intensity

Eight extratropical low-pressure centers were present at 1200Z, 22 April 1976. The impact of each discretionary procedure/effect tested on the predicted intensity of these pressure systems is shown in Table V-23.

By far, the 3X variation in horizontal grid resolution had the greatest impact (probably because the precipitation doubled as the resolution tripled). Precipitation (3MB) is also important, but momentum diffusion can be equally important to the outcome. Also, pressure smoothing (2.5MB) has equal impact to a 50% variation in the initial moisture specification (2.6MB). Both radiation and temporal filtering had no effect on storm intensity.

C. Precipitation

The predicted amounts of precipitation (both large-scale and convective-scale) north of 25°N were tabulated for each model run.

Large variations (∿100%) occurred as a consequence of tripling the horizontal resolution or of a 50% variation in the initial moisture specification. Doubling the vertical resolution from five to ten layers resulted in a 10-15 percent variation in precipitation only. All other parameters/effects tested led to only minor variations in precipitation (less than five percent, generally).

TABLE V-1: EFFECT OF TEMPORAL FILTERING ON FORECAST CHANGES OF MEAN KINETIC ENERGY (IN PERCENT).

RUN	SIGMA LEVEL				
	0.9	0.7	0.5	0.3	0.1
FILTER ACTIVE (RUN SF-3)	18.1	1.0	1.9	-2.6	-23.3
FILTER INACTIVE (RUN SF-15)	18.2	1.0	1.9	-2.6	-23.3

NOTE: THESE ARE 24-HOUR FORECAST CHANGES.

TABLE V-2: EFFECT OF TEMPORAL FILTERING ON FORECAST CHANGES OF MEAN SQUARE VORTICITY (IN PERCENT).

RUN	SIGMA LEVEL				
	0.9	0.7	0.5	0.3	0.1
FILTER ACTIVE (RUN SF-3)	24.1	-13.5	8.0	23.2	-43.1
FILTER INACTIVE (RUN SF-15)	24.3	-13.5	8.0	23.4	-43.1

NOTE: THESE ARE 24-HOUR FORECAST CHANGES.

TABLE V-3: EFFECT OF RADIATION AND SENSIBLE HEATING ON FORECAST CHANGES OF MEAN KINETIC ENERGY (IN PERCENT).

CONDITION/RUN	SIGMA LEVEL				
	0.9	0.7	0.5	0.3	0.1
NO RADIATION OR SENSIBLE HEATING (RUN SF-20)	18.1	0.9	1.9	-2.8	-23.3
STANDARD (RUN SF-3)	18.1	1.0	1.9	-2.6	-23.3

TABLE V-4: EFFECT OF RADIATION AND SENSIBLE HEATING ON FORECAST CHANGES OF MEAN SQUARE VORTICITY (IN PERCENT).

CONDITION/RUN	SIGMA LEVEL				
	0.9	0.7	0.5	0.3	0.1
NO RADIATION OR SENSIBLE HEATING (RUN SF-20)	24.1	-13.5	8.0	23.5	-43.1
STANDARD (RUN SF-3)	24.1	-13.5	8.0	23.2	-43.1

TABLE V-5: EFFECT OF VERTICAL RESOLUTION ON FORECAST CHANGES OF MEAN KINETIC ENERGY (IN PERCENT).

CONDITION/RUN	SIGMA LEVEL				
	0.9	0.7	0.5	0.3	0.1
5-LEVELS (RUN F18)	-4.9	-13.1	-10.9	-19.5	-16.9
10-LEVELS (RUN T4)	-8.4	-12.5	-13.8	-18.4	-11.2
DIFFERENCE	-3.5	0.6	-2.9	1.1	5.7

NOTE: THESE RUNS WERE INITIALIZED WITH A DIFFERENT SET OF ANALYSES THAN THOSE USED FOR THE OTHER SENSITIVITY TESTS.

TABLE V-6: EFFECT OF VERTICAL RESOLUTION ON FORECAST CHANGES OF MEAN SQUARE VORTICITY (IN PERCENT).

CONDITION/RUN	SIGMA LEVEL				
	0.9	0.7	0.5	0.3	0.1
5-LEVELS (RUN F18)	-12.2	-43.2	-37.1	-37.4	-43.4
10-LEVELS (RUN T4)	-25.3	-44.2	-44.3	-33.5	-21.0
DIFFERENCE	-13.1	-1.0	-7.2	3.9	22.4

NOTE: THESE RUNS WERE INITIALIZED WITH A DIFFERENT SET OF ANALYSES THAN THOSE USED FOR THE OTHER SENSITIVITY TESTS.

TABLE V-7: EFFECT OF TEMPERATURE DIFFUSION ON FORECAST CHANGES OF MEAN KINETIC ENERGY (IN PERCENT).

COEFFICIENT/RUN	SIGMA LEVEL				
	0.9	0.7	0.5	0.3	0.1
TDK = 10^5 (RUN SF-4)	22.8	5.2	8.6	3.7	-22.0
TDK = 10^6 (RUN SF-3)	18.1	1.0	1.9	-2.6	-23.3
DIFFERENCE	4.7	4.2	6.7	6.3	1.3

TABLE V-8: EFFECT OF TEMPERATURE DIFFUSION ON FORECAST CHANGES OF MEAN SQUARE VORTICITY (IN PERCENT).

COEFFICIENT/RUN	SIGMA LEVEL				
	0.9	0.7	0.5	0.3	0.1
TDK = 10^5 (RUN SF-4)	23.3	-9.6	24.0	44.3	-41.0
TDK = 10^6 (RUN SF-3)	24.1	-13.5	8.0	23.2	-43.1
DIFFERENCE	1.2	3.9	16.0	21.1	2.1

TABLE V-9: EFFECT OF INITIAL WIND SPECIFICATION ON FORECAST CHANGES OF MEAN KINETIC ENERGY (IN PERCENT).

CONDITION/RUN	SIGMA LEVEL				
	0.9	0.7	0.5	0.3	0.1
ANALYZED WINDS (RUN SF-3)	18.1	1.0	1.9	-2.6	-23.3
BALANCED* WINDS (RUN SF-16)	5.4	-0.4	-3.1	-7.5	-19.4
DIFFERENCE	-12.7	-1.4	-5.0	-4.9	3.9

* FROM NON-LINEAR BALANCE EQUATION; NO SPECIFICATION OF DIVERGENT COMPONENT.

TABLE V-10: EFFECT OF INITIAL WIND SPECIFICATION ON FORECAST CHANGES OF MEAN SQUARE VORTICITY (IN PERCENT).

CONDITION/RUN	SIGMA LEVEL				
	0.9	0.7	0.5	0.3	0.1
ANALYZED WINDS (RUN SF-3)	24.1	-13.5	8.0	23.2	-43.1
BALANCED* WINDS (RUN SF-16)	12.6	-16.8	-16.2	-10.5	-36.7
DIFFERENCE	-11.5	-3.3	-24.2	-33.7	6.4

* FROM NON-LINEAR BALANCE EQUATION; NO SPECIFICATION OF DIVERGENT COMPONENT.

TABLE V-11: EFFECT OF PRECIPITATION ON FORECAST CHANGES OF MEAN KINETIC ENERGY (IN PERCENT).

RUN	SIGMA LEVEL				
	0.9	0.7	0.5	0.3	0.1
MECHANISMS* ACTIVE (RUN SF-3)	18.1	1.0	1.9	-2.6	-23.3
MECHANISMS INACTIVE (RUN SF-14)	4.1	-2.8	2.5	-2.4	-22.0
DIFFERENCE	-14.0	-3.8	0.6	0.2	1.3

* BOTH CYCLONE-SCALE AND CONVECTIVE-SCALE.

TABLE V-12: EFFECT OF PRECIPITATION ON FORECAST CHANGES OF MEAN SQUARE VORTICITY (IN PERCENT).

RUN	SIGMA LEVEL				
	0.9	0.7	0.5	0.3	0.1
MECHANISMS* ACTIVE (RUN SF-3)	24.1	-13.5	8.0	23.2	-43.1
MECHANISMS INACTIVE (RUN SF-14)	-1.2	-23.1	4.6	16.9	-42.7
DIFFERENCE	-25.3	-9.6	-3.4	-6.3	0.4

* BOTH CYCLONE-SCALE AND CONVECTIVE-SCALE.

TABLE V-13: EFFECT OF INITIAL MOISTURE (RH_o) SPECIFICATION ON FORECAST CHANGES OF MEAN KINETIC ENERGY (IN PERCENT).

CONDITION/RUN	SIGMA LEVEL				
	0.9	0.7	0.5	0.3	0.1
RH_o = 25% (RUN SF-17)	2.9	-2.8	2.5	-2.3	-22.0
RH_o = f(VORT)* (RUN SF-3)	18.1	1.0	1.9	-2.6	-23.3
RH_o = 75% (RUN SF-18)	22.2	3.8	5.3	1.6	-24.5
DIFFERENCE (75% - 25%)	19.3	6.6	2.8	3.9	-2.5

* INITIAL RH PARAMETERIZED IN TERMS OF RELATIVE VORTICITY AT EACH PRESSURE LEVEL.

TABLE V-14: EFFECT OF INITIAL MOISTURE (RH_o) SPECIFICATION ON FORECAST CHANGES OF MEAN SQUARE VORTICITY (IN PERCENT).

CONDITION/RUN	SIGMA LEVEL				
	0.9	0.7	0.5	0.3	0.1
RH_o = 25% (RUN SF-17)	-3.6	-23.1	5.1	18.1	-42.7
RH_o = f(VORT)* (RUN SF-3)	24.1	-13.5	8.0	23.2	-43.1
RH_o = 75% (RUN SF-18)	27.7	-13.5	17.7	46.1	-41.8
DIFFERENCE (75% - 25%)	31.3	9.6	12.6	28.0	0.9

* INITIAL RH PARAMETERIZED IN TERMS OF RELATIVE VORTICITY AT EACH PRESSURE LEVEL.

TABLE V-15: EFFECT OF MOUNTAINS ON FORECAST CHANGES OF MEAN KINETIC ENERGY (IN PERCENT).

CONDITION/RUN	SIGMA LEVEL				
	0.9	0.7	0.5	0.3	0.1
MODIFIED* NEAR BORDERS (RUN SF-3)	18.1	1.0	1.9	-2.6	-23.3
UNMODIFIED (RUN SF-19)	14.1	-0.9	0.0	-3.5	-18.9
FLAT EARTH (RUN SF-13)	-3.0	-5.4	1.5	-4.4	-27.7
DIFFERENCE (SF-3 vs SF-13)	21.1	6.4	0.4	1.8	4.4

* FLAT EARTH SOUTH OF 5°N; UNMODIFIED NORTH OF 20°N; TAPERED BETWEEN 5°N AND 20°N.

TABLE V-16: EFFECT OF MOUNTAINS ON FORECAST CHANGES OF MEAN SQUARE VORTICITY (IN PERCENT).

CONDITION/RUN	SIGMA LEVEL				
	0.9	0.7	0.5	0.3	0.1
MODIFIED* NEAR BORDERS (RUN SF-3)	24.1	-13.5	8.0	23.2	-43.1
UNMODIFIED (RUN SF-19)	24.1	-14.4	7.5	23.6	-45.2
FLAT EARTH (RUN SF-13)	-16.5	-31.2	0.0	11.1	-45.6
DIFFERENCE (SF-3 vs SF-13)	40.6	17.7	8.0	12.1	2.5

* FLAT EARTH SOUTH OF 5°N; UNMODIFIED NORTH OF 20°N; TAPERED BETWEEN 5°N AND 20°N.

TABLE V-17: EFFECT OF PRESSURE-SMOOTHING ON FORECAST CHANGES OF MEAN KINETIC ENERGY (IN PERCENT).

COEFFICIENT/RUN	SIGMA LEVEL				
	0.9	0.7	0.5	0.3	0.1
SM = 0.0 (RUN SF-5)	31.6	6.2	3.0	-1.7	-23.3
SM = 0.01 (RUN SF-3)	18.1	1.0	1.9	-2.6	-23.3
SM = 0.02 (RUN SF-6)	3.5	-3.8	0.8	-3.5	-23.9
DIFFERENCE (SF-3 vs SF-6)	14.6	4.8	1.1	0.9	0.6

NOTE: THESE ARE 24-HOUR FORECAST CHANGES.

TABLE V-18: EFFECT OF PRESSURE SMOOTHING ON FORECAST CHANGES OF MEAN SQUARE VORTICITY (IN PERCENT).

COEFFICIENT/RUN	SIGMA LEVEL				
	0.9	0.7	0.5	0.3	0.1
SM = 0.0 (RUN SF-5)	57.8	-2.9	10.9	27.1	-42.7
SM = 0.01 (RUN SF-3)	24.1	-13.5	8.0	23.2	-43.1
SM = 0.02 (RUN SF-6)	0.0	-21.2	5.1	20.2	-42.7
DIFFERENCE (SF-3 vs SF-6)	24.1	7.7	2.9	3.0	-0.4

NOTE: THESE ARE 24-HOUR FORECAST CHANGES.

TABLE V-19: EFFECT OF MOMENTUM DIFFUSION ON FORECAST CHANGES OF MEAN KINETIC ENERGY (IN PERCENT).

COEFFICIENT/RUN	SIGMA LEVEL				
	0.9	0.7	0.5	0.3	0.1
DK = 0.0 (RUN SF-10)	112.0	83.1	91.5	74.1	0.6
DK = 10^5 (RUN SF-2)	85.0	54.0	54.4	42.6	-9.3
DK = 10^6 (RUN SF-3)	18.1	1.0	1.9	-2.6	-23.3
DK = f(K)* (RUN SF-1)	-5.3	-15.9	-14.8	-18.8	-26.4

* DK = { 1.0 E06, K=5; 2.2 E06, K=4; 2.2 E06, K=3; 1.9 E06, K=2; 1.6 E06, K-1

TABLE V-20: EFFECT OF MOMENTUM DIFFUSION ON FORECAST CHANGES ON MEAN SQUARE VORTICITY (IN PERCENT).

COEFFICIENT/RUN	SIGMA LEVEL				
	0.9	0.7	0.5	0.3	0.1
DK = 0.0 (RUN SF-10)	172.1	139.3	251.9	321.1	16.1
DK = 10^5 (RUN SF-2)	131.4	96.3	151.7	200.0	-2.0
DK = 10^6 (RUN SF-3)	24.1	-13.5	8.0	23.2	-43.1
DK = f(K)* (RUN SF-1)	-9.8	-41.6	-35.9	-33.3	-47.3

* DK = { 1.0 E06, K=5; 2.2 E06, K=4; 2.2 E06, K=3; 1.9 E06, K=2; 1.6 E06, K-1

TABLE V-21: EFFECT OF SURFACE FRICTION ON FORECAST CHANGES OF MEAN KINETIC ENERGY (IN PERCENT), UNDER TWO CONDITIONS OF PRESSURE SMOOTHING.

COEFFICIENT/RUN	SIGMA LEVEL				
	0.9	0.7	0.5	0.3	0.1
PRESSURE-SMOOTHING COEFFICIENT = 0.01					
CD = 0.00015 (RUN SF-9)	38.0	8.5	5.8	-0.7	-22.6
CD = 0.0015 (RUN SF-3)	18.1	1.0	1.9	-2.6	-23.3
CD = 0.003 (RUN SF-7)	3.5	-5.7	-1.7	-4.7	-24.5
PRESSURE-SMOOTHING COEFFICIENT = 0.02					
CD = 0.0015 (RUN SF-6)	3.5	-3.8	0.8	-3.5	-23.9
CD = 0.003 (RUN SF-8)	-7.6	-9.5	-2.2	-5.4	-24.5

TABLE V-22: EFFECT OF SURFACE FRICTION ON FORECAST CHANGES OF MEAN SQUARE VORTICITY (IN PERCENT), UNDER TWO CONDITIONS OF PRESSURE SMOOTHING.

COEFFICIENT/RUN	SIGMA LEVEL				
	0.9	0.7	0.5	0.3	0.1
PRESSURE-SMOOTHING COEFFICIENT = 0.01					
CD = 0.00015 (RUN SF-9)	50.6	-2.0	14.9	28.3	-42.3
CD = 0.0015 (RUN SF-3)	24.1	-13.5	8.0	23.2	-43.1
CD = 0.003 (RUN SF-7)	4.8	-21.2	2.9	19.3	-43.5
PRESSURE-SMOOTHING COEFFICIENT = 0.02					
CD = 0.0015 (RUN SF-6)	0.0	-21.2	5.1	20.2	-42.7
CD = 0.003 (RUN SF-8)	-14.4	-27.9	0.6	16.0	-43.5

TABLE V-23: STORM INTENSITY VARIATIONS

ITEM	CENTRAL PRESSURE VARIATION (MBS)	
	AVERAGE	MAXIMUM
Temporal Filtering (on-off)	0	0
Pressure Smoothing (2X variation)	2.5	4
Surface Friction (2X variation)	1.5	4
Precipitation (on-off)	3.0	5
Momentum Diffusion (10X variation)	3.0	8
Temperature Diffusion (10X variation)	1.0	3
Mountains (in-out)	1.1	5
Moisture Specification (50% variation)	2.6	6
Wind Specification (anal-balance)	1.2	2
Radiation (on-off)	0	0
Horizontal Resolution (3X variation)	6.3	11
Vertical Resolution (2X variation)	0.5	2

VI. SUMMARY

A. Description of Modifications

Sensitivity tests using model version PECHCV (63 x 63 x 5 levels) have been completed. Not enough computer time was available to permit the series to be re-run using model version PECHFV (63 x 63 x 10 levels). Modifications to the standard model, together with identifying run numbers, are indicated below:

- Temperature diffusion coefficient (K_T)
  - -- $K_T = 10^6$ (standard); Run SF-3
  - -- $K_T = 10^5$. Run SF-4

- Momentum diffusion coefficient (K_M)
  - -- $K_M = 10^6$ (standard); Run SF-3
  - -- $K_M = 10^5$; Run SF-2
  - -- $K_M = f(\alpha)$; Run SF-1

- Surface drag coefficient (C_D)
  - -- $C_D = 0.0015$ (standard); Run SF-3
  - -- $C_D = 0.003$; Run SF-7
  - -- $C_D = 0.00015$; Run SF-9

- Pressure-smoothing coefficient (ε)
  - -- ε = 0.01 (standard); Run SF-3
  - -- ε = 0.02; Run SF-6
  - -- ε = 0.0; Run SF-5
  - -- ε = f(t); Run SF-12

- Precipitation (large-scale plus convection)
  - -- On (standard); Run SF-3
  - -- Off; Run SF-14

- Temporal filtering
  - -- On (standard); Run SF-3
  - -- Off; Run SF-15

- Multiple modifications
  - -- Standard; Run SF-3
  - -- No diffusion, pressure smoothing, friction, radiation, condensation, evaporation, or sensible heating; Run SF-11
  - -- No radiation, evaporative/sensible exchanges at surface; Run SF-20
  - -- No diffusion (K_T=K_M=0.0); Run SF-10

- Initial wind specification
  - -- Analyzed (standard); Run SF-3
  - -- Derived from balance equation; Run SF-16

- Initial moisture specification
  - -- Parameterized using vorticity patterns (standard); Run SF-3
  - -- RH = 25%; Run SF-17
  - -- RH = 75%; Run SF-18

- Tendency truncation/Terrain tapering
  - -- Tendencies and terrain vanish south of 5°N, and increase smoothly with latitude to full value at 20°N (standard); Run SF-3
  - -- Tendencies and terrain reduced by 50% south of 5°N, with latitudinal increases to full value by 20°N; Run SF-19

- Terrain specification
  - -- Tapered south of 20°N to 5°N equatorward of which it vanishes (standard); Run SF-3
  - -- Smooth earth; Run SF-13

B. Findings

These sensitivity studies have demonstrated that the effects of each process, procedure and parameter contributing to the computer forecast need to be understood, ordered and exploited. Many of the choices are model dependent.

Physical effects are often small when compared to other sources of (possible) variation in a forecast. In fact, some computational/cosmetic devices can mask (or overwhelm) certain physical effects. Consider, for example, pressure smoothing which has a greater impact on the forecast than surface friction, mountains or vertical resolution. Momentum diffusion impacts on the forecast as much as (modeled) precipitation. The coefficients for both pressure smoothing and momentum diffusion should be specified only after careful evaluation of numerous forecasts.

Table VI-1 summarizes some of the variations between two forecasts due to specified modifications in a procedure, coefficient or effect. Precipitation amounts appear to be affected mainly by changes in the horizontal resolution and/or in the initial moisture specification. The average storm intensity is affected by horizontal resolution, too. Vertical resolution increase (from five to ten layers) had minimal

TABLE VI-1: VARIATIONS IN FORECASTS FROM SPECIFIED MODEL CHANGES.

ITEM	DIFFERENCE BETWEEN TWO FORECASTS		
	PRECIPITATION AMOUNT (%)	AVERAGE STORM INTENSITY (MBS)	KINETIC ENERGY CHANGE AT LOWEST LEVEL (%)
RADIATION (ON-OFF)	1	0	0.0
TEMPORAL FILTER (ON-OFF)	1-2	0	0.1
FRICTION (2X CHANGE)	2-3	1.5	14.6
DIFFUSION (10X CHANGE)			
- MOMENTUM	5	3.0	66.9
- TEMPERATURE	3-4	1.0	4.7
PRESSURE SMOOTHING (2X CHANGE)	4-5	2.5	14.6
INITIAL WINDS (ANALYZED-DERIVED)	5	1.2	12.7
MOUNTAINS (IN-OUT)	6	1.1	21.1
PRECIPITATION (ON-OFF)	N/A	3.0	14.0
VERTICAL RESOLUTION (2X CHANGE)	10-15	0.5	3.5
HORIZONTAL RESOLUTION (3X CHANGE)	80-100	6.3	57.7
INITIAL MOISTURES (75%-25%)	50-75	2.6	19.2

impact on storm centers. Pressure smoothing and momentum diffusion have as much effect on lows as precipitation or surface friction. With respect to the kinetic energy change predicted at the lowest model level, note that momentum diffusion has greater impact than tripling the horizontal resolution. Pressure smoothing has the same effect as does surface friction or precipitation. Both radiation and temporal filtering appeared to have only minor (if any) impact on a one-day forecast.

The effects of the model modifications made were selective with respect to model level, to features in the flow patterns, and to the type of condition being examined. The energetics can be affected, for example, without discernible differences being produced in the overall verification statistics. Many of the modifications produced effects which attenuated with altitude (precipitation mechanism; terrain; friction, pressure smoothing, horizontal resolution). These tests were made using one data set. We would expect slightly different results if the sample was enlarged. Indeed, larger variations would be expected if the forecasts were of longer duration. Radiation, for example, would have greater impact on a one-week prediction. Some of the modifications were detrimental. This was expected. The purpose was to define a range of possibilities, rather than to improve the model's performance.